The synthesis and reactions of some small platinum cluster compounds
by Dong Min

A thesis submitted in partial fulfillment of the requirements for the degree of Doctor of Philosophy in Chemistry
Montana State University

Abstract:
The study of the cis Z trans isomerization of PtCl2(Et2S)2 complex is relevant to the synthesis of certain dimeric Pt(III) complexes. Not only is Cis-PtCl2(Et2S)2 a suitable starting material for Pt(III) compounds syntheses, but Cis-PtCl2(Et2S)2 itself also functions importantly in organometallic synthesis. Detailed thermodynamic and kinetic data of the cis and trans isomers, along with x-ray crystallographic structures, are summarized. Binuclear Pt(III) compounds, which have direct metal-metal bonds have been elucidated recently and their structures have been characterized by Cotton's group. Though it has been observed that there is a structural interconversion between head to head and head to tail configuration in some of the Pt(III) compounds, there is no detailed investigation of the mechanism of this interconversion. Our interest is concerned with the synthesis and mechanistic study of these binuclear Pt(III) compounds, especially the formation and rearrangement of metal-metal bonds. Presented here is the mechanism study about this interconversion. Proton NMR is mainly used in the research. Activation entropy (forward -29 vs. reverse 16 J Mol-1K-1) and activation enthalpy (84 vs. 105 kJ Mol-1) of the interconversion are calculated and explained with the results from the experiment. The mechanism of the interconversion is also postulated as a dissociative concerted reaction. A modified synthetic method results in the formation of a hydroxo-bridged Pt(II) dimeric compound and an oxo-bridged Pt(IIrIV) tetrameric compound. Single crystal x-ray crystallographic information is presented, along with infrared data in support of the proposed structures. The Pt(II) compound exhibits strong hydrogen bonding between molecules and its Pt-O-H bridge bond is clearly reflected in the FTIR spectrum. The Pt(II,IV) compound shows the nonequivalent oxidation states of platinum in one molecule. Platinums in the complex are bonded to one another by oxo bridges. Three platinums show pseudo square-planar, and one platinum exhibits octahedral configuration. No such examples exist in current literature. Finally reactivity of the binuclear Pt(III) compounds are studied. Different ligands have been used for axial coordination and variation of torsion angles between two methyl planes is observed. The derivatives of the binuclear platinum(III) compounds are structurally characterized by single crystal x-ray crystallography. Both structures are new to platinum chemistry. 31P NMR is also used to support the structure. It is hoped this work will be helpful in understanding the synthesis and structure of further complicated platinum compounds.

THE SYNTHESIS AND REACTIONS OF SOME SMALL PLATINUM CLUSTER COMPOUNDS

By

Dong Min

A thesis submitted in partial fulfillment
of the requirements for the degree

of

Doctor of Philosophy

in

Chemistry

Montana State University
Bozeman, Montana

August 1989

APPROVAL

of a thesis submitted by

Dong Min

This thesis has been read by each member of the thesis committee and has been found to be satisfactory regarding content, English usage, format, citations, bibliographic style, and consistency, and is ready for submission to the College of Graduate Studies.

August 17 1989 — Date
Edwin H. Abbott — Chairperson, Graduate Committee

Approved for the Major Department

August 17 1989 — Date
Edwin H. Abbott — Head, Major Department

Approved for the College of Graduate Studies

September 15, 1989 — Date
Henry L Parsons — Graduate Dean

STATEMENT OF PERMISSION TO USE

In presenting this thesis in partial fulfillment of the requirements for a doctoral degree at Montana State University, I agree that the Library shall make it available to borrowers under rules of the Library. I further agree that copying of this thesis is allowable only for scholarly purposes, consistent with "fair use" as prescribed in the U.S. Copyright Law. Requests for extensive copying or reproduction of this thesis should be refered to University Microfilms International, 300 North Zeeb Road, Ann Arbor, Michigan 48106, to whom I have granted "the exclusive right to reproduce and distribute copies of the dissertation in and from microfilm and the right to reproduce and distribute by abstract in any format."

Signature 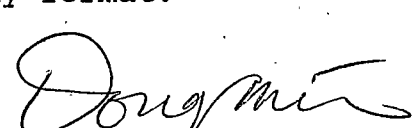

Date August 17, 1989

To my dear Mom and Dad

ACKNOWLEDGEMENTS

There are so many people I would like to thank for making my stay in Bozeman pleasant.

I wish to thank Professor E. H. Abbott for his guidance and support during my graduate career.

I also wish to thank Mr. R. Larson and Professor K. Emerson for the help and technical assistance with the crystallography. I would like to thank Dr. E. S. Peterson for the helpful discussion of synthesis and teaching of NMR. I would also like to thank Dr. D. P. Bancroft for providing the Pt(III) complexes for further research. My colleagues in research, Dan Bedgood, Steven Dunham, deserve great thanks for their encouragement and help.

Finally, I express my deep gratitude for the Graduate Committee which made my trip to the United States possible.

TABLE OF CONTENTS

Page

LIST OF TABLES xi

LIST OF FIGURES xiv

KEY ABBREVIATIONS xvi

ABSTRACT xvii

INTRODUCTION 1

Sulfate Bridged Compounds 3

Phosphate and Pyrophosphite Bridged Compound 6

Platinum Blue Complexes 9

Carboxylate and Dithiocarboxylate Bridged Compounds. 12

Hydroxide and Other Bridged Complexes 15

Oxo-pyridonate Bridged Complexes 20

THE STUDY OF THE CIS TO TRANS ISOMERIZATION OF DICHLOROBIS(DIETHYLSULFIDE) PLATINUM(II) COMPLEX 27

Experimental 27

A. The syntheses of cis-$PtCl_2(Et_2S)_2$ and trans-$PtCl_2(Et_2S)_2$ 27

B. NMR measurements on the equilibrium between cis and trans-$PtCl_2(Et_2S)_2$ 27

C. X-ray crystallograpic determination of the structure of cis-$PtCl_2(Et_2S)_2$ and trans-$PtCl_2(Et_2S)_2$ 29

Discussion 29

THE THERMODYNAMIC AND KINETIC STUDIES ON SOME OF THE BINUCLEAR PLATINUM(III) COMPOUNDS 43

Experimental 43

A. Syntheses of the binuclear Pt(III) compounds 43

B. NMR measurements 43

TABLE OF CONTENTS (continued)

Page

C. NMR spectral assignments for a series of pt(III) compounds 43

D. Equilibrium constant measurement on the HH ⇄ HT interconversion 44

E. Kinetic study of the binuclear Pt(FHPy) HH ⇄ HT interconversion 60

Discussion 61

THE SYNTHESES AND STRUCTURE DETERMINATION OF A GROUP OF PLATINUM COMPOUNDS 81

Experimental 81

A. Preparation of platinum compounds 81

1. Preparation of cis-$PtCl_2(Et_2S)_2$ 1 81

2. Preparation of trans-$PtCl_2(Et_2S)_2$ 2 81

3. Preparation of Ag salts 3 81

4. Preparation of $Pt_2(CH_3)_4[(C^2H^5)^2S]_2$ 4 81

5. Preparation of $K_2[Pt_2(NO_2)_4(OH)_2]\cdot 1\frac{1}{2}H_2O$ 5 .. 82

6. Preparation of $K_5[Pt_4(NO_2)_9(O)_3]\cdot 3H_2O$ 6 82

7. Preparation of $Pt_2(MHPy)_2(CH_3)(Py)$ 7 83

8. Preparation of $[Pt_2(CH_3)_4(MHPy)_2(PPh_3)]\cdot 2CH_3COCH_3$ 8 84

9. Reaction of cis-$PtCl_2(Et_2S)_2$ with pyrizine 9 84

10. Reaction of cis-$PtCl_2(Et_2S)_2$ with PPh_3 10 ... 87

11. Reaction of cis-$PtCl_2(Et_2S)_2$ with NO 11 ... 88

12. Reaction of cis-$PtCl_2(Et_2S)_2$ with $Ag_2C_2O_4$ 12 88

13. Reaction of cis-$PtCl_2(Et_2S)_2$ with $Ag_2C_2O_4$ (modified method) 13 89

TABLE OF CONTENTS (continued)

Page

14. Reaction of cis-$PtCl_2(Et_2S)_2$ with Ag(MHPy) 14 89

15. Reaction of cis-$PtCl_2(Et_2S)_2$ with $AgNO_3$ 15 . 90

16. Reaction of K_2PtCl_4 with PPh_3 16 90

17. Reaction of K_2PtCl_4 with $Ag_2(C_2O_4)$ 17 91

18. Reaction of $K_2Pt(NO_2)_4$ with L-proline ($C_5H_9NO_2$) 18 91

19. Reaction of $K_2Pt(NO_2)_4$ with tartaric acid 19 91

20. Reaction of K_2PtCl_4 with L-proline 20 92

21. Reaction of $K_2Pt(NO_2)_4$ with glycine (H_2NCH_2COOH) 21 92

22. Reaction of $K_2Pt(NO_2)_4$ with D-tartaric acid 22 92

23. Reaction of $Pt_2(HPy)_2(CH_3)_4(Py)_2$ with CCl_3COOH 23 93

24. Reaction of $Pt_2(HPy)_2(CH_3)_4(Py)_2$ with CF_3COOH 24 93

25. Reaction of Pt(MHPy) with CO 25 94

26. Reaction of Pt(MHPy) with KOH 26 95

27. Reaction of Pt(MHPy) with KCN 27 95

28. Reaction of Pt(MHPy) with KSCN 28 96

29. Reaction of Pt(HPy) with CH_3COOH 29 96

30. Reaction of Pt(HPy) with pyrazine 30 97

31. Reaction of Pt(Hpy) with 4-methyl pyridine (picoline) 31 97

32. Reaction of Pt(MHPy) with pyridine 32 98

33. Reaction of Pt(MHPy) with pyrazine 33 98

TABLE OF CONTENTS (continued)

Page

34. Reaction of $Pt(MHPy).Et_2S$ with pyrazine 34 98

35. Reaction of $Pt(HPy)$ with C_2H_4 35 99

36. Reaction of $Pt(HPy)$ with HCl(diluted) 36 .. 100

37. Reaction of $Pt(MHPy)$ with H_2S 37 100

B. Structure Determinations 101

X-ray crystallography data collection 101

Structure solution of $K_2[Pt_2(NO_2)_4(OH)_2]\cdot 1.5H_2O$ 101

Structure solution of $K_5[Pt_4O_3(NO_2)_9\cdot 3H_2O$ 103

Structure solution of $[Pt_2(CH_3)_4(MPy)_2(PPh_3)]\cdot 2CH_3COCH_3$ 104

Structure solution of $Pt_2(CH_3)_4(C_6H_7NO)_2(C_4H_4N_2)$ 106

Structure solution of cis-$PtCl_2(Et_2S)_2$ 109

Structure solution of trans-$PtCl_2(Et_2S)_2$ 111

X-ray crystallographic results 111

Structure of $K_2[Pt_2(NO_2)_4(OH)_2]\cdot 1.5H_2O$ 112

Structure of $K_5[Pt_4(O_3(NO_2)_9]\cdot 3H_2O$ 114

Structure of $Pt_2(CH_3)_4(C_6H_6NO)_2(PPh_2)$ 118

Structure of $Pt_2(CH_3)_4(C_6H_6NO)_2(C_4H_4N_2)$ 124

Structure of cis-$PtCl_2(Et_2S)_2$ 130

Structure of trans-$PtCl_2(Et_2S)_2$ 136

GENERAL DISCUSSION 143

Synthetic procedure 143

Structural comparisons 148

TABLE OF CONTENTS (continued)

Page

NMR and IR studies 159

SUMMARY 162

REFERENCES CITED 165

LIST OF TABLES

Table		Page
1.	Coupling constants for cis-$PtCl_2(Et_2S)_2$ and trans-$PtCl_2(Et_2S)_2$	40
2.	^1H NMR assignments for $Pt_2(CH_3)_4(HPy)_2(Py)$	46
3.	^1H NMR assignments for $Pt_2(CH_3)_4(HPy)_2(Py)_2$	48
4.	^1H NMR assignments for $Pt_2(CH_3)_4(FHPy)_2(Py)$	50
5.	^1H NMR assignments for $Pt_2(CH_3)_4(FHPy)_2(Py)_2$	52
6.	^1H NMR assignments for $Pt_2(CH_3)_4(ClHPy)_2(Py)$	54
7.	^1H NMR assignments for $Pt_2(CH_3)_4(MHPy)_2(Py)$	56
8.	Equilibrium constant and thermodynamic parameters for Pt(FHPy) HH $\rightleftarrows$ HT	60
9.	Rate constant and activation parameters for Pt(FHPy) HH $\rightleftarrows$ HT reaction	64
10.	Chemical shifts of different resonances on Pt(FHPy) (HH) vs. different pyridine concentrations	79
11.	Chemical shifts of different resonances on Pt(FHPy) (HT) vs. different pyridine concentrations	80
12.	^1H and ^{31}P NMR assignments for $Pt_2(CH_3)_4(MHPy)_2(PPh_3)$	87
13.	Crystallographic parameters for $K_2[Pt_2(NO_2)_4(OH)_2]\cdot 1.5H_2O$	103
14.	Crystallographic parameters for $K_5[Pt_4(O)_3(NO_2)_9]\cdot 3H_2O$	105
15.	Crystallographic parameters for $[Pt_2(CH_3)_4(MHPy)_2(PPh_3)]\cdot 2CH_3COCH_3$	107
16.	Crystallographic parameters for $Pt_2(CH_3)_4(MHPy)_2(C_4H_4N_2)$	108
17.	Crystallographic parameters for cis-$PtCl_2(Et_2S)_2$	110

LIST OF TABLES (continued)

Table		Page
18.	Crystallographic parameters for trans-$PtCl_2(Et_2S)_2$	112
19.	Atomic coordinates and isotropic temperature factors ($Å^2$) with standard deviations for $K_2[Pt_2(NO_2)_4(OH)_2]\cdot 1.5H_2O$	116
20.	Anisotropic thermal parameters (Å x 10^3) with standard deviation for $K_2[Pt_2(NO_2)_4(OH)_2]\cdot 1.5H_2O$	116
21.	Bond lengths (Å) with standard deviations for $K_2[Pt_2(NO_2)_4(OH)_2]\cdot 1\frac{1}{2}H_2O$	117
22.	Bond angles (°) with standard deviation for $K_2[Pt_2(NO_2)_2(OH)_2]\cdot 1\frac{1}{2}H_2O$	117
23.	Atomic coordinates and equivalent isotropic temperature factors ($Å^2$) with standard deviations for $K_5[Pt_4(NO_2)_9(O)_3]\cdot 3H_2O$	120
24.	Anisotropic thermal parameters (Åx10^3) with standard deviation for $K_5[Pt_4(NO_2)_9(O)_3]\cdot 3H_2O$	121
25.	Bond lengths (Å) with standard deviations for $K_5[Pt_4(NO_2)_9(O)_3]\cdot 3H_2O$	122
26.	Bond angles (°) with standard deviation for $K_5[Pt_4(NO_2)_9(O)_3]\cdot 3H_2O$	123
27.	Atomic coordinates and isotropic temperature factors (Å) with standard deviations for $[Pt_2(CH_3)_4(C_6H_6NO)_2(PPh_3)]\cdot 2CH_3COCH_3$	126
28.	Anisotropic thermal parameters ($Å^2$x10^3) for $[Pt_2(CH_3)_4(C_6H_6NO)_2(PPh_3)]\cdot 2CH_3COCH_3$	128
29.	Bond lengths (Å) with standard deviation for $[Pt_2(CH_3)_4(C_6H_6NO)_2(PPh_3)]\cdot 2CH_3COCH_3$	128
30.	Bond angles (°) with standard deviation for $[Pt_2(CH_3)_4(C_6H_6NO)_2(PPh_3)]\cdot 2CH_3COCH_3$	129
31.	Atomic coordinates (x10^4) and isotropic thermal parameters ($Å^2$x10^3) with standard deviation for $Pt_2(CH_3)_4$-$C_6H_6NO)_2(C_4H_4N_2)$	132

LIST OF TABLES (continued)

Table		Page
32.	Anisotropic thermal parameters ($Å^2x10^3$) with standard deviation for $[Pt_2(CH_3)_4(C_6H_6NO)_2(C_4H_4N_2)]$	133
33.	Bond lengths (Å) with standard deviation for $Pt_2(CH_3)_4(C6H_6NO)_2(C_4H_4N_2)]$	134
34.	Bond angles (°) with standard deviation for $[Pt_2(CH_3)_4(C_6H_6NO)_2(C_4H_4N_2)$	135
35.	Atomic coordinates and isotropic temperature parameters ($Å^2$) with standard deviations for $cis\text{-}PtCl_2(Et_2S)_2$	138
36.	Anisotropic thermal parameters ($Å^2x10^3$) with standard deviation for $cis\text{-}PtCl_2(Et_2S)_2$	138
37.	Bond lengths (Å) with standard deviations for $cis\text{-}PtCl_2(Et_2S)_2$	139
38.	Bond angles (°) for $cis\text{-}PtCl_2(Et_2S)_2$	139
39.	Atomic coordinates and isotropic thermal parameters ($Å^2$) with standard deviation for $trans\text{-}Pt_(C_2H_5)_2S)_2CL_2$	141
40.	Anisotropic thermal parameters ($Å^2x10^3$) with standard deviation for $trans\text{-}Pt_(C_2G_5)_2S)_2CL_2$	141
41.	Bond lengths (Å) with standard deviation for $trans\text{-}PtC((C_2H_5)_2S)_2Cl_2$	141
42.	Bond angles (°) with standard deviation for $trans\text{-}PtC((C_2H_5)_2S)_2Cl_2$	142
43.	Calculated Hydrogen Atom Coordinates ($x10^4$)	142
44.	Infrared spectral results for $K_2[Pt_2(NO_2)_4(OH)_2]\cdot 1.5H_2O$	150
45.	Infrared spectral results for $K_5[Pt4_2(NO_2)_9(O)_3]\cdot 3H_2O$	154
46.	Relation of the axial ligands vs. torsion angle	158

LIST OF FIGURES

Figure — Page

1. ^1H NMR spectrum of cis-$PtCl_2(Et_2S)_2$ 34
2. ^1H NMR spectrum of trans-$PtCl_2(Et_2S)_2$ 35
3. ^1H NMR spectra of trans-$PtCl_2(Et_2S)_2$ at different temperatures 37
4. ^1H NMR spectra of decoupling of cis-$PtCl_2(Et_2S)_2$ ... 38
5. ^1H NMR spectra of decoupling of trans-$PtCl_2(Et_2S)_2$ 39
6. ^1H NMR spectrum of $Pt_2(CH_3)_4(HP)_2(Py)$ 45
7. ^1H NMR spectrum of $Pt_2(CH_3)_4(HP)_2(Py)_2$ 47
8. ^1H NMR spectrum of $Pt_2(CH_3)_4(FHP)_2(Py)$ 49
9. ^1H NMR spectrum of $Pt_2(CH_3)_4(FHP)_2(Py)_2$ 51
10. ^1H NMR spectrum of $Pt_2(CH_3)_4(ClHPy)_2(Py)$ 53
11. ^1H NMR spectrum of $Pt_2(CH_3)_4(MHPy)_2(Py)$ 55
12. ^1H NMR spectrum of Pt(FHPy) HH → HT 58
13. ^1H NMR spectrum of Pt(HPy) HH → HT 59
14. $-Ln[(HH)-(HH)_{eq}]$ vs. time (hours) plot Pt(FHPy) HH → HT at different pyridine concentrations 68
15. $-Ln[(HH)-(HH)_{eq}]$ vs. time (hours) plot Pt(FHPy) HH → HT at different temperatures 69
16. Eyring plot for Pt(FHPy) HH → HT 70
17. Mechanism 1 for Pt(FHPy) HH → HT 71
18. Mechanism 2 for Pt(FHPy) HH → HT 72
19. ^1H NMR spectrum of Pt(HPy) HT → HH 78
20. ^1H NMR spectrum of $Pt_2(CH_3)_4(MHPy)_2(PPh_3)$ 85

LIST OF FIGURES (continued)

Figure Page

21. ^{31}P NMR spectrum of $Pt_2(CH_3)_4(MHPy)_2(PPh_3)$ 86

22. ORTEP view of $K_2[Pt_2(NO_2)_4(OH)_2]\cdot 1.5H_2O$ 115

23. ORTEP view of $K_5[Pt_4(NO_2)_9(O)_3]\cdot 3H_2O$ 119

24. ORTEP view of $[Pt_2(CH_3)_4(MHPy)_2(PPh_3)]$.....125

25. ORTEP view of $Pt_2(CH_3)_4(MHPy)_2(C_4H_4N_2)$ 131

26. ORTEP view of cis-$PtCl_2(Et_2S)_2$ 137

27. ORTEP view of trans-$PtCl_2(Et_2S)_2$ 140

28. ORTEP view of molecular arrangement in $K_2[Pt_2(NO_2)_4(OH)_2]\cdot 1.5H_2O$ 151

29. ORTEP view of molecular arrangement of Pt(MHPy) with different axial ligands 157

KEY ABBREVIATIONS

Å	=	Angstroms
Et_2S	=	Diethylsulfide [$(H_5C_2)_2S$]
Hz	=	Hertz
MHz	=	Megahertz
NMR	=	Nuclear Magnetic Resonance
ppm	=	part per million
Pt(HPy) (HH)	=	$Pt_2(CH_3)_4(C_5H_4NO)_2(Py)$
Pt(HPy) (HT)	=	$Pt_2(CH_3)_4(C_5H_4NO)_2(Py)_2$
Pt(FHPy)(HH)	=	$Pt_2(CH_3)_4(C_5H_3NOF)_2(Py)$
Pt(FHPy)(HT)	=	$Pt_2(CH_3)_4(C_5H_3NOF)_2(Py)_2$
Pt(ClHPy)	=	$Pt_2(CH_3)_4(C_5H_3NOCl)_2(Py)$
Pt(MHPy)	=	$Pt_2(CH_3)_4(C_6H_6NO)_2(Py)$
Pt(MHPy).Et_2S	=	$Pt_2(CH_3)_4(C_6H_6NO)_2(Et_2S)$
Pt(MHPy).PPh_3	=	$Pt_2(CH_3)_4(C_6H_6NO)_2(PPh_3)$
Pt dimer	=	$K_2[Pt_2(NO_2)_4(OH)_2]\cdot 1\frac{1}{2}H_2O$
Pt tetramer	=	$K_5[Pt_4(NO_2)_9(O)_3]\cdot 3H_2O$
Py	=	Pyridine
X	=	Halogen or specified function group

ABSTRACT

The study of the cis $\rightleftarrows$ trans isomerization of $PtCl_2(Et_2S)_2$ complex is relevant to the synthesis of certain dimeric Pt(III) complexes. Not only is cis-$PtCl_2(Et_2S)_2$ a suitable starting material for Pt(III) compounds syntheses, but cis-$PtCl_2(Et_2S)_2$ itself also functions importantly in organometallic synthesis. Detailed thermodynamic and kinetic data of the cis and trans isomers, along with x-ray crystallographic structures, are summarized. Binuclear Pt(III) compounds, which have direct metal-metal bonds have been elucidated recently and their structures have been characterized by Cotton's group. Though it has been observed that there is a structural interconversion between head to head and head to tail configuration in some of the Pt(III) compounds, there is no detailed investigation of the mechanism of this interconversion. Our interest is concerned with the synthesis and mechanistic study of these binuclear Pt(III) compounds, especially the formation and rearrangement of metal-metal bonds. Presented here is the mechanism study about this interconversion. Proton NMR is mainly used in the research. Activation entropy (forward -29 vs. reverse 16 J $Mol^{-1}K^{-1}$) and activation enthalpy (84 vs. 105 kJ Mol^{-1}) of the interconversion are calculated and explained with the results from the experiment. The mechanism of the interconversion is also postulated as a dissociative concerted reaction. A modified synthetic method results in the formation of a hydroxo-bridged Pt(II) dimeric compound and an oxo-bridged Pt(II,IV) tetrameric compound. Single crystal x-ray crystallographic information is presented, along with infrared data in support of the proposed structures. The Pt(II) compound exhibits strong hydrogen bonding between molecules and its Pt-O-H bridge bond is clearly reflected in the FTIR spectrum. The Pt(II,IV) compound shows the nonequivalent oxidation states of platinum in one molecule. Platinums in the complex are bonded to one another by oxo bridges. Three platinums show pseudo square-planar, and one platinum exhibits octahedral configuration. No such examples exist in current literature. Finally reactivity of the binuclear Pt(III) compounds are studied. Different ligands have been used for axial coordination and variation of torsion angles between two methyl planes is observed. The derivatives of the binuclear platinum(III) compounds are structurally characterized by single crystal x-ray crystallography. Both structures are new to platinum chemistry. ^{31}P NMR is also used to support the structure. It is hoped this work will be helpful in understanding the synthesis and structure of further complicated platinum compounds.

INTRODUCTION

Platinum, first discovered as a 50-80% alloy with gold and silver, was considered to be water-born grain in ancient times. Because of the difficulties in its separation from other materials and its high melting point, it was not until 1741 that the first pure sample of platinum was under investigation by European scientists (1).

Since then, many remarkable properties of this element have been discovered. Early ones were its strong resistance to corrosion, even under the attack of aqua regia, and its excellent electrical conductivity. As early as 1840, chemists found the metal had the ability to form complicated networks of bonds under fairly moderate conditions with various ligands. A Pt-Pt metal bond was reported in a journal at that time (2). Thereafter platinum not only interested chemists for its shining surface and value but also for its chemical activity. In recent years, the development of research on this metal has further revealed its important catalytic activity in organic synthesis and petroleum industrial processes. There is also more and more focus on the biochemical activity of platinum compounds, especially the anti-tumor properties of several of its compounds (3). Modern research is directed at determining systematic aspects of Pt chemical properties and even investigating the potential application of using platinum

clusters for electronic circuitry which could change the electronic industry dramatically (4).

Our purpose in research has centered in the area of new methods for synthesis of platinum compounds with Pt-Pt bonds. We are also interested in structure elucidation and chemical properties. Our efforts have been directed towards two objectives:

1. Synthesis of platinum dimer, trimer, tetramer cluster compounds and their structure determination.

2. Determining the mechanisms of certain platinum clusters rearrangement reactions.

Because we are interested in making platinum compounds which have one or more Pt-Pt bonds, the basic understanding of the platinum oxidation states verses the electron configuration of the compound needs to be considered first.

Recently, a group of the platinum(III) binuclear compounds, first characterized in detail by F. Albert Cotton's group, has been shown to have a net single bond between platinum metal atoms and the $\underline{\sigma^2\pi^4\delta^2\delta^{*2}\pi^{*4}}$ electronic configuration (5). Such a configuration enables this system to form two bridging ligands bonding with the metal atoms and axial bonding with appropriate monodentate ligand as is commonly seen in the Rh^{+4}_2 system (6-8) which is isoelectronic with the Pt^{+6}_2 system. Numerous examples have been characterized structurally in the Rh^{+4}_2 system.

Therefore one object of our work was to develop the methodology for the synthesis of Pt^{+6}_2 groups where only a few structures are known and to extend it to the development of platinum cluster formation. Let us begin by reviewing the current state of knowledge of Pt_2^{6+} groups.

Sulfate Bridged Compounds

In 1893 Vezes reported that the reaction of dilute mineral acids with $K_2[Pt(NO_2)_4]$ resulted in the formation of copper red needles (9, 10) which he formulated as $K_2H_4Pt_3(NO_2)_6O\cdot 3H_2O$. In 1905, Blondel prepared the first well-characterized compound in this category which he suggested to be a Pt(III) complex (11). In this reaction, Pt(IV) oxide was reacted with aqueous sulphuric acid and subsequently reduced by the addition of oxalic acid. At the time, Blondel formulated this Pt complex as $K[Pt(SO_4)_2]\cdot H_2O$. His work was later confirmed by Wohler and Frey who independently prepared this compound along with other related species (12). It was not until 1976, with the use of x-ray crystallography that this compound was correctly formulated as $K_2[Pt_2(SO_4)_4(H_2O)_2]\cdot 9.5H_2O$--a binuclear Pt(III) compound [1](13).

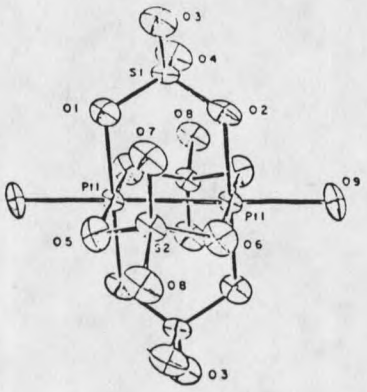

[1]

In 1977, new investigations of Vezes' red salt also reformulated the compound as $K_2[Pt_3(NO_2)_6O]\cdot 3H_2O$ [2](14).

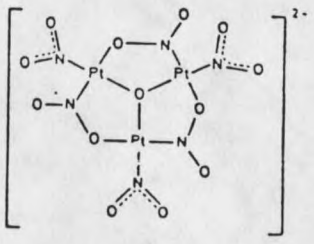

[2]

The potassium salt $K_2[Pt_2(SO_4)_4(H_2O)_2]$ was the first structurally characterized Pt_2^{6+} binuclear complex (15-17). This work was later improved by using the reaction of $K_2[Pt(NO_2)_4]$ with H_2SO_4 in which a oxidation reaction occurs during the process. The conditions for the reaction are fairly simple. The basic requirement for this reaction is to dissolve the potassium salt with aqueous sulphuric acid followed by 10 minutes heating of the solution in an oil

bath at 353 K. Slow evaporation in vacuum results in a change of color of the solution from colorless to light blue, blue, green, yellow and, finally, when exposed to air with the addition of H_2O, a red precipitate form. In this process, each color may represent an individual compound and structure determination confirmed one of the compounds as $K[Pt(NO_2)_4(NO)(H_2O)]\cdot H_2O$ [3](18).

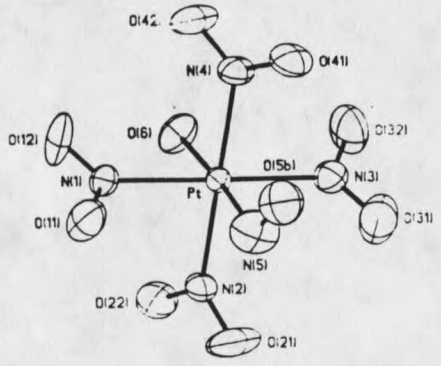

[3]

A few derivatives of the sulfato-bridged platinum compound containing neutral or anionic axial ligands were also reported such as $K_2[Pt_2(SO_4)_2(OSMe)_2]\cdot 4H_2O$ (13). Most reactions take place at the axial position of this platinum(III) complex. Generally the Pt-Pt bond length is about 2.50-2.60 Å.

Although the reaction between $K_2Pt(NO_2)_4$ and H_2SO_4 was first performed about 80 years ago, the correct structure of the product was not determined until 1984 (19). Similar types of the sulfato-bridged, metal-metal bonded compounds were also seen for $[Re_2(SO_4)_4(H_2O)_2]^{-4}$ and $[Mo_2(SO_4)_4(H_2O)_2]^{-4}$ that were characterized in the mid 70's

(15-16).

Phosphate and Pyrophosphite bridged complexes

Binuclear platinum(III) phosphate compounds were discovered in 1980 (20). Their structures were determined shortly thereafter (21). The structure is very similar to that of sulfato bridged platinum complexes. The structure of the sulfate and phosphate complexes is referred to as a "lantern" structure. This lantern form represents a comparatively short metal-metal bond, four bridging ligands coordinated to the two platinum atoms and either one or two axial ligands as illustrated above [1].

A variety of derivatives has been synthesized with pyridine as an axial ligand and characterized by x-ray crystallography (22).

Another class of compounds is arrived at via an oxidation reaction of a binuclear platinum(II) complex which was synthesized from K_2PtCl_4 with bridging pyrophosphite [$H_2P_2O_5$,$(POP)^{-2}$] ligands in 1982. POP is the anhydride of phosphorous acid (H_3PO_3) with two oxygen ions available for coordination [4]. The formation of binuclear platinum(III) complexes with methyl iodide or halogens as oxidizing agents in the axial position was first observed [5](23-26).

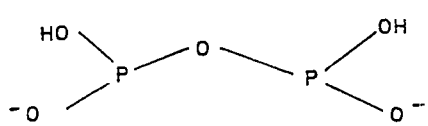

[4]

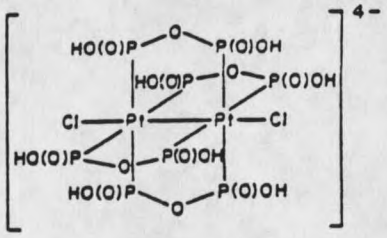

[5]

The general formula for these Pt(III) complexes is $[Pt_2(POP)_4X_2]^{-4}$. They all have the lantern structures. The formation of Pt-Pt single bond apparently results from loss of the two antibonding σ electrons in $[Pt_2(POP)_4]^{-4}$ in the $\underline{\sigma^2\pi^4\delta^2\delta^{*2}\pi^{*4}\sigma^{*2}}$ electron configuration. The two antibonding σ electrons are transferred to the incoming X_2 molecule in $[Pt_2(POP)_4X_2]^{-4}$ to form $\underline{\sigma^2\pi^4\delta^2\delta^{*2}\pi^{*4}}$ electron configuration. The decrease of bond length (from 2.925 Å to 2.695 Å) supports the explanation. This interpretation is also supported by electronic absorption spectra of the complex where a higher energy, intense component has been assigned to a dσ --> dσ* transition (24).

More interesting results came from the oxidation of $[Pt_2(POP)_4]^{-4}$ by bromine water in which a final product $[Pt_2(POP)_4Br]\ H_2O$ formed [6](26).

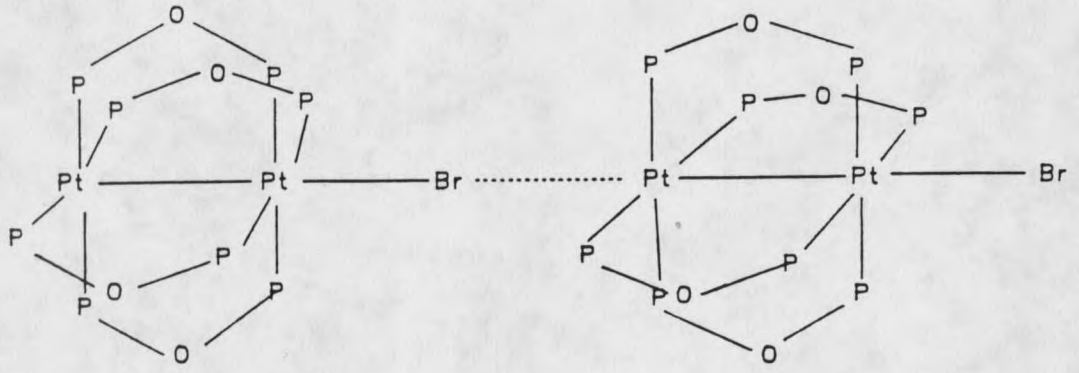

[6]

This complex has distinct semi-conductor properties. The structure showed the one dimensional packing along Pt-Pt-Br direction. This paired stacking provides the pathway for conduction. The Pt-Pt bond length is 2.793 Å and the Pt-Br distance is 2.699 Å. The longer distance between Pt-Pt in the pyrophosphite bridged complex was due to the large bite distance of the POP bridge ligands. With the use of ^{31}P and ^{195}Pt NMR, one can study the platinum-phosphine complexes which have magnetically different platinum and phosphine atoms by measuring the coupling constant and chemical shifts, as Pt-Pt coupling constants and Pt-P coupling constants are directly measured from spectra, usually from an AB pattern. With different bridging and axial ligands, the coupling constants and chemical shifts vary in magnitude; this coupling constant and chemical shift provide a way to study the interaction between the Pt ions and Pt-P atoms as well. Infrared spectra are also helpful in

studying the Pt-Pt and Pt-X stretching modes.

Platinum Blue Complexes

"Platinum blues" are mixed valence polynuclear Pt compounds with an intense blue absorption. The first platinum blue compound was prepared in 1908 when the German chemists Hoffman and Bugge ran the reaction of $Pt(CH_3CN)_2Cl_2$ with K_2PtCl_4 and obtained a blue product with the formula $Pt(CH_3CONH)_2 \cdot H_2O$ (27). Though the early platinum blue complex had historical significance, it was not until the discovery of the anti-tumor activity of the platinum blue synthesized from cis-$Pt(NH_3)_2(H_2O)_2$ that there was much interest in this group of compounds. Since the discovery of the powerful anti-cancer drug cis-$Pt(NH_3)_2Cl_2$ (28-30), many platinum blue compounds have been prepared. In 1977, the first platinum blue complex was structurally characterized by x-ray crystallography. The crystals are found in the reaction of α-pyridone with cis-$PtCl_2(NH_3)_2$ in dilute HNO_3 acid solution for [7](31).

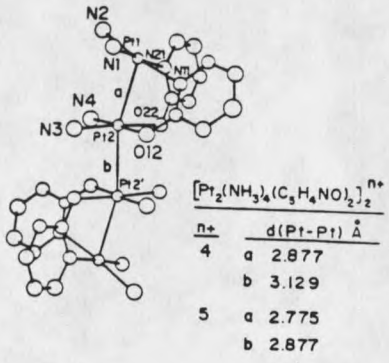

[7]

This compound had two binuclear platinum complexes coordinated together by a Pt-Pt bond. Each binuclear platinum complex had the same configuration. Two cis-ammine groups were coordinated to each Pt atom and two α-pyridone ligands bridged the two Pt atoms in a cis orientation. This platinum blue complex was further studied and it was found that the oxidation of the platinum tetramer by HNO_3 resulted in red crystals. It was characterized as cis-$[Pt_2(NH_3)_4(Pyr)_2(NO_3)(H_2O)]$ with a head-to-head configuration of the α-pyridone bridges. In this head-to-head form labeled as HH, platinum is bonded to both nitrogens or oxygen ions of the bridging ligands. It was later found that HH would form cis-$[Pt_2(NH_3)_4(Pyr)_2(NO_3)_2]$ (HT) (head to tail configuration) with the addition of HNO_3 [8](32-33).

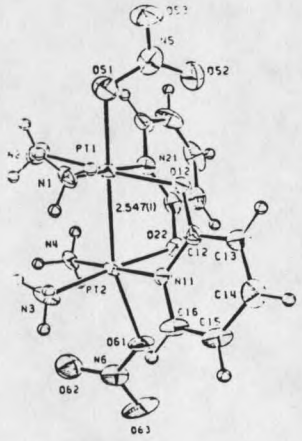

[8]

The difference between HH and HT is whether or not the Pt atoms are coordinated to both nitrogens or oxygens on the α-pyridone bridge. In the HH Pt complex, each Pt is coordinated to either both N atoms or to both O atoms on

bridging ligands. For the HT Pt complex, each Pt is coordinated to N and O atoms on the bridging ligands. The reaction was studied electrochemically which revealed that the formation of the Pt-Pt bond was either due to a concerted two electrons oxidation, (HT), or through two one electron steps, (HH) (33). This result was informative as the binuclear platinum (III) complex had two coordinated axial ligands that were not present in the starting binuclear Pt(II) complex.

Recently a related platinum-nucleobase complex with a Pt-C bond was reported [9](34).

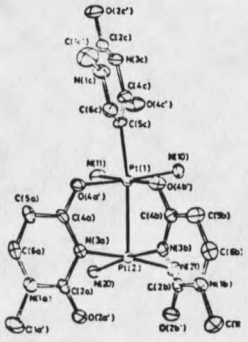

[9]

This complex has nonequivalent sites of platinum coordination which are useful in ^{195}Pt NMR studies. The bridging ligand used in this complex was 1-methyluracil in a head-to-head fashion. Another methyluracil ligand in the axial position is bonded to a platinum atom through C(5) on its ring.

Research on this catagory of platinum blue encourages chemists to investigate areas in which interactions between

metal and biological active ligands occur and where a lot of challenging questions are still unanswered.

Carboxylate and Dithiocarboxylate Bridged Compounds

The first studies on the carboxylate bridged platinum(III) compound were reported in 1976 and in 1977 (35-36). Ag(I) salts oxidized platinum(II) compounds according to the following reaction:

$$Pt_2R_4(R^2{}_2S)_2 + 2AgO_2CR' \longrightarrow Pt_2R_4(O_2CR')_2(R^2{}_2S)_2 + 2Ag$$

R=Ph, p-tolyl, Me, R'=Me, CF_3, R^2=Et, Pr.

The series of complexes with two bridging carboxylate groups coordinated to the platinum atoms in a cis position were studied and formulated as $Pt_2R_4(O_2CR')_2(R^2{}_2S)_2$. For most reactions, the starting materials were the cis-$Pt(R^2{}_2S)_2Cl_2$ compounds. They react with CH_3Li to form binuclear complexes in which each Pt is bonded to two methyl groups and is bridged by two $R^2{}_2S$ ligands. Further oxidation by a Ag(I) carboxylate or possibly by Hg(II) or Tl(III) carboxylate salts, made these reactions proceed as follows (37):

$$Pt_2R_4(Et_2S)_2 + 2Hg(O_2CCH_3)_2 \longrightarrow Pt_2R_4(O_2CCH_3)_2(Et_2S)_2 + Hg_2(O_2CCH_3)_2$$

$$Pt_2R_4(Et_2S)_2 + Tl(O_2CCH_3)_3 \longrightarrow Pt_2R_4(O_2CCH_3)_2(Et_2S)_2 + Tl(O_2CCH_3)$$

R=CH_3, Ph, p-tolyl

In 1978, a binuclear Pt(III) complex was fully characterized by x-ray crystallography [10](38).

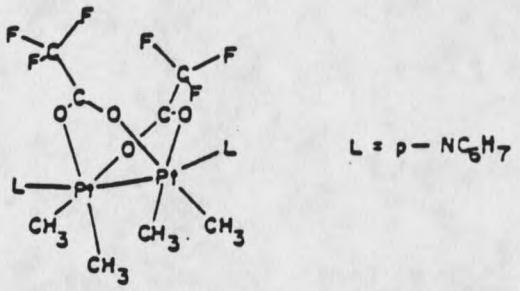

[10]

The structure of the complex was similar to the α-pyridone bridged complex with two trifloroacetate ligands bridging the two platinum atoms and a net single bond forming in between (Pt-Pt bond length 2.557 Å). Each platinum atom was coordinated by two methyl groups in a cis orientation and two 4-Methylpyridine groups in the axial position. There was a torsional twist along the N-Pt-Pt-N direction by 26 degree from linearity due to methyl steric repulsions.

Dithiocarboxylate ligands also bridge two platinum atoms forming similar types of compound (39).

$$K_2PtCl_4 + CH_3CS_2H \longrightarrow [Pt_2(CH_3CS_2)_4]^{-2} \quad (A)$$

$$A + X_2 \longrightarrow [Pt_2(CH_3CS_2)_4X_2] \quad X=Cl, Br, I.$$

$$A + 1/2\ I_2 \longrightarrow Pt_2(CH_3CS_2)_4I \quad (B)$$

The distance between the Pt-Pt was 2.677 Å and compound B was proven to have semiconductive properties. It was suggested that this property was caused by the stacking of the regular units along Pt-Pt-I direction as a pathway to transport the electrons.

As the studies on carboxylate bridged compounds increased, more new compounds were structurally characterized and different synthetic routes were explored. In 1976, a tetrameric carboxylate complex was studied. It was suggested that its structure was a planar square of four platinum(II) atoms bridged by eight acetate ions [11](40).

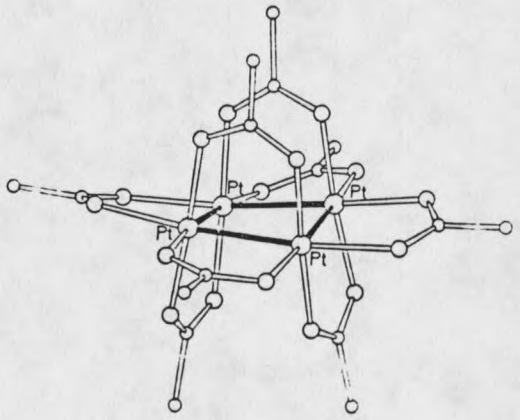

[11]

There was direct bonding between Pt(II)-Pt(II) in the square so as to create pseudo-octahedral coordination around each platinum(II). X-ray crystallography confirmed this structure. Such an arrangement of bridge ligands in this complex led us to study more complex carboxylate ligands. Efforts were made to synthesize structure-similar bridging

compounds using $K_2Pt(NO_2)_4$, K_2PtCl_4 and even cis-$PtCl_2(Et_2S)_2$ with tartaric acid($C_4O_6H_6$) and Ag(I) oxalate salt, etc.

Derivatives of the carboxylate bridged platinum(II) tetramer were studied and a carbonyl bridged compound was discovered and characterized structurally [12](18).

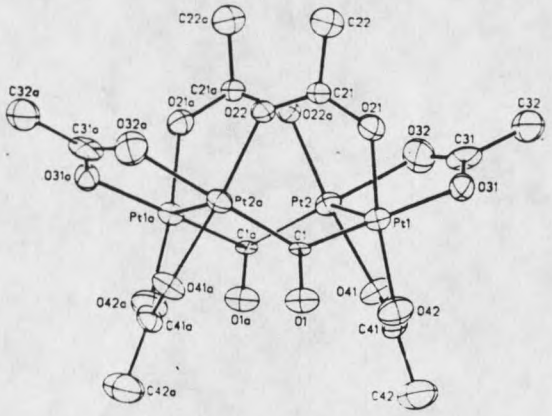

[12]

Studies showed that this platinum complex was stable in air and the Pt tetramer frame kept intact under the various ligand substitutions. IR and XPS data indicated the postulated structures when a single crystal was impossible to obtain (18).

Hydroxide and Other Bridged Complexes

In 1974, Russian chemists claimed a reaction product ($K_2Pt(NO_2)_4$ + H_2SO_4 under 100°c) $K_2(H_3O)[Pt_2(SO_4)_4(H_2O)(OH)]$ formed. While this compound was filtered the residue was extracted by acetone (41). They formulated the final product as peroxide O_2^{-2} bridged $[Pt_2(O_2)_2(OH)_2(H_2O)_2]_n$.

$KHSO_4$. Unfortunately the work was not verified by X-ray crystallography and the structure was totally inferred from infrared spectroscopy, microanalysis and potentiometric titration.

In 1974, Italian chemists reported the synthesis and structures of platinum carbonyl clusters $[Pt_3(CO)_3(\mu\text{-}CO)_3]_n^{-2}$ (n=2, 3, 4, 5)[13](42).

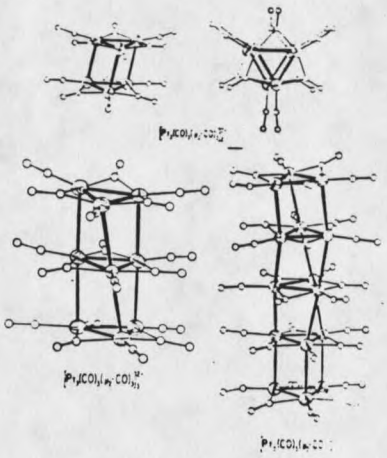

[13]

This series of platinum clusters is of particular interest, because it displays a basic $M_3L_3(\mu\text{-}X)_3$ type building block with direct metal-metal interactions. The 2.66 Å intracluster Pt-Pt distances are within the expected Pt-Pt single bond range. The intercluster Pt-Pt distances averaged 3.03-3.05 Å which indicated the metal-metal interactions were not very strong and the whole stacking was twisted. This kind of cluster represented an approach to the synthesis of a unique type of one dimensional metal cluster polymer with potential desirable conductivity.

In recent years, another kind of cluster was synthesized

and the structure was characterized as $[Pt_5(CO)(\mu\text{-}CO)_2(\mu\text{-}SO_2)_3\text{-}(PPh_3)_4]$ [14](43).

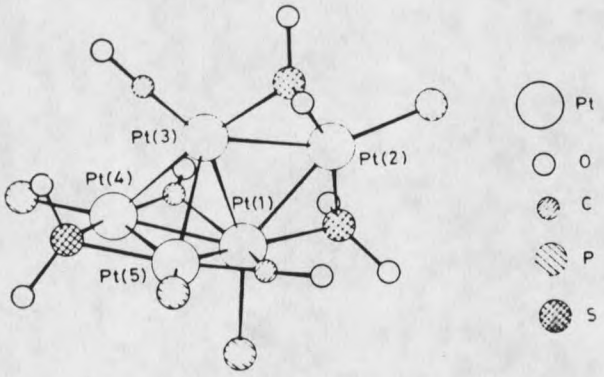

[14]

The unbridged Pt-Pt bond lengths radiating from Pt(3) in the complex averaged 2.78 Å. The cluster might be more correctly described in terms of two orthogonal triangular-clusters which share a common metal atom. The investigator involved also indicated that SO_2 was a better sigma donor than CO and CO was a better pi acceptor electronically. Hence this complex not only had a CO bridging bond but also had a SO_2 bridging bond between platinum atoms. The synthesis of the cluster required passing SO_2 gas through a toluene solution of $Pt(C_2H_4)(PPh_3)_2$. The product was formulated as $Pt_3(SO_2)_3(PPh_3)_3$ which was the starting material for synthesis of the platinum cluster compound $Pt_5(CO)(\mu\text{-}CO)_2(\mu\text{-}SO_2)_3(PPh_3)_4$ (44). The diversity of the SO_2 bridged platinum complexes opened up an entirely different chemistry. The lability of the SO_2 ligand may be useful synthetically.

Several platinum coordination compounds with hydroxide bridges have been isolated and characterized [15](45).

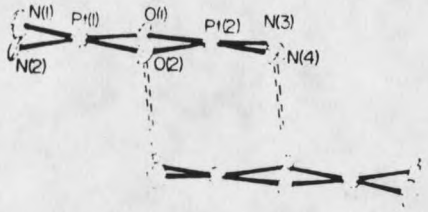

[15]

The structures of the complexes showed that the two OH groups bridged the two platinum atoms in a cis fashion forming two square-planar configurations. Each platinum dimer in the unit cell was stacked over another. Strong interaction between each layer was most likely caused by hydrogen bonding. The dimer unit was essentially planar although a twist of the planes and the distortion such that Pt(2)(a) and Pt(2)(b) moved out of the square planes away from each other could be seen. The interdimer distance was 2.81 Å (a and b indicate different molecules).

The synthesis was strongly dependent upon controlling the pH of the solvent and crystal formation only occurred in basic solution. Infrared spectroscopy showed a Pt-O-H bending mode which indicated that the compound was hydroxide bridged. Similar syntheses also resulted in the formation of hydroxide bridged platinum trimer and tetramer (46-47). The platinum trimer had roughly C_{3v} symmetry. All the

bridging hydroxide groups lay on the same side of the three platinum plane. Each platinum atom and its ligands formed an essentially planar configuration error. The platinum tetramer might be visualized as consisting of a tetrahedral core of oxygen atoms, with platinum atoms bridging four of the six edges of the tetrahedron. The four Pt atoms defined a plane and were located approximately on the corner of a square. Coordination around each platinum atom was square planar. An oxo-bridged platinum complex was only recently reported (48) and the structure was characterized by crystallography [16]. This Pt(I)-Pt(II) complex contained a metal-metal bonded diplatinum(I) unit. One $Pt_2Cl_2(DMSO)_2$ unit fused into a dimeric $Pt_2O_2(DMSO)_4$ unit by the formation of two μ-oxo bridges. The geometry about each platinum atom was nearly square planar.

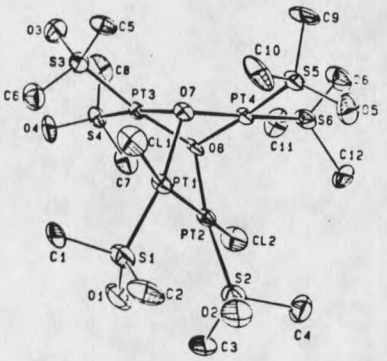

[16]

Oxo-Pyridonate Bridged Complexes

Some α-pyridone bridged platinum complexes have been discussed. The platinum blue compounds were chiefly prepared by either chemical or electrochemical oxidation of the mixed-valent platinum compounds (49-51). However, the syntheses for these products have been found to be non-repeatable or the yields too low to represent a systematic route for obtaining them. Precursors for these complexes tend to be unstable in air and do not have good solubility as well. A research group led by F. A. Cotton has synthesized a series of platinum(III) binuclear compounds bridged by a series of oxopyridonate ligands in high yields. These Pt(III) complexes are stable in air and soluble in the organic solvents. The syntheses are based on Vrieze's method (35) in which platinum(II) compounds react with Ag(I) carboxylate to form carboxylate bridging bonds between the two platinum atoms.

By using a variation of Vrieze's method, Bancroft has synthesized a new class of platinum binuclear compounds which have been confirmed by x-ray crystallography and NMR spectroscopy. This has resulted in interesting geometric and mechanistic insights (52).

This series of the binuclear platinum(III) compounds existed as head-to-head (HH) and head-to-tail (HT) isomers. This HH and HT classification not only depends upon the geometry in which HT has both axial positions occupied while

HH has only one axial position occupied and another axial position is available for ligand bonding, but also depends on the size of the substituent on the bridges. If the substituent is large in size like Cl or CH_3, then the complexes form HH or the polar-arrangement. If the substituent is small like H or F, then the complexes can have either polar (HH) or nonpolar (HT) arrangements [17].

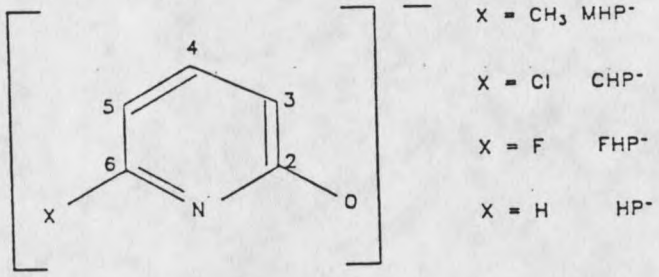

Oxopyridonate ligands and their derivatives

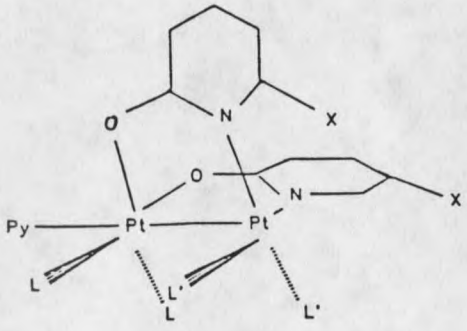

L=L'=CH_3
Head to Head configuration

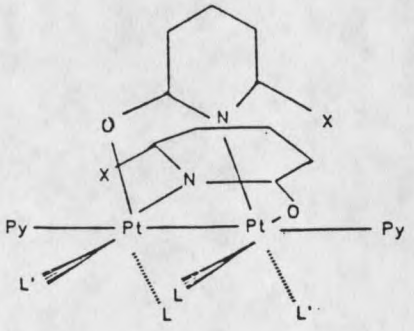

L = L'=CH_3
Head to tail configuration

The oxopyridonate bridged complexes are prepared by the following reactions:

$$K_2PtCl_4 + 2R_2S \longrightarrow cis\text{-}PtCl_2(R_2S)_2 + 2KCl$$

$$cis\text{-}PtCl_2(R_2S)_2 + 2CH_3Li \longrightarrow 1/2\ Pt_2(CH_3)_4(R_2S)_2 + 2LiCl + R_2S$$

$$Pt_2(CH_3)_4(R_2S)_2 + 2Ag(XHPy) \longrightarrow [Pt_2(CH_3)_4(XHPy)_2(R_2S)_n] + 2Ag$$

$$Pt_2(CH_3)_4(XHPy)_2(R_2S)_2 + Pyridine \longrightarrow Pt_2(CH_3)_4(XHPy)_2(Py) + nR_2S$$

$R=C_2H_5$, X=H, F, Cl, Br, CH_3, n=1, 2

The platinum(III) complexes are stable in the solid state. NMR studies show that some HH polar complexes are stable in solution while HT complexes are converted to a HT and HH equilibrium mixture in the solution over a period of a few hours.

In summary, much is yet to be learned about platinum cluster chemistry in view of the great structure diversities of the clusters. The objectives of my project were to develop general methods for the synthesis of multinuclear platinum compounds, to characterize the bond formation in these complexes and to investigate the mechanisms of some of the platinum reactions.

The $cis\text{-}PtCl_2(Et_2S)_2$ complex is not considered to be a Pt cluster, but in this special category, I'd rather include

this complex into the consideration due to its importance in the synthesis of the platinum cluster and its functionality in organometallic chemistry. It has been observed that cis-$PtCl_2(Et_2S)_2$ isomerizes to trans-$PtCl_2(Et_2S)_2$ in solution and trans-$PtCl_2(Et_2S)_2$ is the thermodynamically favored product in certain solvents. It is also true that cis-$PtCl_2(Et_2)_2$ is a common starting material for further synthesis because of the labile Pt-Cl bond. A review of the reactions involving related compounds can benefit the understanding of the current investigation.

As my research has been concerned with the formation and breakage of chemical metal-metal bonds, it is important for me to find out and trace reactions involving direct metal-metal bonds or metal atoms bonded by a bridge. There is a interconversion of binuclear platinum(III) complex as I describe earlier in this chapter. Thus, it is my intention to study this interconversion thermokinetically and to learn more detail about this kind of arrangement. The binuclear platinum(III) complex, from the electronic configuration, has a metal-metal bond. Initially, I will attempt to determine whether the metal-metal bond is broken during the HH $\rightleftarrows$ HT interconversion. Then I will examine the rearrangement of the bridge ligands as these ligands in one state "bite" the metal centers and transfer into another state without giving up chelating the metals. Factors affecting this interconversion have been found. Lastly,

theoretical comparison of experimental data brings us to a conclusion that the interconversion happens as a concerted step, neither the metal-metal bond nor the bridging ligand is completely dissociated. Therefore the question of a mixed valence d^6-d^8 (Pt(IV) and Pt(II)) electronic configuration or a d^7-d^7 (Pt(III) and Pt(III)) electronic configuration in the interconversion has been partially clarified as the intact metal-metal bond in the rearrangement. Pt(III) is more reasonable in explaining the metal-metal bond formation. Systematic substitution chemistry of the binuclear Pt(III) compounds reveals the influence of the axial ligand on the metal-metal bond and the torsion angles between the Pt-CH_3 group planes. Different axial ligands result in different torsion angles and bond length changes. The torsion angle is not related to the trans-effect of the axial ligand, it is rather related to the bulk of the axial ligand. The change of the metal-metal bond length seems to be closely related to the trans-effect of the axial ligand.

In the last part of this dissertation, the synthesis and characterization of a group of yellow platinum clusters has been pursued. The synthesis suggested by Blondel (11) by using Pt(IV) oxide reacting with sulfuric acid and oxalic acid has been modified such that a simpler and safer reaction between $Pt(NO_2)_4^{-2}$ and dilute sulfuric acid develops into a new series of platinum complexes. This

reaction is strongly influenced by the pH value of the solution and generates a series of color changes. The synthesis results in a yellow platinum dimer and a yellow platinum tetramer [18].

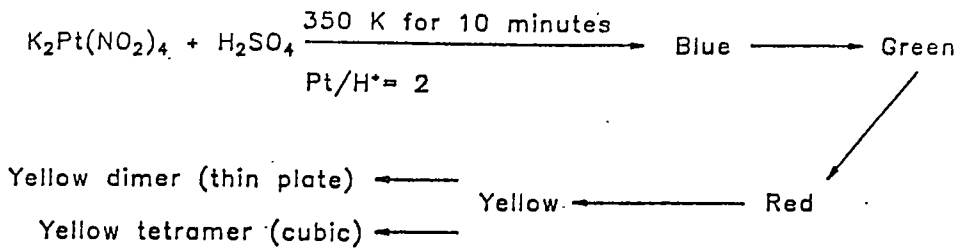

Synthesis of yellow dimer and tetramer

[18]

While a binuclear platinum(III) sulfato-bridged complex forms in a classic sense of the synthesis (I), compounds characterized by Lippert have similar structures (45). But one should notice the unique aspect of the yellow platinum clusters that nonequivalent oxidation states are found in the platinum tetramer. The research of this particular reaction has given some insights into the formation, structure and reactivity of the platinum cluster. Modern techniques have been used during the investigation. They include nuclear magnetic spectroscopy, single crystal x-ray crystallography, infrared spectroscopy, chromatography and elemental analysis.

My thesis is divided into three parts. Part one deals with cis- and trans-$PtCl_2(Et_2S)_2$. Their structures were determined by x-ray crystallography and their isomerization reactions were studied. The second part is the kinetic and thermodynamic study on the HH-HT interconversion for $Pt(CH_3)_4(C_5H_3FNO)_2(C_5H_5N)$ by NMR. Part three is the synthesis of a platinum binuclear compound and platinum tetranuclear compound. Structures were characterized by x-ray crystallography, NMR and FTIR. The last part also includes the different substitution reactions for the binuclear platinum(III) compounds. Any implications concerning structure details, thermodynamic results and reaction routes are discussed after each part. General discussion contains the summary of the work and achievement of this investigation.

THE STUDY OF THE CIS TO TRANS ISOMERIZATION OF DICHLOROBIS(DIETHYLSULFIDE)PLATINUM(II) COMPLEX

Experimental

A. The syntheses of cis-$PtCl_2(Et_2S)_2$ and trans-$PtCl_2(Et_2S)_2$

Synthetic methods have been published (53) and compounds were made for the purpose of the investigation.

B. NMR measurements on the equilibrium between cis and trans-$PtCl_2(Et_2S)_2$

^1H NMR spectra were recorded on a Bruker AC-300 NMR spectrometer. Low temperature experiments were carried out on a Bruker WM-250 spectrometer operating at 250.132 MHz and on a Bruker AM-500 equipped with a variable-temperature probe. Single frequency decoupling experiments were performed and coupling constants were measured. Chemical shifts were referenced to tetramethylsilane.

Equilibrium constants for the cis to trans-$PtCl_2(Et_2S)_2$ isomerization were determined by ^1H NMR. The measurement of the equilibrium constant for the isomerization was at 298 K. Pure cis-$PtCl_2(Et_2S)_2$ and trans-$PtCl_2(Et_2S)_2$ were used as starting materials, respectively. The equilibrium constant was expressed as K, (K= [trans]/[cis]). The concentrations of cis and trans Pt complexes were determined by integration methylene resonances on Et_2S ligands of each complex in NMR spectrum. As the methylene resonances are not well

separated one from another, but are proportional to the concentration, the equilibrium constant was calculated by the formula (K=[b-a]/[2a], 2a=[cis], b=[trans + cis/2]). Both a and b were methylene proton resonances directly measured from NMR spectrum. The equilibrium mixtures were measured several times over two weeks until calculated constants no longer varied. The value of the equilibrium constant for cis $\rightleftarrows$ trans-$PtCl_2(Et_2S)_2$ isomerization in chloroform was 2.2. In comparison, the isomerization went much more quickly in benzene and took only about half as much time as it did in chloroform. The value of the equilibrium constant was 22.40 in benzene.

The kinetics of the cis $\rightleftarrows$ trans-$PtCl_2(Et_2S)_2$ isomerization has been previously investigated (54-55). Though the investigation of the cis to trans-$PtCl_2(Et_2S)_2$ isomerization had been studied for a long time, most of the reports were only concerned with the cis or trans Pt complexes themselves. Because of the instrumentation's limitations, some of the data about the complexes were not well characterized. Recently the study of the cis and trans Pt(II) complexes has shifted to mechanistic research, including oxidation-reduction pathways and synthetic availability of further platinum clusters. Hence, it is useful to summarize this part of the work as a reference to further study.

C. X-ray crystallographic determination of the structure of cis-$PtCl_2(Et_2S)_2$ and trans-$PtCl_2(Et_2S)_2$

The synthetic products from the reactions have different colors and crystalline shapes. The crystals of the cis-$PtCl_2(Et_2S)_2$ complex are greenish yellow and flake-like, while the crystals of the trans-$PtCl_2(Et_2S)_2$ are orange yellow and tiny needle-like. Both crystals have a metallic shining surface. Single crystals of these two complexes were picked up for x-ray crystallographic determination. Structures for both cis-$PtCl_2(Et_2S)_2$ and trans-$PtCl_2(Et_2S)_2$ complexes were solved. They were refined routinely following the standard procedure as described on pages 112 and 114.

Discussion

Platinum(II) complexes have been known for many years to have square-planar structures, but it is only in recent years that people began to realize their important role in organometallic and coordination chemistry studies. When we started the Pt cluster research, we found that the cis isomer was a ideal starting material for binuclear Pt(III) complex formation due to the labile metal-ligand interaction. Meanwhile, the cis to trans isomerization was observed and studied by NMR. Therefore, we intended to report the details about the cis and trans isomer structures in this part.

As early as 1888, Blondtrad (56) found that diethylsulfide united with platinum chloride to form a Pt(II) complex with a Pt-S bond. Klason (57) extended this observation and reformulated the structure of the product, in which platinum was quadrivalent. Neither author contemplated a planar configuration or gave satisfactory proof of the structure, although useful and accurate data were accumulated. It was not until Werner (58) attributed the isomerism to the presence of cis and trans-planar forms that it was recognized that platinum exhibited four coordination, as is universally accepted at the present time.

Although many square-planar Pt(II) compounds have been isolated in their cis and trans forms, only a few of them have an observable isomerization in solution. The first study on the cis $\rightleftarrows$ trans dichlorobis(dialkylsulfide) platinum(II) complexes occurred in 1930 (59) when Angell and Drew observed qualitatively that a cis $\rightleftarrows$ trans isomerization took place in alcohol. Studies on the thermodynamics of this process were reported in 1952 (60), in which a comparison of equilibrium between cis- and trans-$(MEt_3)_2PtCl_2$ where M=P, As, Sb. In this paper, the thermodynamic data for the system were collected and the steric effect of the ligands in the cis position was discussed. In 1970, cis-bis(trialkylphosphine)dichloro-platinum(II) was studied kinetically for the cis $\rightleftarrows$ trans isomerization and the

investigator of this paper postulated that the isomerization took place through the pseudorotation of the phosphine group in a five-coordinate intermediate and the cis ⇄ trans isomerization was catalysed by free phosphine (61). Meanwhile, extensive studies of these platinum-phosphine complexes gave conclusive evidence for the mechanism which required two consecutive steps to effect the cis ⇄ trans isomerization, involving an ionic intermediate and known ligand trans effect. At the early 70's, there was no clear reason for invoking the pseudorotation mechanism for cis ⇄ trans isomerization. Almost at the same time, proton NMR was first used to study the cis ⇄ trans dichlorobis(dialkyl-sulfide)platinum(II) complexes and the mechanism of the inversion at sulfur was first reported [19](62).

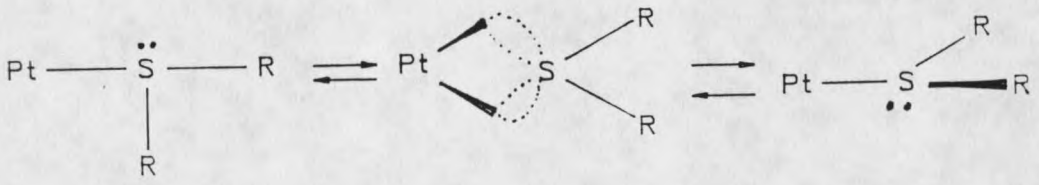

[19]

The observation that the retention of Pt-S-C-H coupling above the coalescence temperature is consistent with the proposal that the inversion process is really an internal displacement of one sulfide electron pair by another sulfide electron pair in a rearrangement mechanism involving pentacoordinate configuration, since bond weakening and bond strengthening are involved. In the isomerization, there is

no sign for the loss of Pt-S-C-H, thus dissociation of the sulfide ligand is impossible. Thus, a reasonable hypothesis is that there is bonding to both sulfur unshared electron pairs so that the platinum atom has a distorted pentacoordinate configuration or an inversion through a partially dissociated state. In this report, the vicinal platinum-proton coupling constants in the cis and trans forms were calculated (62). Several years later, the cis ⇄ trans bis(dialkylsulfide) dihaloplatinum(II) reaction was studied again using ^1H NMR. Different ΔH, ΔS, ΔG and corresponding equilibrium constants were measured. The mechanism for the cis ⇄ trans isomerization of bis(dialkylsulfide)-platinum(II) complex was proposed as a double displacement [20] (55).

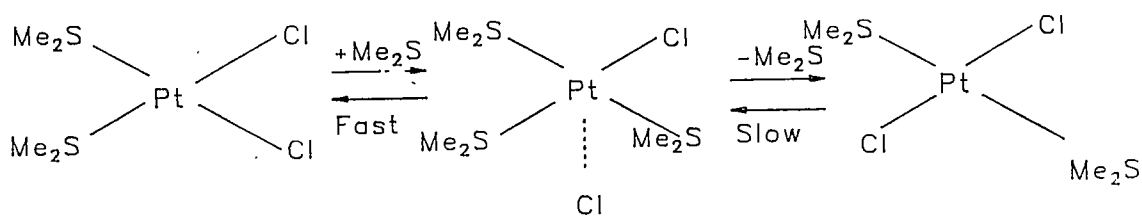

[20]

In recent years, study focused on the isomerization has been transferred to cis ⇄ trans-$PtCl_2(Et_2S)_2$ and isomer reactivities; the availability of an oxidative addition pathway has been discovered. Cis-$PtCl_2(Et_2S)_2$, with the addition of mesityllithium, produced trans-$PtCl_2(Mes)(Et_2S)_2$ (Mes=2, 4, 6 trimethyl phenyl). With the addition of LiBr,

the reaction is accelerated and $Pt(Br)(Mes)(Et_2S)_2$ was obtained (63).

The mechanism of the conversion from cis-$PtCl_2(Et_2S)_2$ to trans-$PtBr(Mes)(Et_2S)_2$ involved the nucleophilic substitution of halide by a mesityl anion and substitution of a chloro ligand by a bromide ligand (63).

Trans-PtX_2L_2(X=Cl, Br; L=Et_2S, Et_2Se) reactions with phenyl, O-tolyl were reported in the early 70's (65). As the bonding between a sulfide ligand and Pt(II) ion is fairly labile, a sulfide group could easily be replaced by other ligands like phosphine, pyridine and carbonyl groups (64). Hence Pt(II) complex with sulfide ligands is a useful precursor of various organoplatinum complexes. It was also reported that cis-$PtCl_2(Et_2S)_2$ is an important starting material for the synthesis of a series of binuclear platinum(III) complexes (52). Earlier work supplied a lot of information about this type of complex, but because of the instruments' limitations (e.g. low sensitivity of NMR and shortage of structure data), there are still quite a few points which have not been explained. It was our goal to collect accurate thermodynamic and kinetic data for the cis $\rightleftarrows$ trans-$PtCl_2(Et_2S)_2$ process and to structure the complexes in order to improve the synthesis.

^1H NMR data showed (Figures 1-2) that the cis-$PtCl_2(Et_2S)_2$ has the two quintet and one triplet resonances in the spectrum due to the sterically nonequivalent

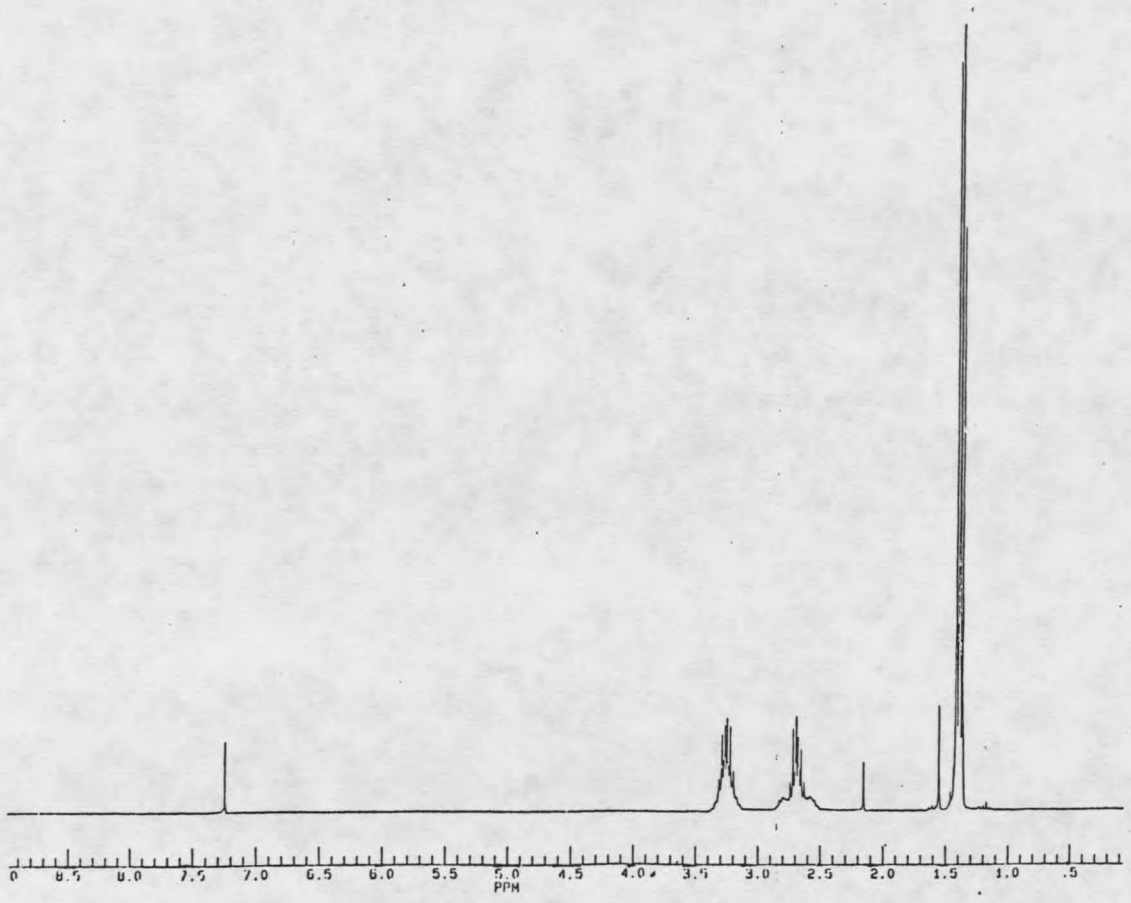

Figure 1. ^{1}H NMR spectrum of cis-$PtCl_2(Et_2S)_2$

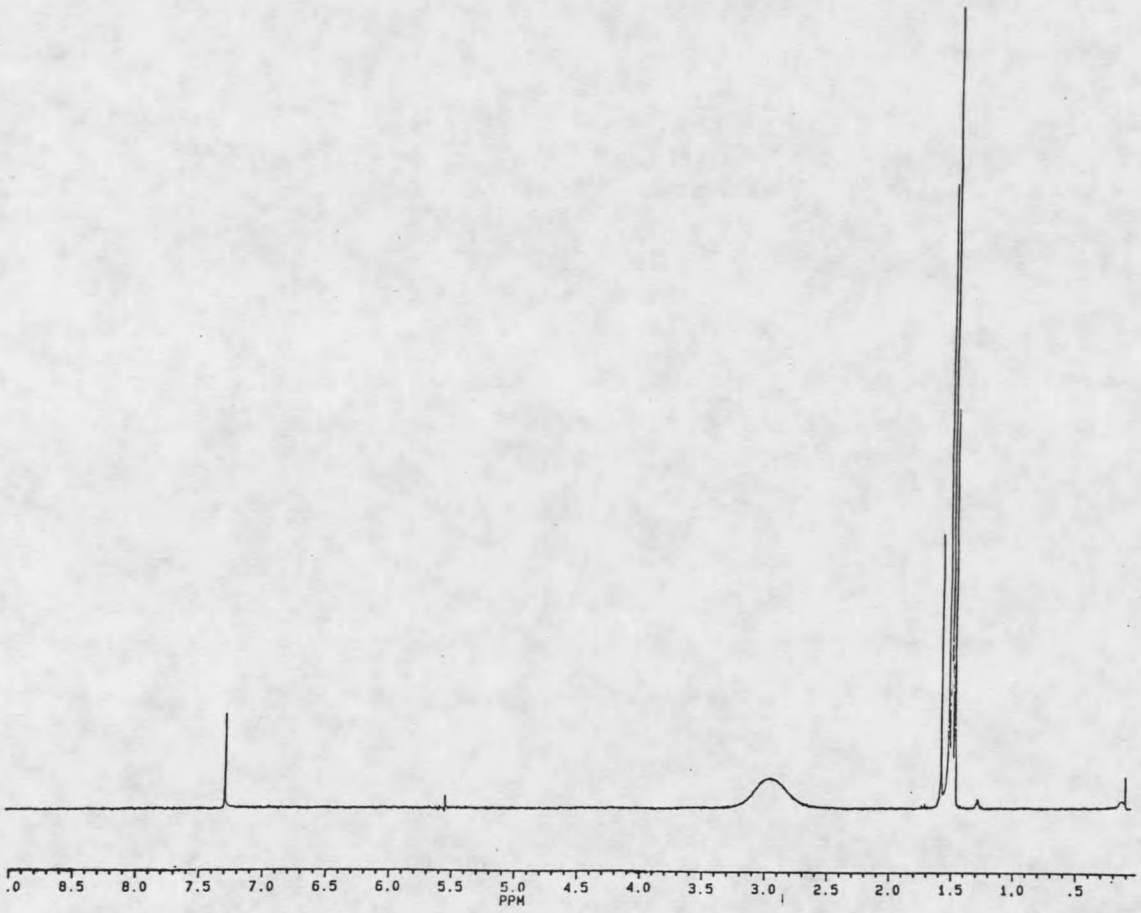

Figure 2. ^{1}H NMR spectrum of trans-$PtCl_2(Et_2S)_2$

methylene protons and equivalent methyl protons of coordinated diethylsulfide. Trans-$PtCl_2(Et_2S)_2$ showed a broad unresolved resonance in methylene region at room temperature in the spectrum. This broad resonance was caused by the methylene protons, as methylene groups in trans-$PtCl_2(Et_2S)_2$ were fluxional on the NMR time scale. Once the temperature of the experiment was lowered, the fluxionality rate of the $-CH_2-$, which was either caused by the methylene protons' rotation around S-C1-C2 axis or by the inversion at the sulfur, was slowed down; therefore one could observe the nonequivalent $-CH_2-$ resonances in the spectrum (Figure 3).

The proton single frequency decoupling experiment not only helps to determine the relation between one proton and another, but it also determines the coupling constant which indicates the interaction between the nuclei. From the decoupling data, we determined that the Pt-H coupling constant is much larger than the H-H coupling, indicating the strong interaction with the heavy atom (Figures 4-5, Table 1). We also notice that coupling constant of cis complex is always larger than that of trans complex. The explanations are based on the coupling through σ and π bond. In this case, the amount of π bond between Pt-S is small. Therefore the larger coupling constant of the cis isomer must have a larger amount of σ bond between Pt-S, so the bond strength between Pt-S increases which also means that

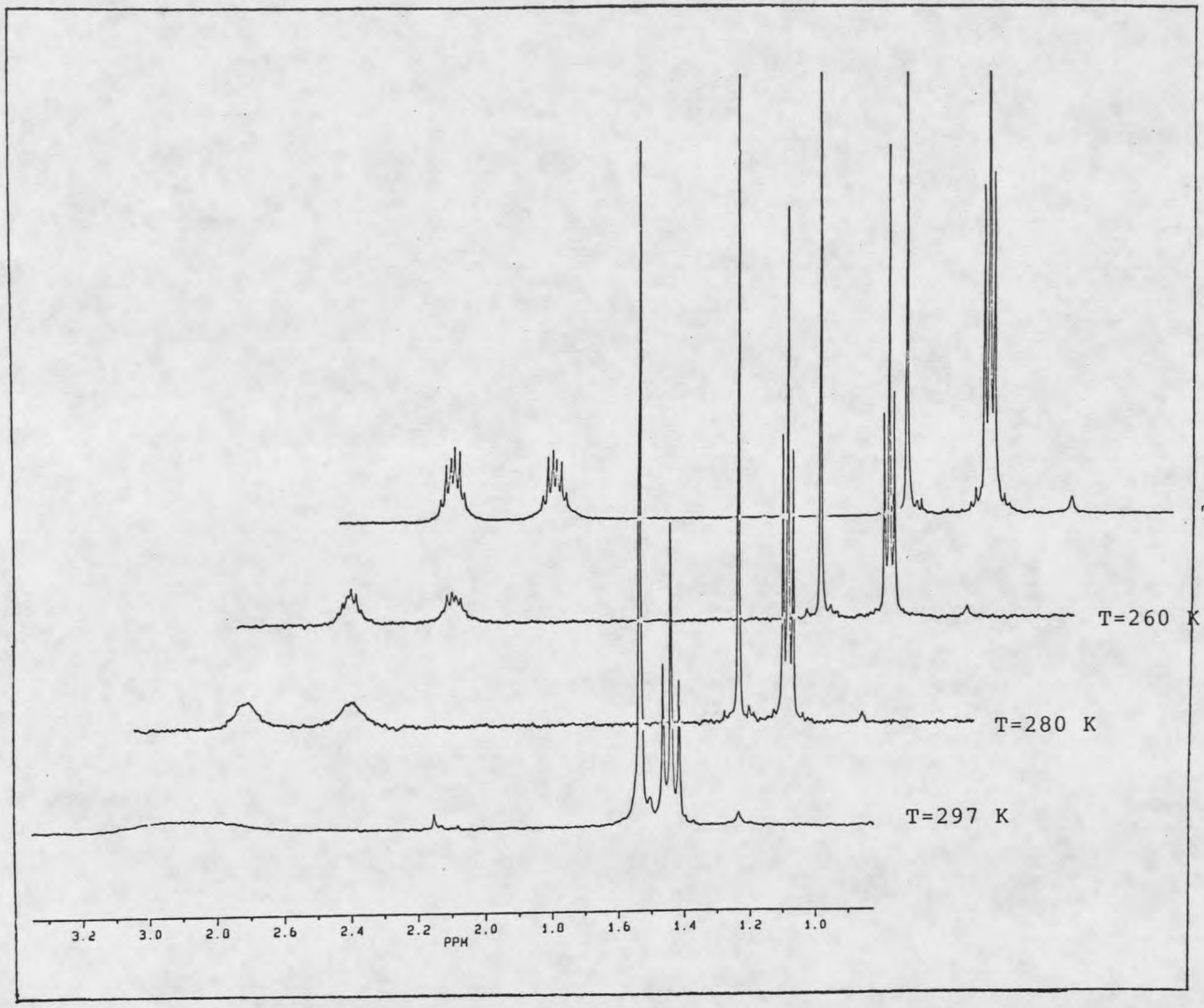

Figure 3. ^{1}H NMR spectra of trans-$PtCl_2(Et_2S)_2$ at different temperatures

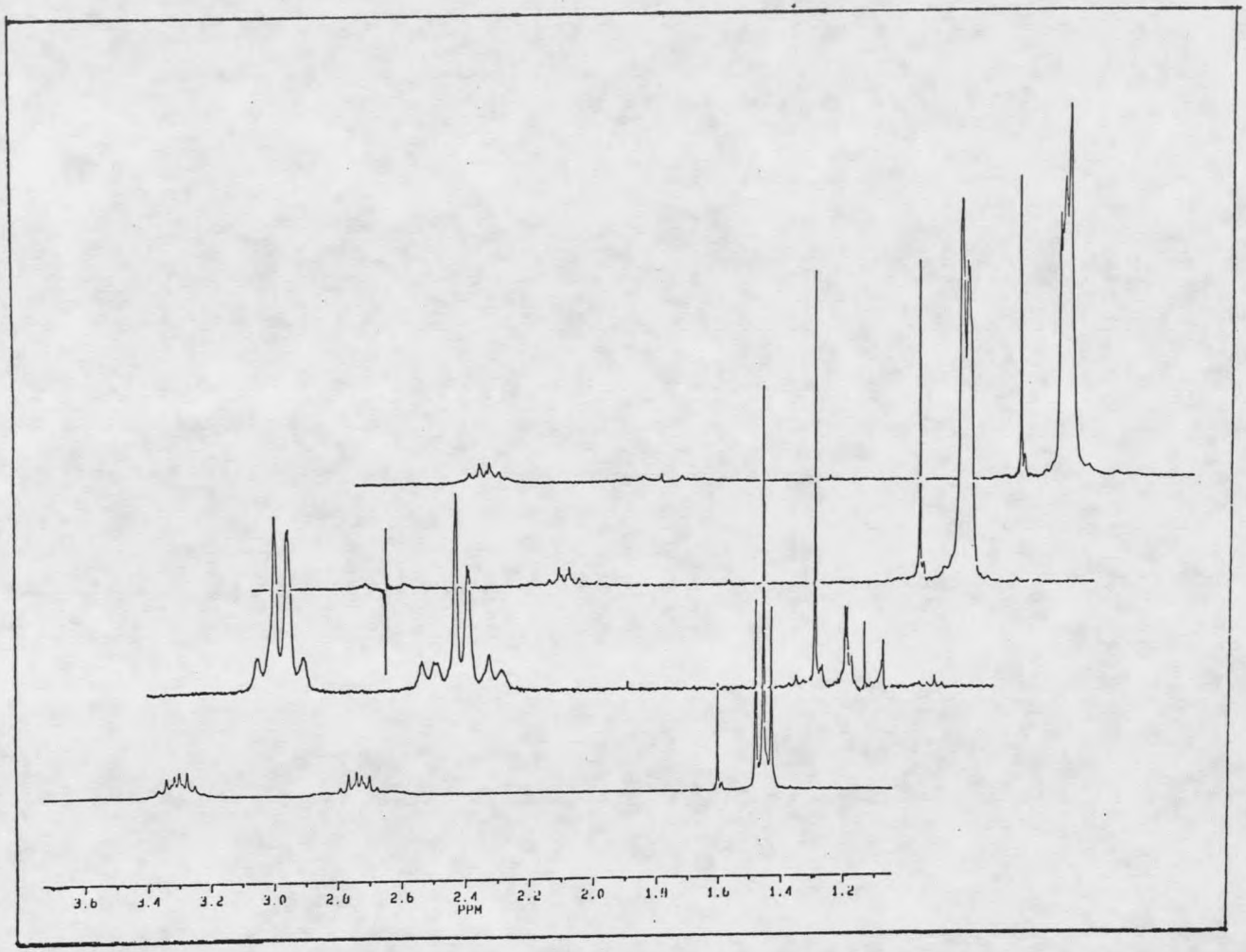

Figure 4. ^1H NMR spectra of decoupling of cis-$PtCl_2(Et_2S)_2$

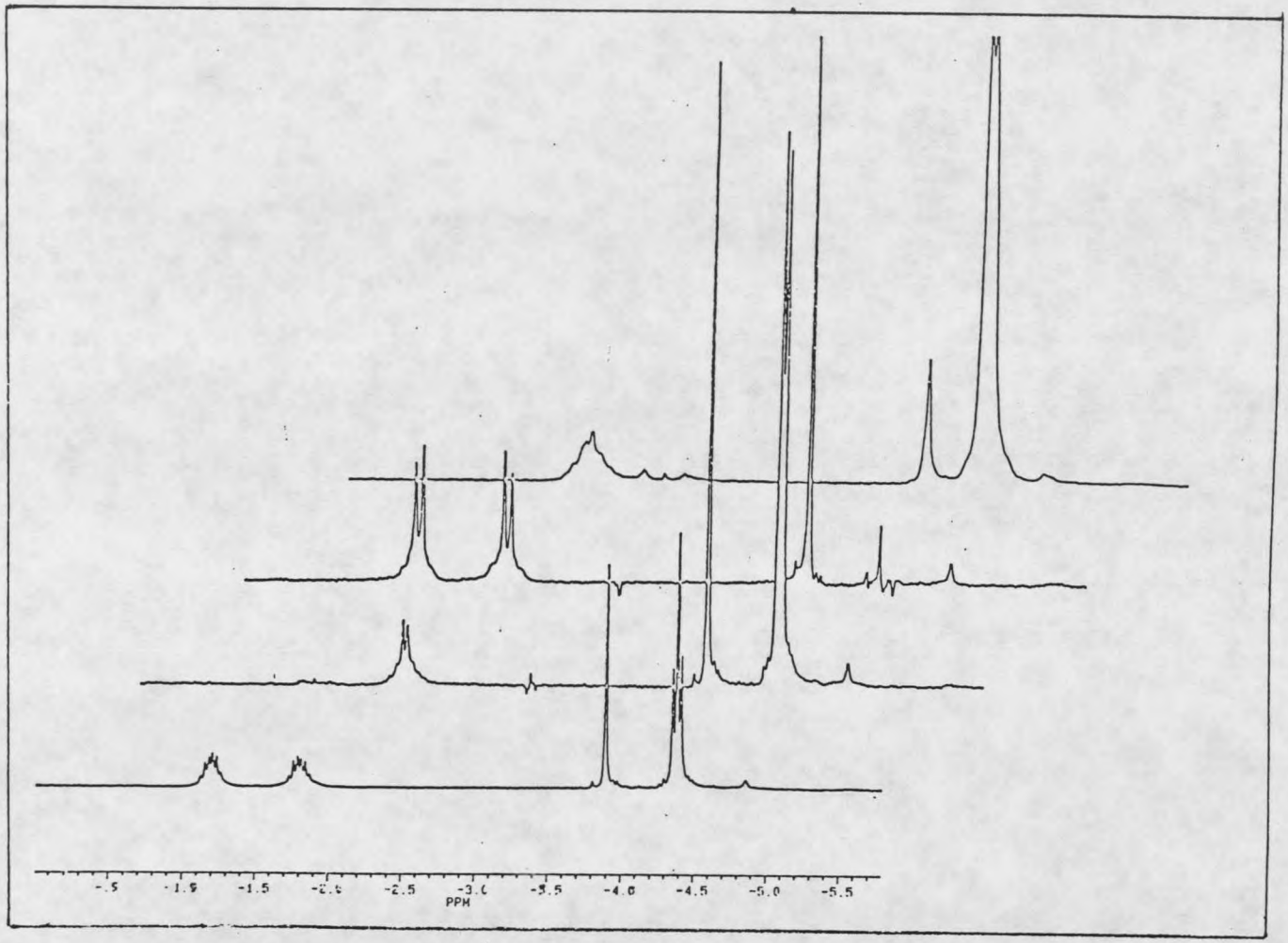

Figure 5. ^{1}H NMR spectra of decoupling of trans-$PtCl_2(Et_2S)_2$

Table 1. Coupling constants for cis-$PtCl_2(Et_2S)_2$ and trans-$PtCl_2(Et_2S)_2$

	cis-$PtCl_2(Et_2S)_2$	trans-$PtCl_2(Et_2S)_2$
J_{ab}*	11.4 Hz	7.6 Hz
J(Pt-a)	63.8 Hz	38.8 Hz
J(Pt-b)	34.3 Hz	28.5 Hz
J(a-CH_3)	9.5 Hz	7.9 Hz
J(b-CH_3)	6.6 Hz	6.3 Hz

* a and b refer to the methylene protons on Et_2S.

Et_2S is a better ligand in the cis isomer than in trans isomer. The equilibrium constant varies with solvents. Equlibrium constants were measured for $CDCl_3$ and C_6D_6. Isomerization also occurred in acetone, resulting in a unclear spectrum. Besides cis-$PtCl_2(Et_2S)_2$ was quite soluble in methanol and quite insoluble in hexane. Those results could indicate that cis-$PtCl_2(Et_2S)_2$ has considerable polarity.

From the equilibrium constant data, it was concluded that cis $\rightleftarrows$ trans-$PtCl_2(Et_2S)_2$ isomerization tended to go to less-polar trans-$PtCl_2(Et_2S)_2$ in less polar media. Because C_6D_6 is less-polar than $CDCl_3$, the equilibrium constant in C_6D_6 is 10 times larger than that in $CDCl_3$.

X-ray crystallography was used to characterize cis- and trans-$PtCl_2(Et_2S)_2$ structures. Both structures show a Pt-S bond length of 2.226-2.301 Å, similar to the Pt-S bond length in Pt(III) complex with Et_2S in an axial position

(2.292-2.303 Å). One might think that the trans-$PtCl_2(Et_2S)_2$ should be non-polar due to the symmetry of the complex. But it turns out from structure characterization that since the four $-C_2H_5-$ groups lie on the same side of the plane containing platinum, chlorine, and sulfur atoms, the trans complex keeps certain polarity as had been previously determined (2.41 D for trans isomer, 9.5 D for cis isomer (58)).

Finally the rate of cis to trans-$PtCl_2(Et_2S)_2$ isomerization, despite the different postulated mechanisms, is directly related to the solvent, because different solvents change the rate of the reaction. The solvent effect on the isomerization is nevertheless related to the ligand substitution. As the enthalpy of the formation of trans-$PtCl_2(Et_2S)_2$ is positive (ΔH=15 kcal/mole), thus the cis to trans process is quite endothermic. ΔH for the internal bond strength change and ΔH of solvation are the two major contributions to this enthaply term. As sulfide ligands have a larger trans-effect than chloro groups, the isomer which allows the greater amount of Pt-sulfur π back donation would have the larger overall bond strength, simply because the isomer with more efficient π bonding would have the greater total bond strength. This is the cis-Pt isomer in which the sulfides ligands are trans to the chloro ligands. As for the ΔH of solvation, the dipole-dipole interaction between the complex and the solvent are greater

in the more polar cis-Pt complex than in the less-polar trans-Pt isomer (55).

For the entropy of the process, obtaining a positive ΔS (3 eu) would favor the trans-Pt(II) complex, since the cis-Pt(II) complex would have more associated solvent molecules than the less-polar trans Pt complex due to the stronger interaction between cis-$PtCl_2(Et_2S)_2$ and the solvent. The rate determining step of the isomerization has been claimed to be the formation by a slow substitution of one chloride by a sulfide, followed by the fast substitution of one of the two sulfides trans to each other by a chloride (55).

It is up to this point that cis $\rightleftarrows$ trans-$PtCl_2(Et_2S)_2$ isomerization has been studied.

THE THERMODYNAMIC AND KINETIC STUDIES ON SOME OF THE BINUCLEAR PLATINUM(III) COMPOUNDS

Experimental

A. Syntheses of the binuclear Pt(III) compounds

The preparation of a series of platinum(III) complexes for the purpose of this investigation has been described (52). These binuclear Pt(III) compounds include Pt(HPy) (HH and HT), Pt(FHPy) (HH and HT), Pt(CHPy) (HH) and Pt(MHPy) (HH).

B. NMR measurements

The NMR assignments on these binuclear Pt(III) compounds were carried out with a Bruker WM-250 operating at 250.132 MHz for proton spectroscopy, 62.80 MHz for carbon-13 and 53.518 MHz for platinum-195. Chemical shifts are referred to tetramethylsilane for proton and carbon-13 spectra. For platinum-195, the standard is 1 M H_2PtCl_6. Nuclear Overhauser enhancements were measured by the difference method. All solvents were bought from Aldrich and used without further purification.

C. NMR spectral assignments for a series of Pt(III) compounds

The molecular structures of the series of binuclear Pt(III) compounds have been elucidated (52). There are two kinds of structures for some of the Pt(III) compounds, one

is known as head to head (HH) or the polar Pt(III) complex, another is known as head to tail (HT) or the non-polar Pt(III) complex. The differences between HH and HT are whether the axial positions are occupied by one ligand or two ligands and the coordination around each Pt as described on page 21. There is an interconversion between HH and HT when addition or removal of axial ligands happens. The proton NMR assignments for these Pt(III) compounds are listed in Tables 2-7 and the NMR spectra are shown in Figures 6-11. Protons on the hydroxypyridine ligands were readily assigned by comparison of the unsubstituted complex with the 6-substituted complexes. The 5-H on the hydroxypyridine ligand is a multiplet in the former case but is a doublet in the latter case. The 3 and 4-H's are the remaining doublet and triplet, respectively. Single frequency decoupling and a COSY experiment confirmed these assignments.

D. Equilibrium constant measurement on the HH ⇌ HT interconversion

The equilibrium constant for the HH ⇌ HT binuclear Pt(III) compounds interconversion has been determined by proton NMR. The equilibrium between HH to HT is expressed as:

$$\text{Pyridine} + \text{HH} \rightleftharpoons \text{HT}$$

The equilibrium constant is $K = [HT]/\{[HH]x[Py]\}$. The measurement starts with the addition of free pyridine to the

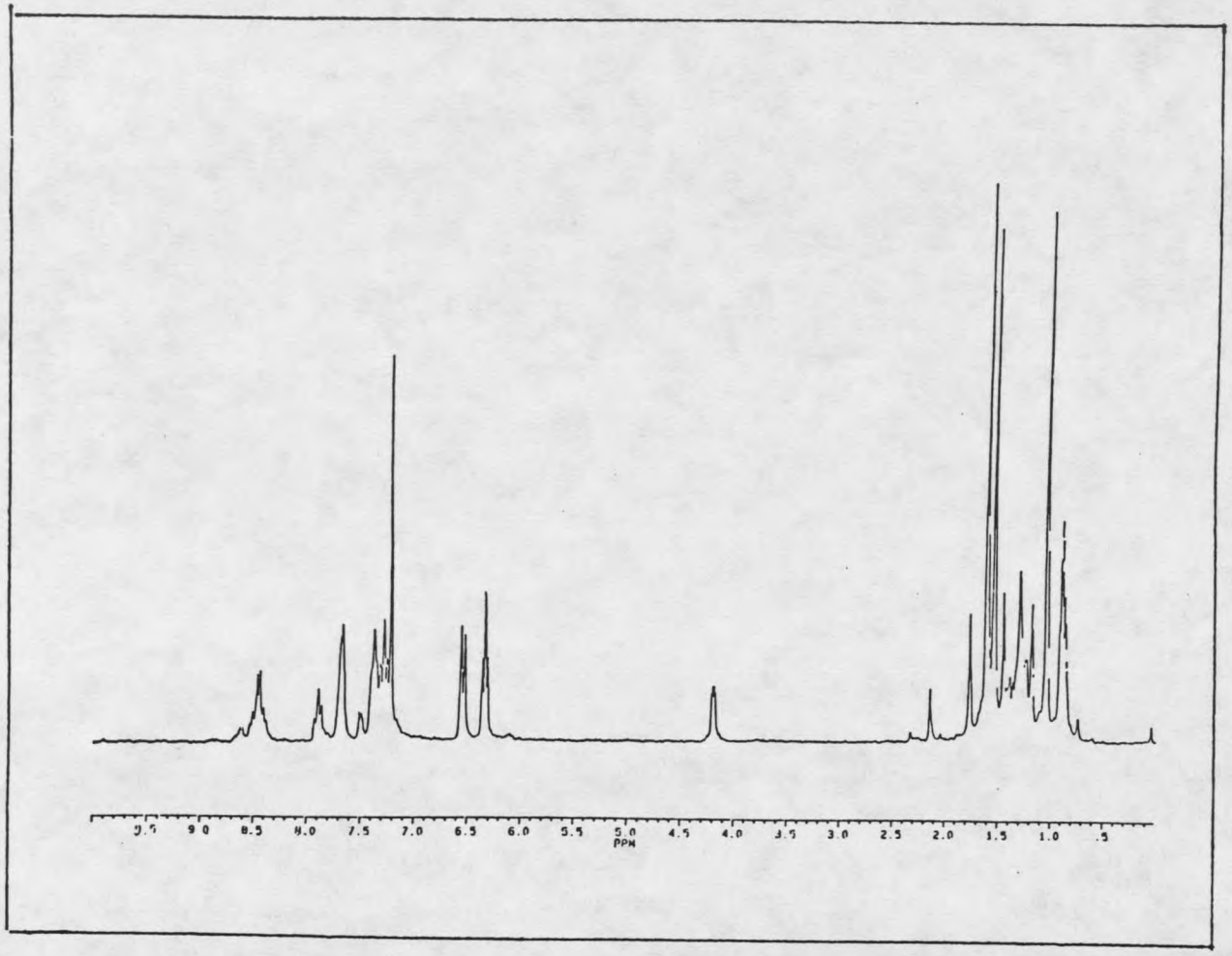

Figure 6. ^{1}H NMR spectrum of $Pt_2(CH_3)_4(HP)_2(Py)$

Table 2. ^{1}H NMR assignments for $Pt_2(CH_3)_4(HPy)_2(Py)$

Chemical shift (ppm)	Assignment	Coupling constant (^{2}J Pt-CH_3)
1.05	CH_3(I)	72.1 Hz
1.62	CH_3(II)	80.5 Hz
6.35	5-H	
6.56	3-H	
7.30	4-H	
7.40	6-H	
7.24	$CDCl_3$	
7.70	ß H-pyridine	
7.92	γ H-pyridine	
8.47	α H-pyridine	

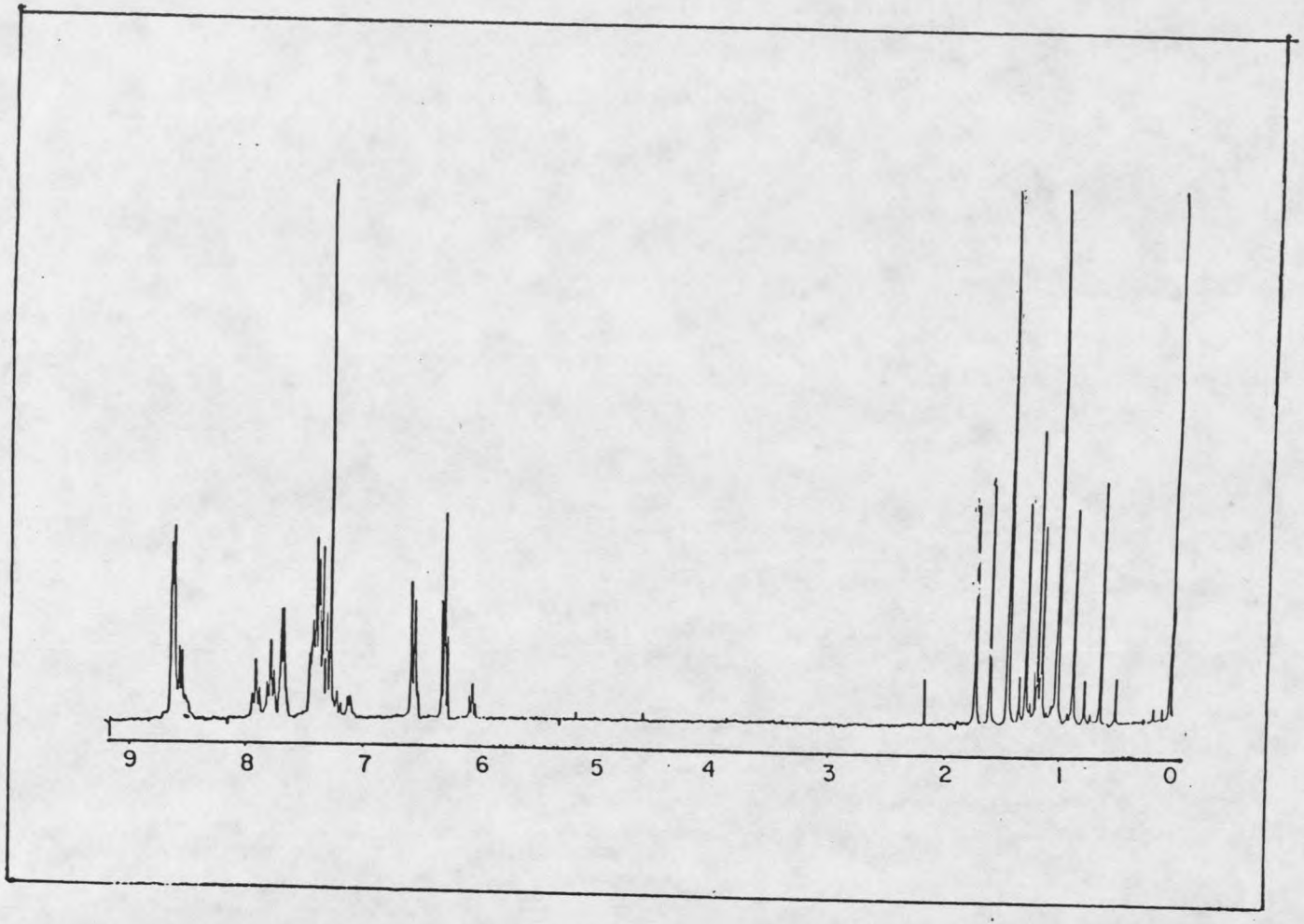

Figure 7. ^{1}H NMR spectrum of $Pt_2(CH_3)_4(HP)_2(Py)_2$

Table 3. ^{1}H NMR assignments for $Pt_2(CH_3)_4(HPy)_2(Py)_2$

Chemical shift (ppm)	Assignment	Coupling constant (^{2}J Pt-CH_3)
0.64	CH_3(I)	69.9 Hz
1.16	CH_3(II)	78.7 Hz
5.72	5-H	
7.22	4-H	
7.36	3-H	
7.24	$CDCl_3$	
7.40	ß H-pyridine	
7.85	γ H-pyridine	
8.70	α H-pyridine	

* Note 6-H not observed

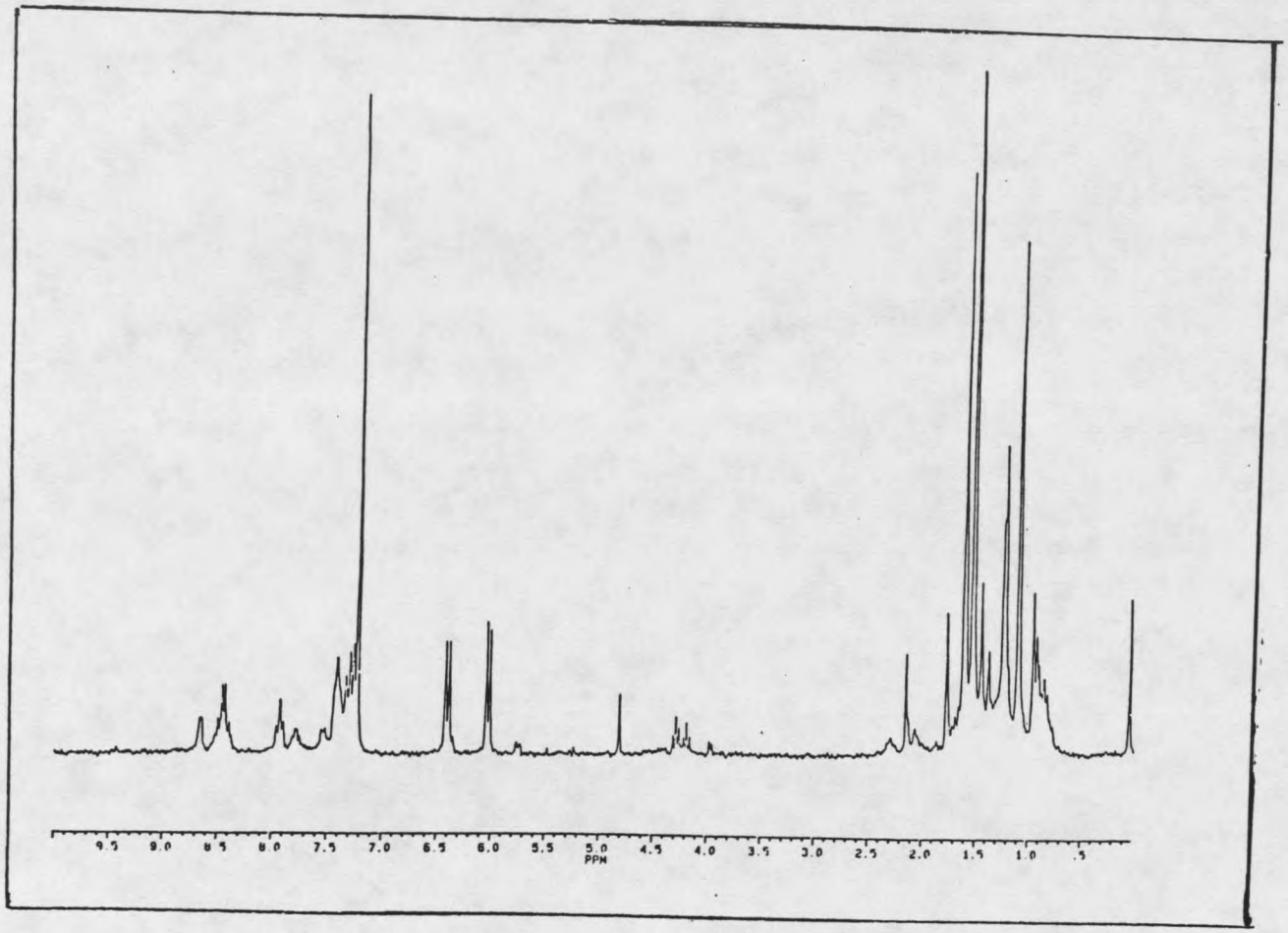

Figure 8. ^{1}H NMR spectrum of $Pt_2(CH_3)_4(FHP)_2(Py)$

Table 4. ^1H NMR assignments for $Pt_2(CH_3)_4(FHPy)_2(Py)$

Chemical shift (ppm)	assignment	Coupling constant (^2J Pt-CH_3)
1.11	CH_3(I)	69.8 Hz
1.77	CH_3(II)	79.3 Hz
6.07	5-H	
6.43	3-H	
7.26	4-H	
7.24	$CDCl_3$	
7.30	ß H-pyridine	
7.80	γ H-pyridine	
8.46	α H-pyridine	

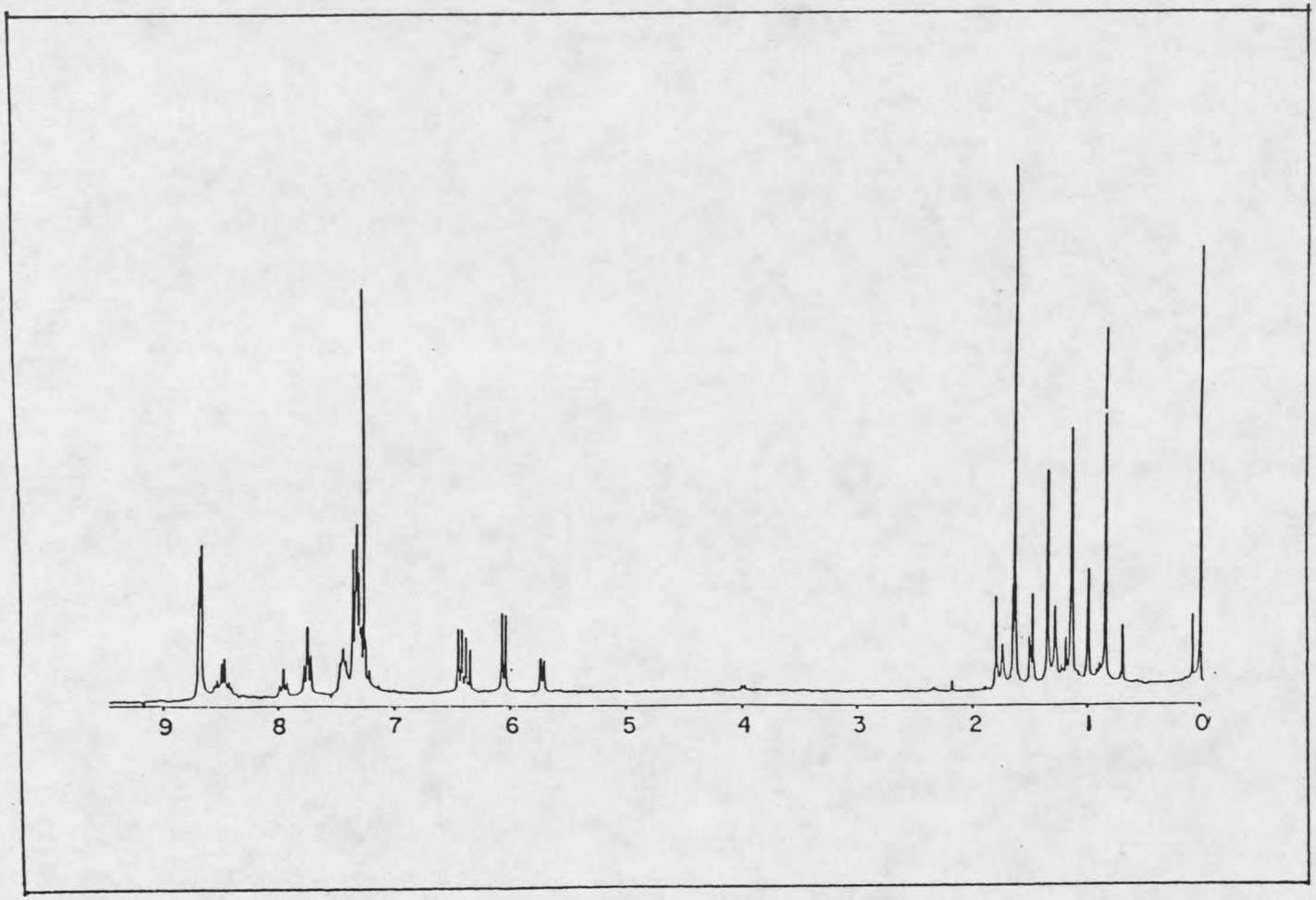

Figure 9. ^{1}H NMR spectrum of $Pt_2(CH_3)_4(FHP)_2(Py)_2$

Table 5. ^{1}H NMR assignments for $Pt_2(CH_3)_4(FHP_y)_2(Py)_2$

Chemical shift (ppm)	Assignment	Coupling constant (^{2}J Pt-CH_3)
1.13	CH_3(I)	80.5 Hz
1.61	CH_3(II)	72.6 Hz
5.69		
5.73	5-H	
6.34		
6.38	3-H	
7.30	4-H	
7.24	$CDCl_3$	
7.45	ß H-pyridine	
7.74	γ H-pyridine	
8.52	α H-pyridine	

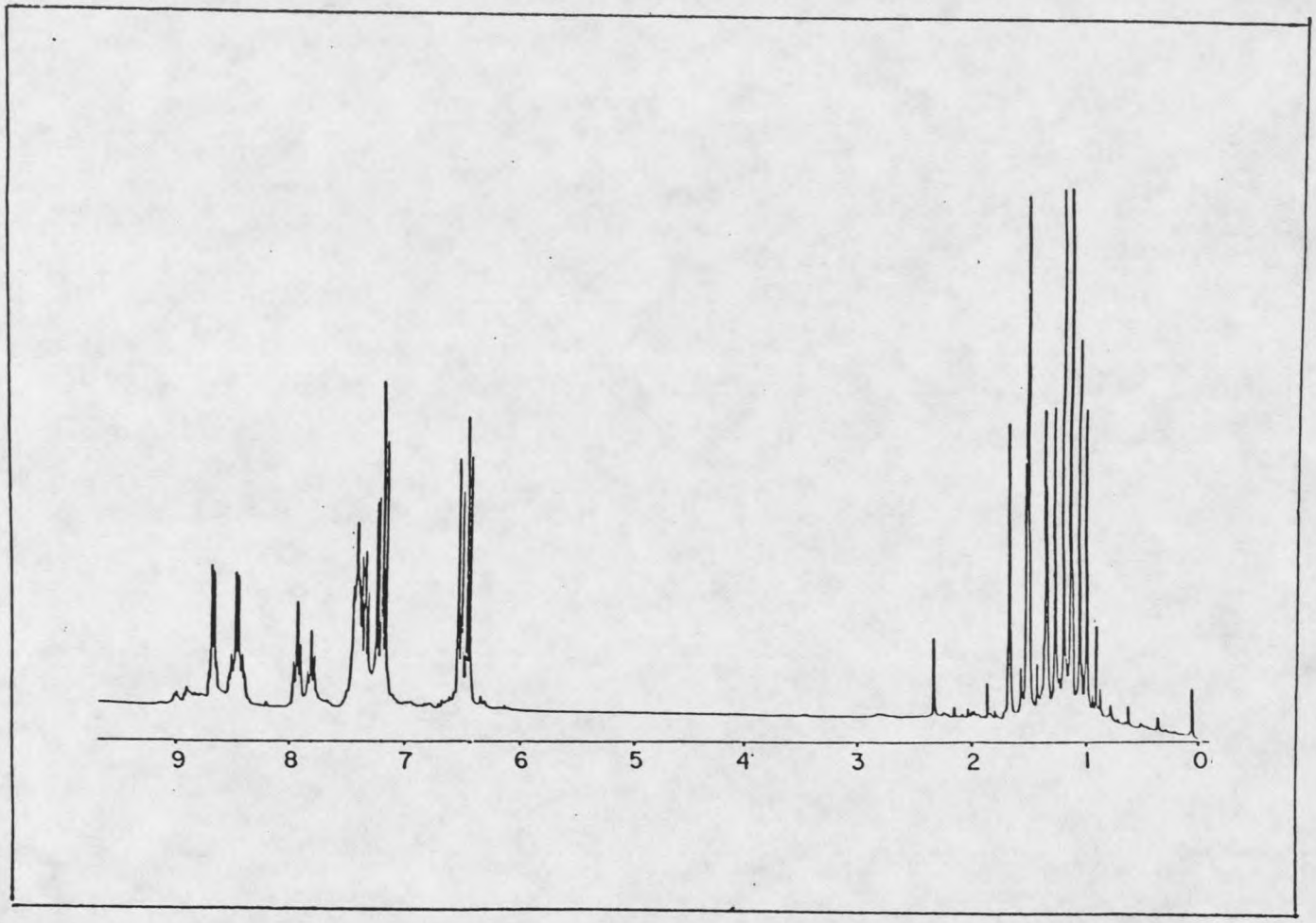

Figure 10. ^{1}H NMR spectrum of $Pt_2(CH_3)_4(CHPy)_2(Py)$

Table 6. ^{1}H NMR assignment for $Pt_2(CH_3)_4(ClHPy)_2(Py)$

Chemical shift (ppm)	Assignment	Coupling constant (^{2}J Pt-CH_3)
1.15	CH_3(I)	70.2 Hz
1.46	CH_3(II)	79.6 Hz
6.40	5-H	
6.45	3-H	
7.14	4-H	
7.24	$CDCl_3$	
7.36	ß H-pyridine	
7.88	γ H-pyridine	
8.40	α H-pyridine	

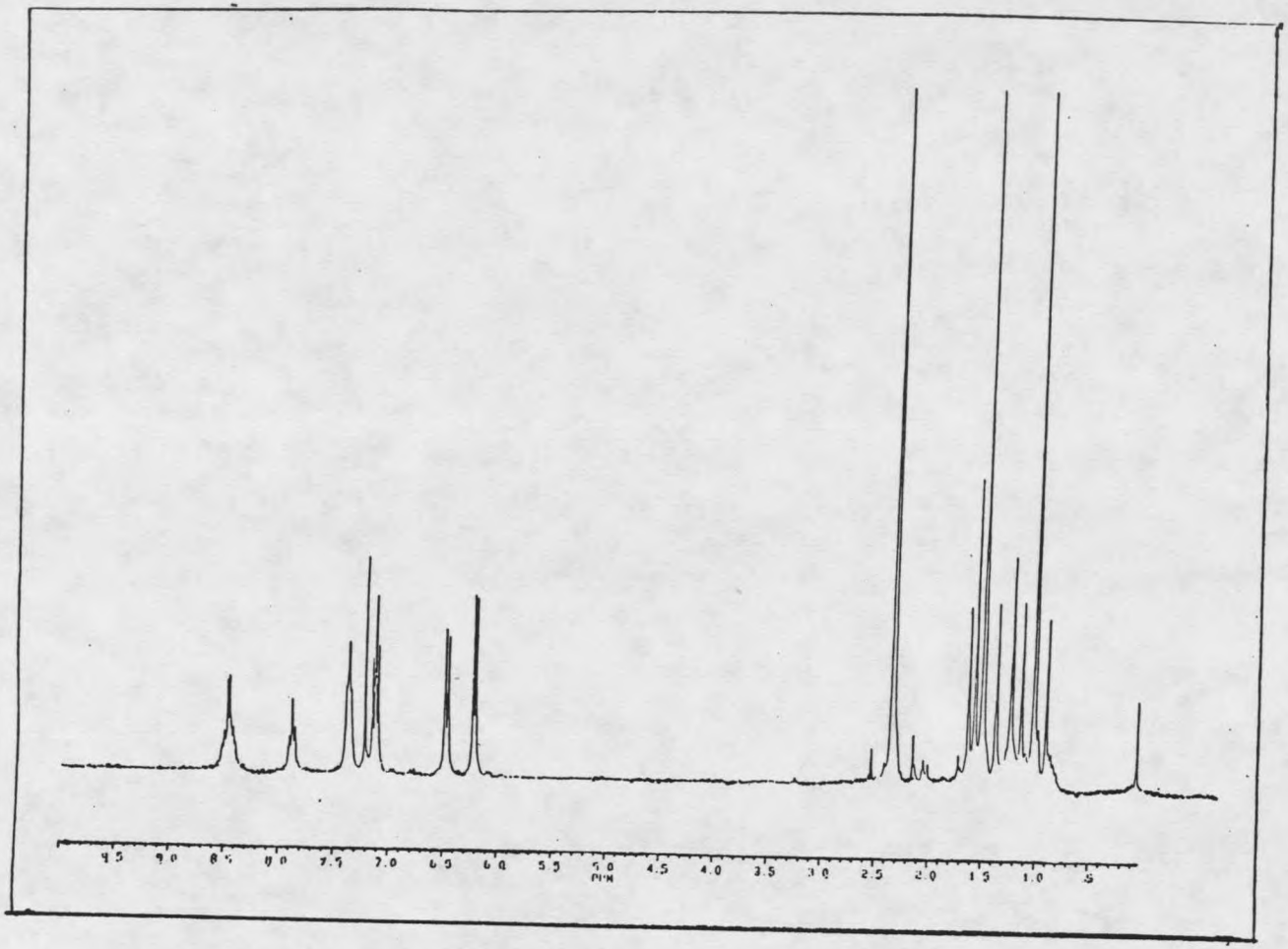

Figure 11. ^{1}H NMR spectrum of $Pt_2(CH_3)_4(MHPy)_2(Py)$

Table 7. ^1H NMR assignments for $Pt_2(CH_3)_4(MHPy)_2(Py)$

Chemical shift(ppm)	Assignment	Coupling constant (^2J Pt-CH_3)
1.03	CH_3(I)	69.8 Hz
1.50	CH_3(II)	79.3 Hz
2.36	CH_3 on the ring	
6.23		
6.25	5-H	
6.48		
6.52	3-H	
7.15	4-H	
7.24	$CDCl_3$	
7.39	ß H-pyridine	
7.91	γ H-pyridine	
8.49	α H-pyridine	

Pt(III) compound (HH), or through dissociation of pure HT isomers into equilibrium mixtures of HH complex and free pyridine. The HT complex is in fast exchange with free pyridine while the HH complex is in slow exchange with the pyridine, leading to different pyridine resonances in the NMR spectra.

Integration of the α proton resonance on the axial coordinated pyridine gives the measure of ratio of HH complex to the HT complex plus the free pyridine. The 5-H proton resonance on the oxo-pyridonate bridge of the HH complex is well separated from the one of the HT, so integration of that region gives the ratio of the HH to HT. An understanding of the total Pt(III) complex concentration makes it possible to calculate all relevent concentrations from these equations:

[HH] / [HT] = ratio

[HH] + [HT] = known concentration

The interconversion between HH ⇌ HT reaches equilibrium slowly, hence the Pt(III) sample was kept in a water bath at constant temperature and measured periodically. The equilibrium constant was measured at different pyridine concentrations and at different temperatures. The data, (Table 8), indicated the interconversion between HH ⇌ HT thermodynamically favors the HT state. Equilibrium constants and thermodynamic parameters for Pt(FHPy) are tabulated in Table 8. Spectra are shown in Figures 12-13.

The size of the substituent on the oxopyridonate bridge determines whether the HH ⇌ HT interconversion happens or not. Addition of pyridine to the Pt(HPy) and Pt(FHPy) (both are HH) complexes resulted in the progressive conversion to the HT isomer. Addition of free pyridine to the Pt(MHPy) (HH) and Pt(ClHPy) (HH) resulted in no detectable formation of the HT Pt(III) complex even after several months. Comparison of the size of the substituents on bridging ligand from x-ray crystallographic data indicates that pyridine can interact sterically with the substituent. Larger substituents are able to block the portion that pyridine uses to coordinate with the platinum ion, while smaller substituents do not hinder this pathway for bonding.

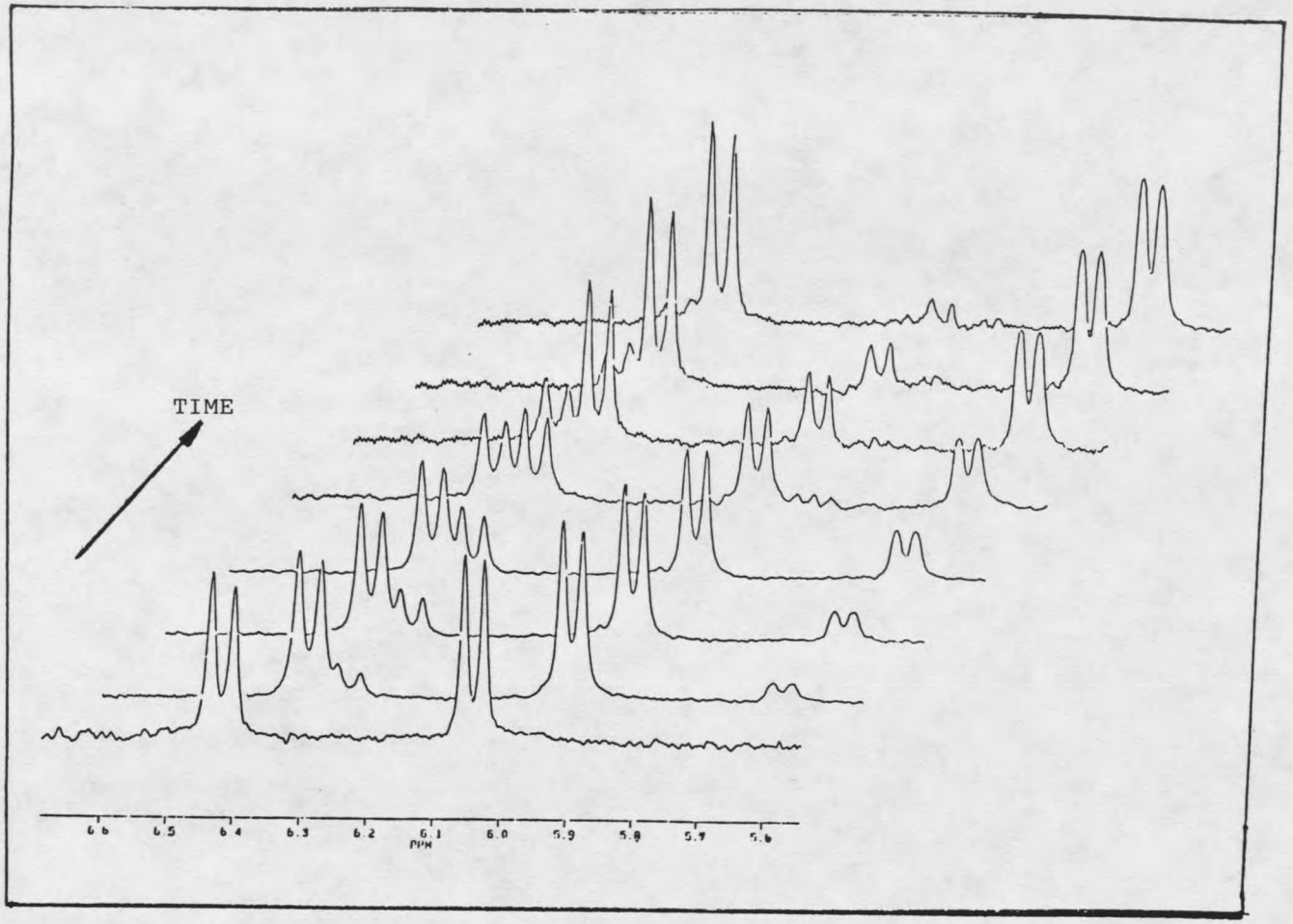

Figure 12. ^{1}H NMR spectrum of Pt(FHPy) HH $\rightarrow$ HT

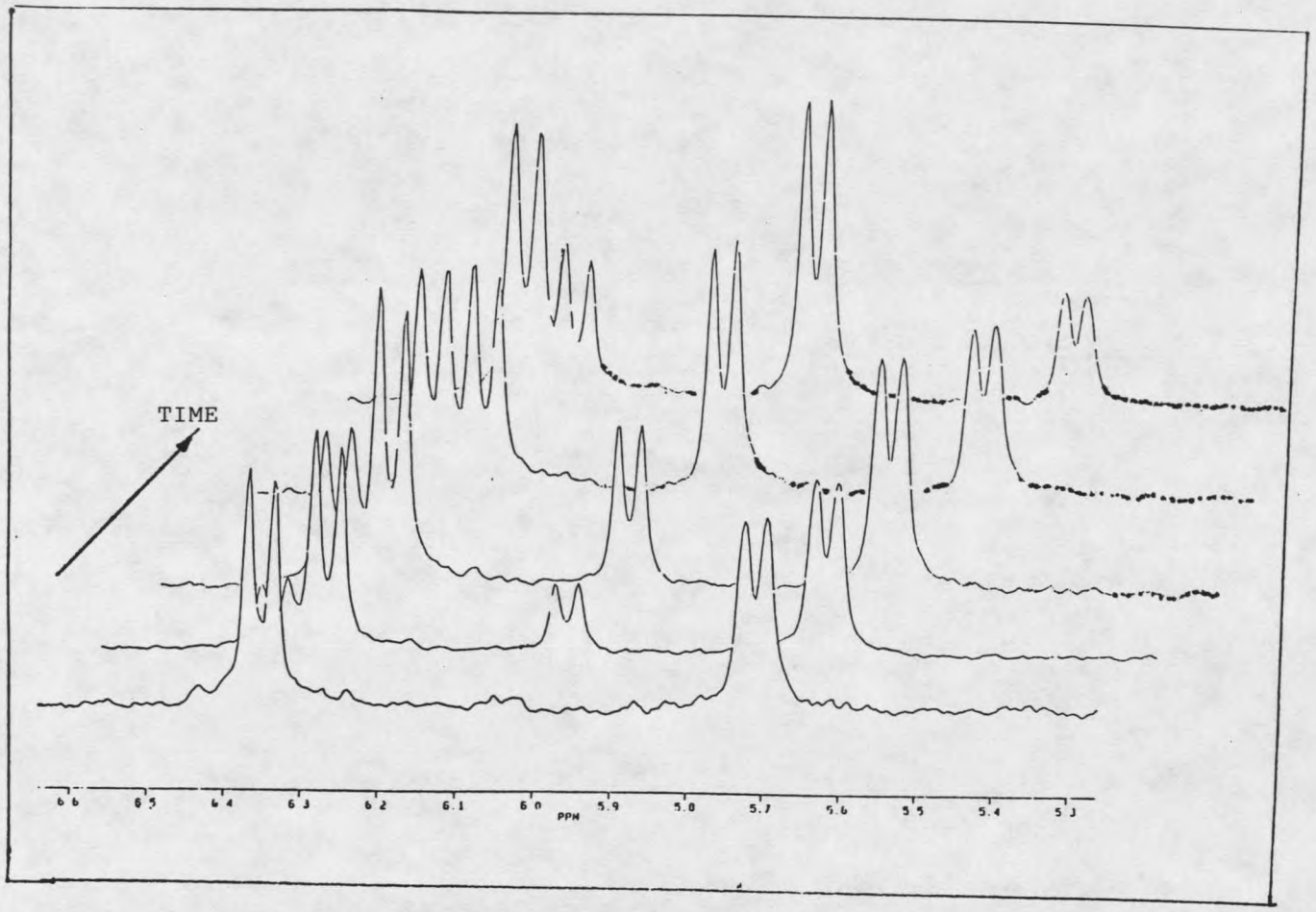

Figure 13. ^{1}H NMR spectrum of Pt(HPy) HH $\rightarrow$ HT

Table 8. Equilibrium constant and thermodynamic parameters for Pt(FHPy) HH $\rightleftarrows$ HT

[a]Equilibrium constant K (M^{-1})	[P_y] (M)
26	0.173
24	0.320
21	0.375
27	0.468

K (M^{-1})	[b]ΔG° (kJ./Mol)	Temperature (K)
26	-8.0	296
20	-7.6	307
15	-7.2	318

ΔS°= -38 J./(K. Mol.) ΔH°= -19 kJ./Mol.

a. Temperature = 298 K; standard deviation is ±2.

b. $\Delta G^\circ = -RTLn(K)$

E. Kinetic study of the binuclear Pt(FHPy) HH $\rightleftarrows$ HT interconversion

The kinetic study on the HH $\rightleftarrows$ HT interconversion for Pt(FHPy) was conducted by proton NMR spectroscopy. The sample of Pt(FHPy) (HH) was kept in a constant temperature water bath and different concentrations of pyridine added into the sample dissolved in $CDCl_3$. Rate constants were derived and calculated based on the integration ratio of the HH/HT resonance from NMR measurements. The temperature dependence of this interconversion was also determined. $\Delta S^{\neq}$

and $\Delta H^{\neq}$ values of the reaction were calculated based on the microscopic reversibility principle and Eyring plot (Table 9).

Discussion

Tables 1-6 present the chemical shift and coupling constant data for these binuclear Pt(III) series complexes. Protons on the oxopyridonate ligand are readily assigned by the comparison of the unsubstituted hydroxypyridine with the 6-substituted F, Cl or CH_3 group complex, the nearby 5-H proton is a triplet in the former case where it is a doublet in the substituted F, Cl or CH_3 group case. The 3-H and 4-H are assigned by the single frequency decoupling and remained as a doublet and triplet in the ^1H NMR spectra in either case.

The methyl resonances of the complexes are easily assigned by the interaction with the platinum ion which has 30% spin 1/2 nucleus, forming an apparent triplet. This triplet resonance results from the magnetic field caused by the 1/2 spin of platinum nucleus. If the magnetic field is along the direction of the external magnetic field, the nuclear magnetic momentum of the proton nucleus would be enhanced, so the chemical shift of the proton would go downfield. If, however, the magnetic field of the nucleus spin is against the direction of the external field, the nuclear magnetic momentum of the proton would be decreased,

and the chemical shift of the proton would go upfield. The center of the apparent triplet is due to methyl groups on Pt with no spin. The triplet 1:4.67:1 ratio is due to the 30% of platinum nuclear spin. A measurement of the distance between the outer wings of the triplet would determine the Pt-CH_3 coupling constant.

In the HH case, two chemically equivalent methyl groups are on each Pt ion while each Pt ion has two different methyl groups on it in the HT case [17]. This is due to the CH_3 group trans to nitrogen and oxygen atom on the oxopyridonate ligands in HT form or cis to these atoms in HH case. The chemical shifts for the methyl group in HH and HT cases have been measured. If a HT arrangement with a single axial ligand existed, the methyl resonances would be different from those observed in the di-axial substituted case in that one ought to see four different methyl resonances. This is not the situation encountered in the measurement.

Nuclear Overhauser enhancement serves to identify the methyl groups in the HH and HT cases respectively if the axial ligand is pyridine. In the HH case, irradiation of the downfield methyl resonance results in the enhancement of the α proton resonance on the axial pyridine (α, β, γ refer the resonances on Py), while the upfield methyl resonance shows no interaction with the proton resonance on pyridine proving that a downfield methyl resonance is closer to the

coordinated pyridine. In the HT case, irradiation of each of the methyl resonances separately results in the same enhancement of the α proton on the axial pyridine, supporting the diaxial substituted structure.

Carbon-13 and platinum-195 NMR assignment for these binuclear Pt(III) compounds were previously described (18), giving a fully-described structure of these Pt(III) complexes.

For the equilibrium HH + free pyridine $\rightleftarrows$ HT, the variation of the pyridine concentration is shown in Table 9. The equilibrium constant obtained by the method described in the experimental section for Pt(HPy) and Pt(FHPy) is thermodynamically reasonable, in which K for Pt(HPy) is about 150 $LMol^{-1}$ and for Pt(FHPy) is about 25 $LMol^{-1}$ at room temperature in $CDCl_3$, meaning there is more HT formation in Pt(HPy) compared with HT formed in the Pt(FHPy) at the same pyridine concentration. The reason for the difference in the equilibrium constant for Pt(HPy) and Pt(FHPy) might be due to steric bulk of the substituent on Pt(FHPy). Pt(HPy) is less hindered. It is Pt(HPy) that is more likely to accept the coordinating axial pyridine and transforms to HT form. The failure of Pt(MHPy) and Pt(ClHPy) to form HT complexes is attributed to the steric bulk of the 6-X substituent as well. Therefore, the value of K is directly related to the substituent.

Table 9. Rate constant and activation parameters for Pt(FHPy) HH ⇄ HT reaction

[a]Rate constant (s^{-1})	Pyridine concentration (M)
7.94×10^{-5}	0.173
1.96×10^{-4}	0.320
2.30×10^{-4}	0.375
3.64×10^{-4}	0.468

[b]Rate constant(s^{-1})	Temperature (K)
7.94×10^{-5}	296
3.18×10^{-4}	307
7.36×10^{-4}	318

	$\Delta S^{\neq}$	$\Delta H^{\neq}$
For Pt(FHPy) HH -> HT	-29 J $Mol^{-1}K^{-1}$	84 KJ Mol^{-1}
For Pt(FHPy) HT -> HH	16 J $Mol^{-1}K^{-1}$	105 KJ Mol^{-1}

a. Temperature = 298 K

b. Pyridine concentration is a constant

Table 9 shows the rate constants and activation parameters of Pt(FHPy) interconversion.

Proton NMR spectroscopy has been used to identify and follow the interconversion of Pt(FHPy) (HH ⇄ HT) in $CDCl_3$.

Kinetic study of the reaction is based on the rate law, $-d[HH]/dt=k_f[HH]-k_r([HH]_o-[HH])$. With the assumption that

pyridine concentration is much larger than the HH Pt(III) complex concentration, so that Py functions as a constant. One sets up the model for HH $\rightleftarrows$ HT, an approach to equilibrium expression for which $K_{eq}=k_f/k_r$, $[HT]=[HH]_o-[HH]$. The time dependence of the decrease of the HH Pt(III) complex concentration and the appearance and increase of the HT Pt(III) complex concentration, with the addition of the free pyridine, fit the integrated form of the rate law which describes the pseudo first-order approach:

$$-d[HH]/dt=k_f[HH]-k_r([HH]_o-[HH])$$

Integrated form: $$Ln(k_f[HH]_o/\{(k_f+k_r)[HH]-k_r[HH]_o\}$$

$$=(K_f+k_r)t$$

At equilibrium: $d[HH]/dt= 0$

$$k_f[HH]_{eq}=k_r([HH]_o-[HH]_{eq})$$

$$[HH]_{eq}=k_r[HH]_o/(k_f+k_r)$$

Substitution into the integrated form result:

$$Ln([HH]_o-[HH]_{eq}/[HH]-[HH]_{eq})=(k_f+k_r)t$$

Therefore $-Ln([HH]-[HH]_{eq})$ vs. time should result in a straight line if analysis is correct. The slope of this straight line is k_f+k_r and one can determine the rate constant by the following equations if the equilibrium constant for the interconversion is known.

$$K = k_f / k_r$$

$$slope = k_f + k_r$$

Recently a similar HH to HT rearrangement was studied in a very different system (66). In the Pt(II) complexes studied hydroxypyridine bridge breakage and formation were involved. Similar kinetic models and equations were used. Unlike the system we studied, there were no Pt-Pt bonds nor were axial ligands present in product or reactant. The data obtained from that study should be compared to our data for the HT $\rightleftarrows$ HH reaction. As that system was studied in water, while our reaction was carried out in chloroform, detailed comparison is unreasonable. Nevertheless, comparison of their results to ours for the HT to HH interconversion is illuminating. In both results, the activation entropy is consistent with a dissociative concerted mechanism for bridge isomerization.

The changes of the reaction rate of HH Pt(III) complex on NMR spectra are directly proportional to the changes in concentration of pyridine. The higher the concentration of pyridine, the faster the increase of HT peak height forms on

NMR spectra and the quicker the final equilibrium is reached (Figure 14).

The changes of reaction rate of HH Pt(III) complexes are also related to the temperature. The higher the temperature, the faster the reaction goes (Figure 15).

The different temperature measurement for the interconversion determines the reaction activation enthalpy and activation entropy using Eyring plot (Figure 16).

Rate studies reveal the reaction rate is greatly influenced by the concentration of pyridine and temperature. Reaction at varying pyridine concentrations established that the reaction is first order in pyridine and first order in HH complex. Addition of free hydroxypyridine to the reaction mixture showed no formation of a mixed HPy, FHPy platinum complex even after 20 half-lives for the HH to HT rearrangement. These facts taken together suggest one of two mechanisms. In route 1, a preequilibrium in which pyridine binds the HH complex is followed by a rate determining step, which involves a somewhat dissociative but concerted rearrangement of an FHPy bridge (Figure 17). In route 2, pyridine attacks in a rate determining associative step displacing one bond to the FHPy bridge. The FHPy bridge subsequently converts to form an HT complex (Figure 18). The possibility of a mechanism involving rupture of the metal-metal bond was also considered. Theoretically,

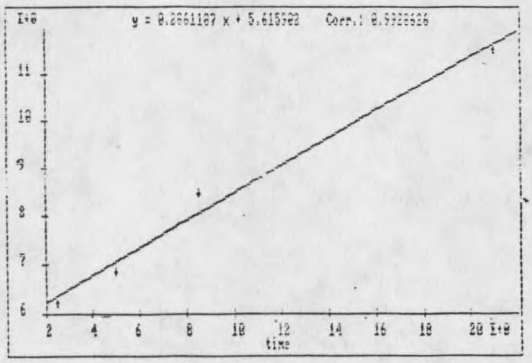

-Ln([HH]-[HH]$_{eq}$) vs. Time (hours)

[Py]=10 µL T=296K

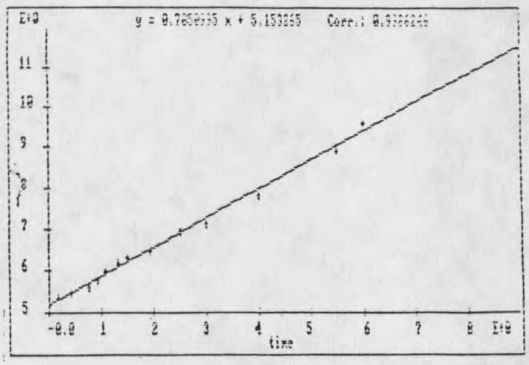

-Ln[(HH)-[HH]$_{eq}$) vs. Time (Hours)

[Py]=20 µL T=296K

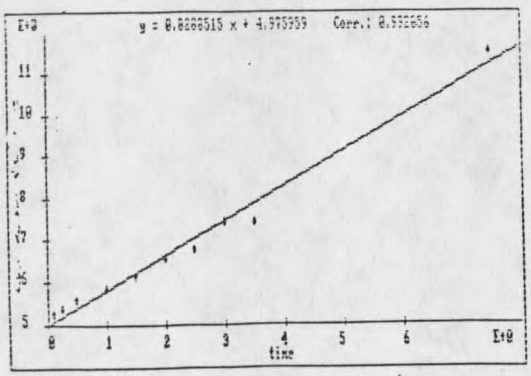

-Ln([HH]-[HH]$_{eq}$) vs. Time (hours)

[Py]=25 µL T=296K

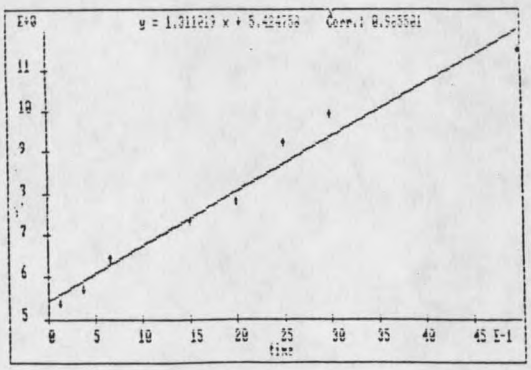

-Ln([HH]-[HH]$_{eq}$) vs. Time (hours)

[Py]=50 µL T=296K

Figure 14. **-Ln[(HH)-$(HH)_{eq}$] vs. time (hours) plot Pt(FHPy) HH → HT at different pyridine concentrations**

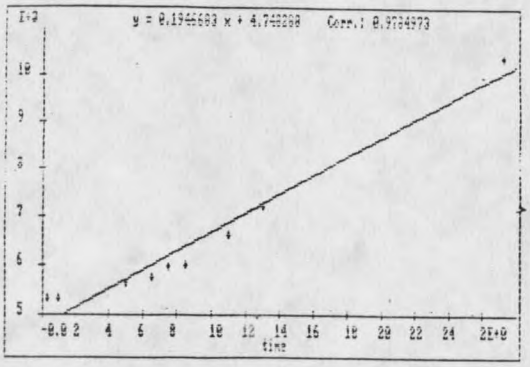

-Ln([HH]-[HH]$_{eq}$) vs. Time (hours)

[Py]=10 µL T=283K

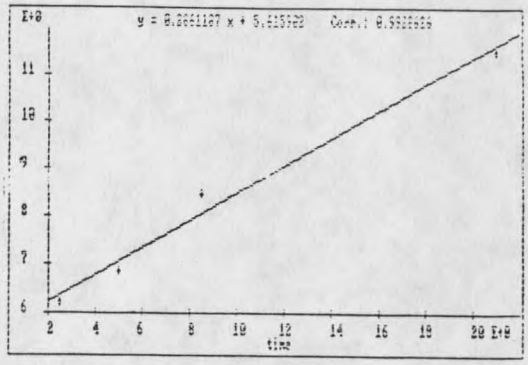

-Ln([HH]-[HH]$_{eq}$) vs. Time (hours)

[Py]=10 µL T=296K

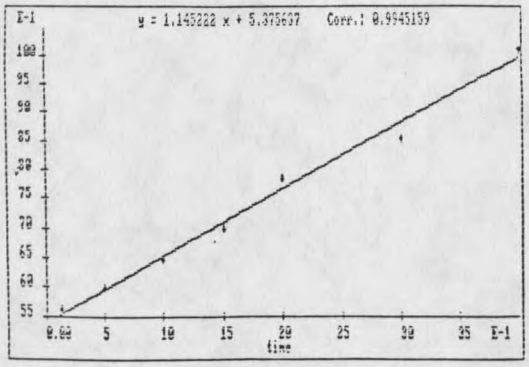

-Ln([HH]-[HH]$_{eq}$) vs. Time (hours)

[Py]=10 µL T=307K

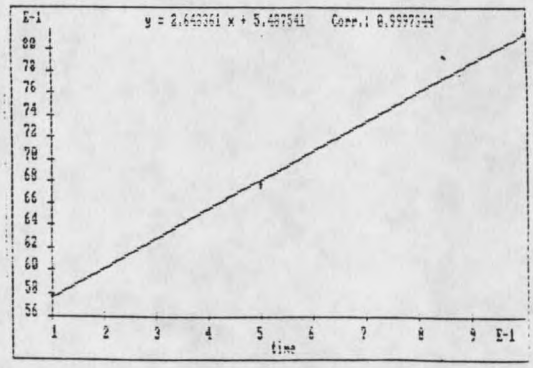

-Ln([HH]-[HH]$_{eq}$) vs. Time (hours)

[Py]=10 µL T=318K

Figure 15. -Ln[(HH)-(HH)$_{eq}$] vs. time (hours) plot Pt(FHPy) HH → HT at different temperatures

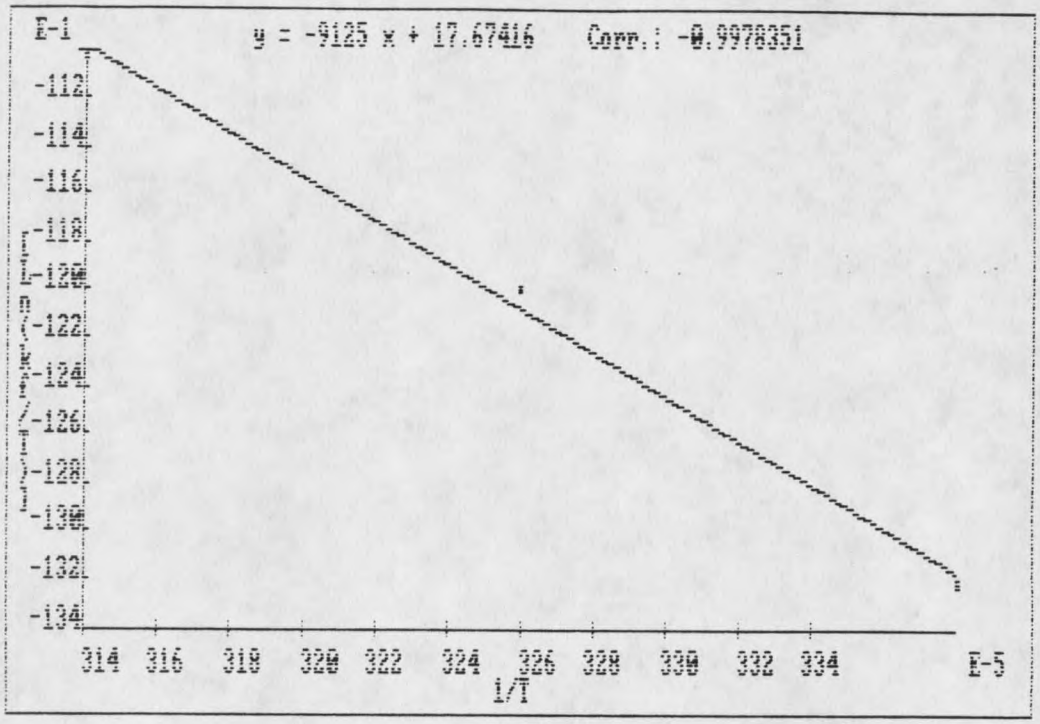

Ln(k/T) vs. 1/T

Figure 16. Eyring plot for Pt(FHPy) HH → HT

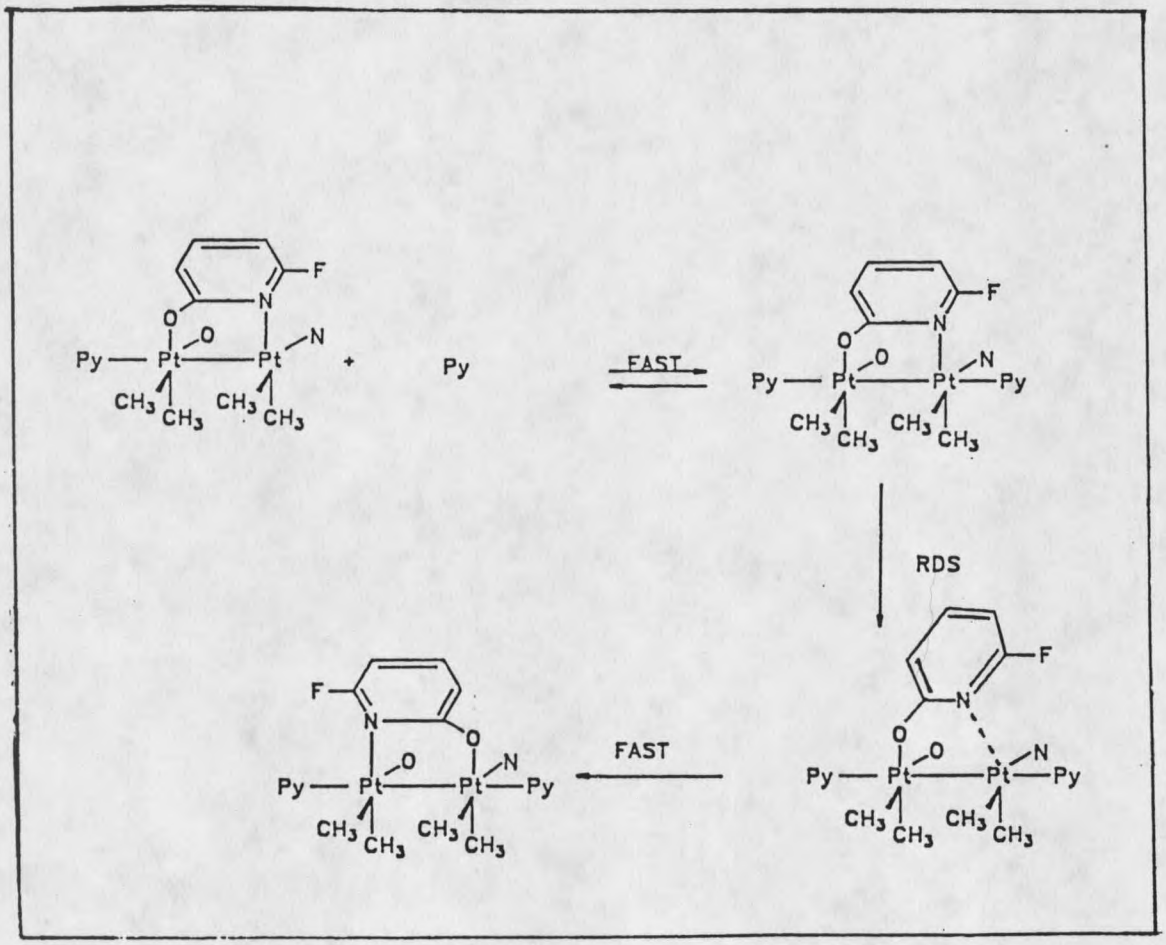

Figure 17. Mechanism 1 for Pt(FHPy) HH → HT

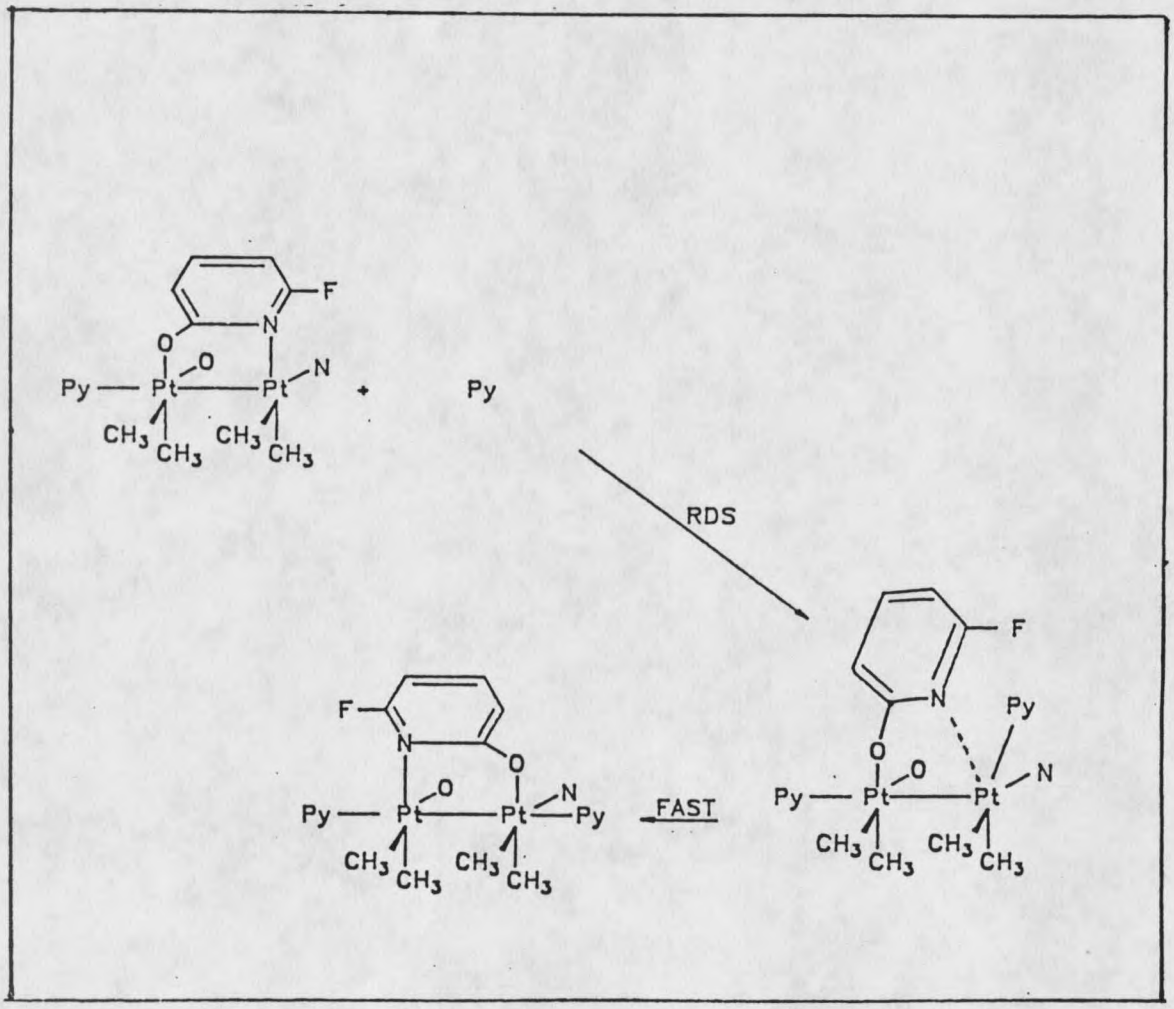

Figure 18. Mechanism 2 for Pt(FHPy) HH → HT

addition of pyridine to the HH complex might occur on the same platinum to which the first pyridine is coordinated. If this was followed by disproportionation, it would result in a mononuclear four-coordinate Pt(II) complex and a six-coordinate Pt(IV) complex. Each complex would contain one bidentate FHPy bridge if Pt(FHPy) complex was used. Recombination of these two monoplatinum complexes could result in HT formation. This consideration was rejected by the experiment in which the Pt(FHPy) and Pt(HPy) complexes (both are HH) were present in the same solution. With the addition of pyridine and 10 half-lives for the HH to HT conversion, no mixed-bridged platinum complex could be detected. This observation does not preclude the mechanims in which the metal-metal bond is broken but one XHPy continues to bridge the metal ions.

The validity of the equilibrium in this interconversion is supported by the observation that a state is eventually reached in which HH and HT concentrations keep a fairly stable ratio under the influence of changes in pyridine concentration.

There is a considerable difference between the rate constants of Pt(FHPy) and Pt(HPy) in interconversion. The rate constant for Pt(FHPy) is 5.43×10^{-4} s^{-1} M^{-1} and is 2.33×10^{-5} s^{-1} M^{-1} for Pt(HPy) forward reaction (HH $\rightarrow$ HT). It takes about 36 hours to reach the equilibrium for Pt(FHPy) and about 10 days to get the equilibrium for

Pt(HPy). So the Pt(FHPy) reacts much faster than Pt(HPy) does with addition of same amount of pyridine. The Pt-N bond length (N on the bridge ligand) in Pt(FHPy) (HH) is 2.162 Å while it is 2.119 Å in Pt(HPy) (HH). This difference in bond length provides the insight about the lability of Pt-N bond in Pt(FHPy) (HH) and why it is easier to convert. Even in the HT form, Pt-N bond length is 2.19 Å for Pt(FHPy), while it is only 2.14 Å in Pt(HPy). This is possibly another reason for which in HT $\rightleftarrows$ HH reverse reaction, Pt(FHPy) (HT) goes back to (HH) faster than Pt(HPy) (HT)(2.05×10^{-5} s^{-1} vs. 2.11×10^{-7} s^{-1}). Presumably this is a consequence of a weaker bond between platinum and the hydroxypyridine nitrogen in the Pt(FHPy) complex, as might be expected on inductive grounds. For both Pt(FHPy) and Pt(HPy) complexes, the bond from Pt to the nitrogen on hydroxypyridine is longer in HT than that in HH. Assuming that this lengthening is due to the presence of a second axial pyridine, then a preequilibrium mechanism as route 1 should weaken the Pt-N bond and thus accelerate a dissociative rate determining step, as indicated in mechanism 1.

Another plausible reason for this happening might be due to the substituent on the bridge ligands. Because fluorine is larger than hydrogen in size, it is more susceptible to be repelled by the steric interaction of hydrogens on the pyridine ring while pyridine attacks the axial position in

the HH → HT case. That repulsion helps tear the bonds between FHPy ligands and Pt ions and makes Pt(FHPy) easier to convert to HT orientation, hence the reaction rate is faster.

The dissociative reaction mechanism best explains the activation enthalpy and entropy data. As a preequilibrium concerted step, activation entropy and enthalpy ($\Delta S^{\neq}$= -29 J $mol^{-1}K^{-1}$, $\Delta H^{\neq}$= 84 kJ mol^{-1}) were calculated from experiment(HH → HT), meaning the activated complexes do not have a significant difference in number. The positive enthalpy term represents that there is a bond dissociation step which is just the rearrangement of the oxo-pyridonate bridge ligand and in which the HH form converts to HT form.

Different attacking ligands result in different rates in forming HT from HH. Pyrazine ($C_4H_4N_2$) and picoline (C_6H_7N) were used. Compared with pyridine, picoline is a better nucleophilic ligand. A better base would donate electrons easily, and in so doing form Pt-ligand bonds, hence to accelerate the HH ⇄ HT interconversion.

The evidence that the interconversion may be sterically accelerated is based on the result from HH ⇄ HT in Pt(HPy) and Pt(FHPy) case. Comparison of the x-ray structures of corresponding compounds reveals that Pt-Pt bond length in HH binuclear Pt(III) complexes changes from 2.556 Å to 2.550 Å for Pt(HPy) in HT, and from 2.554 Å to 2.551 Å for Pt(FHPy) in HT form. The change in bond length of Pt(HPy) is larger

than that of Pt(FHPy) during interconversion. Though it is not a substantial change in bond length, the decrease does play a role in accommodating the increased electron density given by the incoming axial pyridine ligand. The more bonding electrons involved, the stronger the interaction between the metal ions, so the stronger bonding. Clearly Pt(HPy) is more sensitive to the second pyridine coordination than Pt(FHPy).

The arrangement of the two adjacent oxo-pyridonate rings would certainly be a part in this interconversion. These bridging ligands are coordinated with Pt ions through chelate bonds, and the chelate bonds are not broken at the bonding sites spontaneously, so as to keep out other chelate ligands for substitution. Evidence showed using a free pyridonate ligand to substitute FHPy bridges ligand in Pt(FHPy) case during HH $\rightleftarrows$ HT was unsuccessful, because there was no new resonance showing in NMR spectra. Therefore the inter-rearrangement must be due to other factors. That the Pt_2^{6+} unit keeps intact in the process has been proved by an experiment mentioned earlier. The possibility of the intramolecular conversion caused by the addition of an electron donating ligand is also likely to be explained as electron imbalance in the metals. Absence of observable quantities of mononuclear species indicate the conversion does not involve complete dissociation of the binuclear complex. The rearrangement is so fast that more detailed

data could not be collected at this time about the conversion.

Further evidence in favor of the mechanism also came from the activation parameters for the reverse reaction (HT → HH) in which $\Delta H^{\neq}$= 105 kJ mol^{-1} and $\Delta S^{\neq}$= 16 J $mol^{-1}K^{-1}$ were obtained (Figure 19). If the mechanism route 2 is right, a much larger positive $\Delta S^{\neq}$ would be expected and there would be a substantial difference in $\Delta H^{\neq}$ value in the forward reaction. Additional evidence for the preequilibrium of HH complex with pyridine was also studied by the dependence of the chemical shift of the proton resonances of HH and HT on attacked pyridine. Different chemical shifts of HH caused by the added pyridine were closely related to the amount of pyridine and moved to different directions (Table 10). However, all the resonances of the HT complex shifted uniformly to the lower field as pyridine is added (Table 11). This observation would be more consistent with the assumed mechanism as rapid equilibrium between free pyridine and the HH complex; it could not be interpreted further in terms of a detailed mechanism.

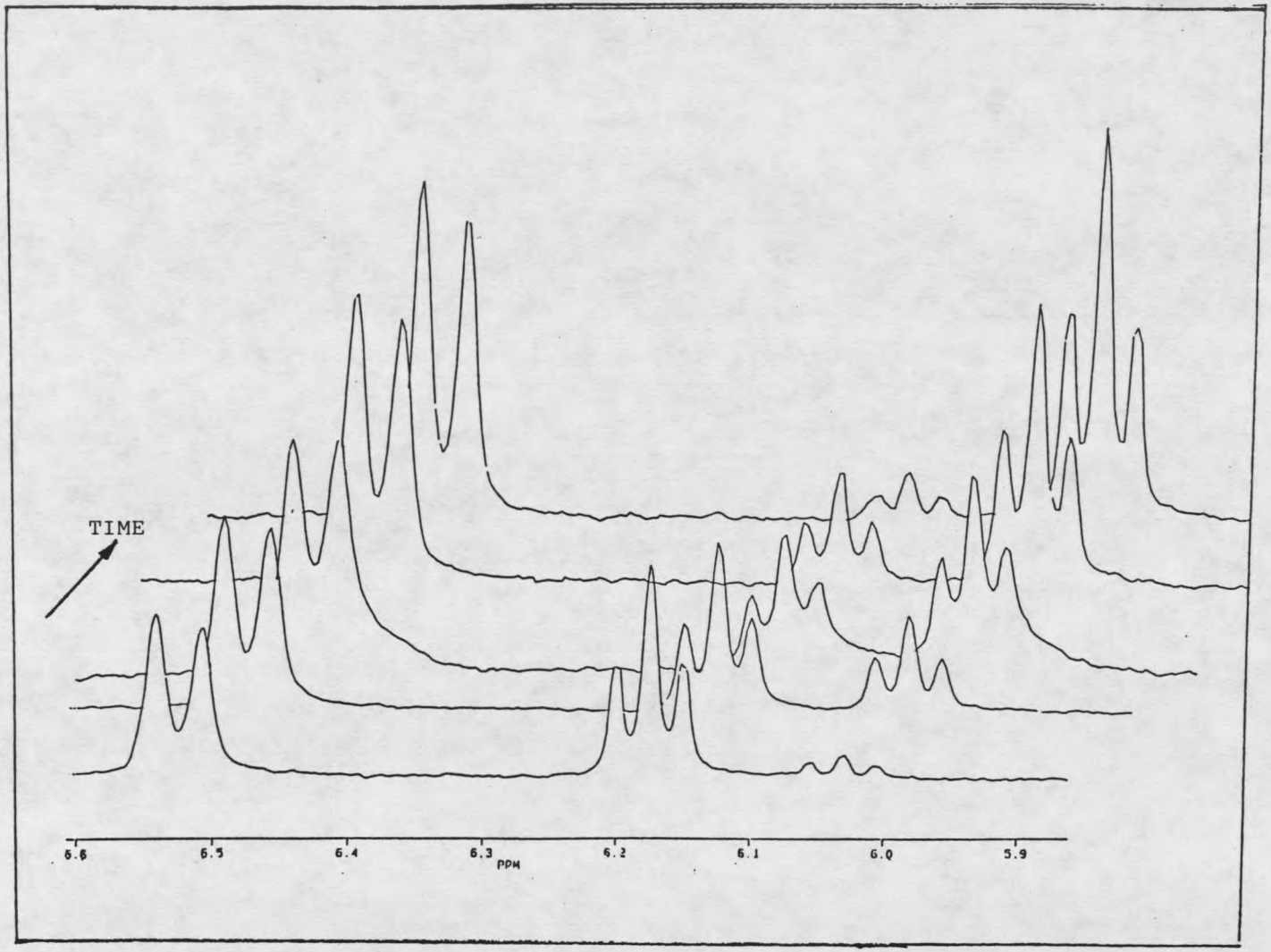

Figure 19. ^{1}H NMR spectrum of Pt(HPy) HT → HH

Table 10. Chemical shifts of different resonances on Pt(FHPy)(HH) vs. different pyridine concentrations

[Py](μl)	3-H(ppm)	5-H(ppm)	CH_3(ppm)	CH_3'(ppm)
0	0.81	1.19	5.62	6.12
10	0.83	1.22	5.65	6.13
20	0.81	1.21	5.65	6.11
25	0.81	1.21	5.65	6.11
50	0.80	1.22	5.66	6.08

[Py](μl)	[a]D_{H3-H5} (ppm)	[b]$D_{CH3-CH3'}$ (ppm)
0	0.37	0.50
10	0.38	0.48
20	0.40	0.46
25	0.40	0.45
50	0.42	0.41

a. Difference in chemical shift between H3 and H5 resonance in HH complex.

b. Difference in chemical shift between CH_3 and CH_3' resonance in HH complex.

Table 11. Chemical shifts of different resonances on Pt(FHPy) (HT) vs. different pyridine concentrations

[Py](µl)	3-HT(ppm)	5-HT(ppm)	CH_3[a](ppm)	CH_3[b](ppm)
10	0.90	1.56	5.92	6.43
20	0.88	1.54	5.90	6.41
25	0.89	1.54	5.90	6.41
50	0.87	1.53	5.87	6.38

[Py](µl)	[c]$D_{HT3-HT5}$(ppm)	[d]$D_{CH3a-CH3b}$(ppm)
10	0.65	0.50
20	0.65	0.50
25	0.65	0.50
50	0.66	0.50

a. CH_3 group on Pt(FHPy)(HT)

b. CH_3' group on Pt(FHPy)(HT)

c. difference in chemical shift between H3 and H5 resonance in HT complex

d. difference in chemical shift between CH_{3a} and CH_{3b} resonance in HT complex

THE SYNTHESES AND STRUCTURE DETERMINATION OF A GROUP OF PLATINUM COMPOUNDS

Experimental

A. Preparation of platinum compounds

1. Preparation of cis-$PtCl_2(Et_2S)_2$

cis-$PtCl_2(Et_2S)_2$ was prepared as described (54).

$K_2PtCl_4 + 2Et_2S$ (excess) -----> cis-$PtCl_2(Et_2S)_2 + 2KCl$

2. Preparation of trans-$PtCl_2(Et_2S)_2$

trans-$PtCl_2(Et_2S)_2$ was prepared as described (54).

K_2PtCl_4 (excess) + $2Et_2S$ -----> trans-$PtCl_2(Et_2S)_2$ + $2KCl$

3. Preparation of Ag salts

Ag(MHPy) was prepared by addition of $AgNO_3$ solution to the aqueous solution of sodium salt of the MHPy ligand, which was previously prepared by the addition of $NaOCH_3$ in methanol to the MHPy ligand. The Ag salt precipitated immediately in all cases when $AgNO_3$ was added. It was filtered, washed with water, ethanol, ether, and air dried. All Ag salts were off-white in color and stored in a brown bottle to avoid decomposition by light.

4. Preparation of $Pt_2(CH_3)_4[(C_2H_5)_2S]_2$

$Pt_2(CH_3)_4[(C_2H_5)_2S]_2$ was prepared as described (52).

cis-$PtCl_2(Et_2S)_2 + CH_3Li$ -----> $Pt_2(CH_3)_4(Et_2S)_2$

The complex was recrystalized from $CHCl_3$ prior to use to remove an impurity present after the initial preparation.

5. Preparation of $K_2[Pt_2(NO_2)_4(OH)_2]\cdot 1\frac{1}{2}H_2O$

0.100 g $K_2Pt(NO_2)_4$ (2.18×10^{-4} mole) was dissolved in 2 mL of H_2SO_4 (0.219 M) and heated to T=85°C for 10 minutes. After that, the colorless solution in the vessel was concentrated under reduced pressure until the solvent was gone. During that time, the color of the solution changed from colorless to light blue, blue, green, orange and finally became a red solid. This red solid was dissolved with a minimum amount of water and the pH of the solution was approximately 1. Addition of K_2CO_3 resulted in bubbling of the solution (CO_2) and color change from red to yellow until pH=7. Leaving the yellow solution in the cold room (5°C) for 30 days yielded the formation of crystals. Transparent ones were determined to be K_2SO_4. Yellow crystals were determined to be $K_2[Pt_2(NO_2)_4(OH)_2]\cdot 1/2H_2O$.

6. Preparation of $K_5[Pt_4(NO_2)_9(O)_3]\cdot 3H_2O$

0.050 g of $K_2Pt(NO_2)_4$ (1.09×10^{-4} mole) was dissolved in 1 mL of H_2SO_4 (0.219 M). The solution was heated to T=85°C for 10 minutes and a colorless solution formed. Removing the solvent under reduced pressure resulted in the color change from colorless to light blue, blue, green, orange and finally red when the liquid was gone. Addition of a few drops of acidified water left the product entirely red.

Addition of a minimum amount of water and K_2CO_3 to neutralize the solution turned the color of the solution from red to yellow, single yellow crystals were grown from the yellow solution by leaving it in the cold room for a month. Transparent crystals which were later determined to be K_2SO_4 were by-products. Hence manual separation was required. The yield of the yellow compound was 20-30%. Elemental analysis calculated for $H_6N_9O_{24}K_5Pt_4$, N= 8.45%, Pt= 52.30%. Found N= 8.20%, Pt= 50.81%.

7. Preparation of $Pt_2(MHPy)_2(CH_3)_4(Py)$

This modified preparation of the title complex was carried out by dissolving 0.500 g (0.80 mmole) $Pt_2(CH_3)_4[(C_2H_5)_2S]_2$ in 40 mL dry benzene. With the addition of Ag(MHPy) (0.35 g 1.60 mmole), the solution, initially white, turned dark brown, then black once they were mixed. This solution was stirred for 72 hours while the Ag coated on the reaction vessel. Repeated filtration eventually changed the color of the solution from black to brown. Excess pyridine was used as the eluting solvent to get the brown solution off the silica gel column, resulting in the orange-red solution. This orange-red complex was confirmed by the NMR spectrum as the title compound. The yield of the reaction before chromatography was about 40%, while after that it was only 20%.

8. Preparation of $[Pt_2(CH_3)_4(MHPy)_2(PPh_3)]\cdot 2CH_3COCH_3$

0.030 g of $Pt_2(CH_3)_4(MHPy)_2(Py)$ (4.05×10^{-5} mole) was dissolved in about 2 mL of chloroform. With the addition of 2 eq.of PPh_3 (0.021 g) at room temperature, the solution changed color from orange to light orange over the course of several days. Meanwhile, ^1H (Figure 20), ^{31}P (Figure 21) and ^{195}Pt NMR were used to trace this reaction (Table 12). Spectra showed the beginning and completion of the reaction. No crystals were formed when the solvent was removed. Crystallization from hexane or methanol failed. Finally metallic-like small crystals were grown from acetone at low temperature when free PPh_3 in the solution had been eliminated by extraction with ethanol. The structure of the complex was characterized by x-ray crystallography.

9. Reaction of $cis\text{-}PtCl_2(Et_2S)_2$ with pyrazine

0.050 g of $cis\text{-}PtCl_2(Et_2S)_2$ (1.4×10^{-4} mole) was dissolved in 10 mL chloroform and 2 mL DMSO. Addition of 0.0448 g (4 eq.) of pyrazine caused no immediate change in color in solution. This yellow solution was stirred at room temperature for 6 hours and left in the cold room for slow evaporation. Needle-like pale yellow crystals were obtained. X-ray crystallography was tried, but the quality of the crystal was not good enough to solve the structure of the complex.

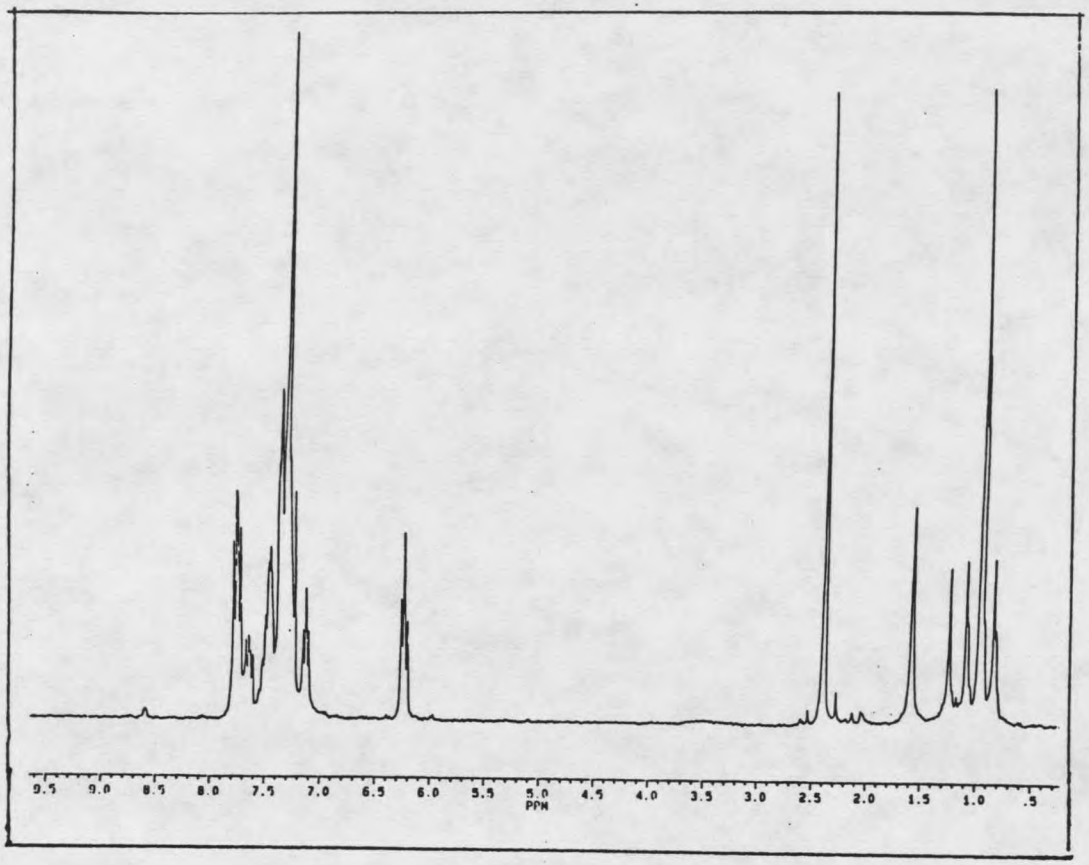

Figure 20. ^{1}H NMR spectrum of $Pt_2(CH_3)_4(MHPy)_2(PPh_3)$

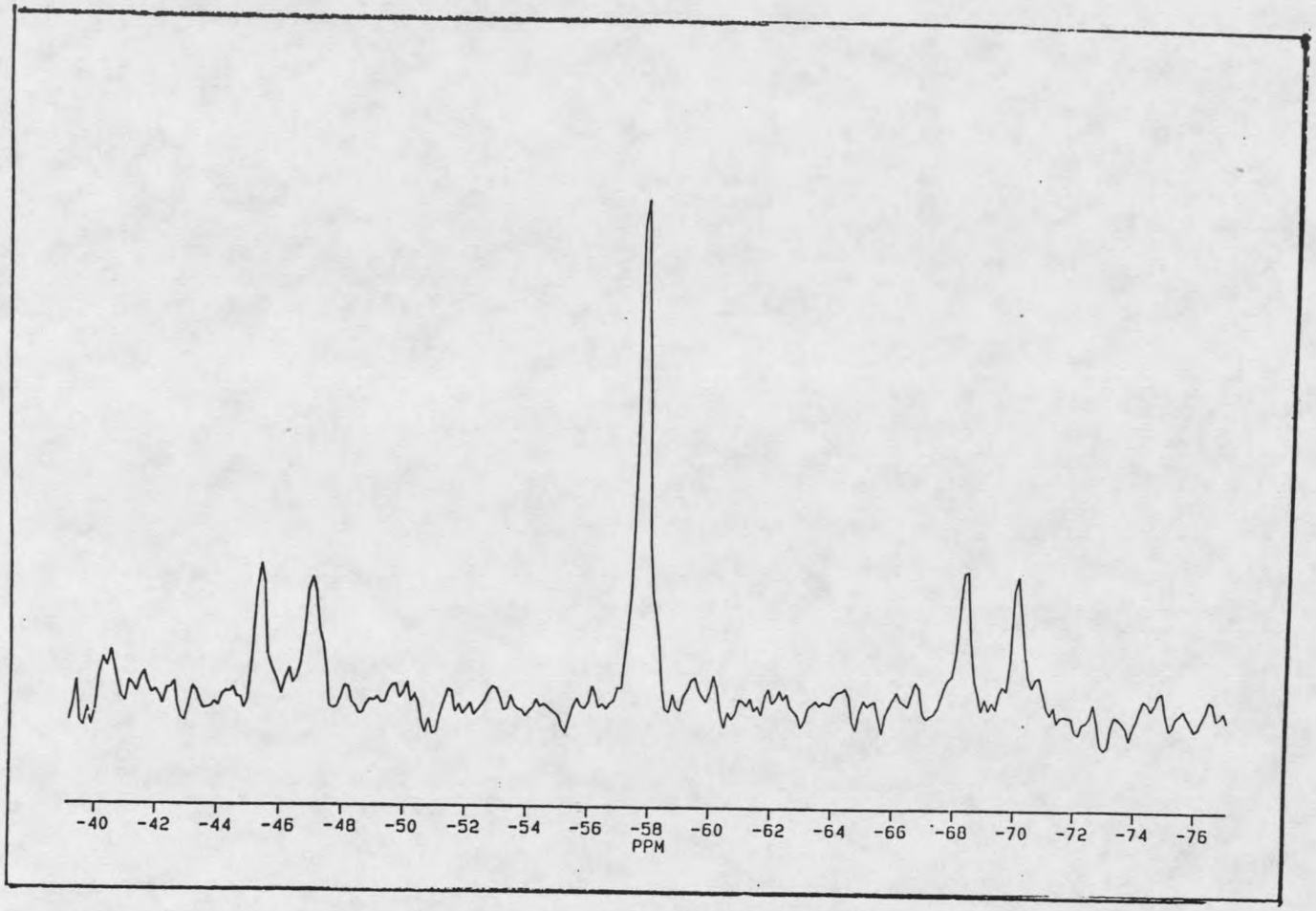

Figure 21. ^{31}P NMR spectrum of $Pt_2(CH_3)_4(MHPy)_2(PPh_3)$

Table 12. 1H and ^{31}P NMR assignment for $Pt_2(CH_3)_4(MHP_y)_2(PPh_3)$

Chemical shift(ppm)	Assignment	Coupling constant (^2J Pt-CH_3)
Proton Assignments		
0.94	CH_3(I)	75.3 Hz
0.96	CH_3(II)	76.2 Hz
2.39	CH_3 on the ring	
6.24	5-H	
7.14	3-H	
7.31	4-H	
7.24	$CDCl_3$	
7.37	ß H-pyridine	
7.48	γ H-pyridine	
7.78	α H-pyridine	
Phosphorus-31 Assignments		
-57.683 (3)	P on PPh_3	J(P-Pt1) = 1257 Hz J(P-Pt2) = 1086 Hz

10. Reaction of cis-$PtCl_2(Et_2S)_2$ with PPh_3

0.050 g of cis-$PtCl_2(Et_2S)_2$ ($1.4x10^{-4}$ mole) was dissolved in toluene. 2 eq.of PPh_3 (0.0868 g) was added into the solution. After the solution was well mixed-up, NO gas was bubbled through the solution for 5 minutes. The color of the solution changed from yellow to light green, then green. This green solution turned color to dark brown when left in refrigerator. The attempt to get crystals for x-ray study failed.

11. Reaction of cis-$PtCl_2(Et_2S)_2$ with NO

NO gas was bubbled through a solution of cis-$PtCl_2(Et_2S)_2$ (0.025 g, 7.0×10^{-5} mole) in 5 mL toluene until the color changed to light green. After stopping the gas bubbling and leaving the solution in the refrigerator, I obtained dark brown solution. Separating the brown solution with a silica gel column, I obtained two kinds of solutions with different color. The green part was only soluble in toluene while the light brown was only soluble in acetone.

12. Reaction of cis-$PtCl_2(Et_2S)_2$ with $Ag_2(C_2O_4)$

0.050 g of cis-$PtCl_2(Et_2S)_2$ (1.28×10^{-4} mole) was dissolved in 10 mL of dry benzene. With addition of 0.156 g $Ag_2(C_2O_4)$ (4 eq.), the color of the solution changed from yellow to white and light black mixture. The white precipitate was believed to be AgCl while the black one was thought to be Pt metal. The solution was stirred for 24 hours at room temperature and finally the solution turned purple. The solvent was removed in vacuum and the purple residue was extracted with water. Then different solvents were used to try to dissolve this purple compound, but none was effective. The structure of this purple complex was likely to be a Pt-Ag polymer. Crystallization of this complex is being attempted.

13. Reaction of cis-$PtCl_2(Et_2S)_2$ with $Ag_2C_2O_4$ (modified method)

0.100 g of cis-$PtCl_2(Et_2S)_2$ was dissolved in 5 mL methanol. With the addition of 4 eq.of $Ag_2C_2O_4$ (0.311 g), the solution was stirred at room temperature for 15 hours. Then another 4 eq.of oxalic acid (0.046 g) added and the whole solution was heated in an oil bath (T=96°C) for 10 minutes. After that, purple precipitate appeared in the methanol solution. Addition of formic acid did not change the solubility of the purple compound. Different solvents were tried, but were not able to dissolve the compound and separate it from silica gel column. No crystal was obtained from evaporation.

14. Reaction of cis-$PtCl_2(Et_2S)_2$ with Ag(MHPy)

0.200 g of cis-$PtCl_2(Et_2S)_2$ (5.13×10^{-4} mole) was dissolved in 20 mL of dry benzene. 2 eq. of Ag(MHPy) (0.222 g) was added in the solution. The solution was stirred at room temperature for 72 hours, the solution finally was brown without Ag coating. Then the solution was put in an oil bath (T=82°C) for 9 hours and color of the solution turned into grey. A purple layer coated on the wall of the reaction vessel. Attempt to dissolve this purple precipitate failed due to the unsoluble nature of the compound. A possible structure for the compound might involve a Pt-Ag polymer because of the blue color.

15. Reaction of cis-$PtCl_2(Et_2S)_2$ with $AgNO_3$

0.100 g of cis-$PtCl_2(Et_2S)_2$ (2.18×10^{-4} mole) was dissolved into 4 mL of distilled water and 4 mL of methanol with the addition of 74.4 mg of $AgNO_3$ (4.37×10^{-4} mole). This mixed solution was stirred at room temperature for 6 hours. During that time, there was a color change from green to yellow and a white precipitate formed. After filtering off the precipitate, the solution looked pale-green. Rotovaping the solution to the minimum volume enabled it to grow crystals at low temperature. After several days crystallization, pale-green single crystals were obtained. Though we were unable to solve the structure so far, we got the unit cell of the crystal. It was assumed that the product was a Pt dimer bridged by Et_2S ligands.

Unit cell: a=12.660 Å, b=9.984 Å, c=13.424 Å

α=89.95°, β=109.87°, γ=90.05°, V=1595.69 $Å^3$,

Space group: monoclinic B

16. Reaction of K_2PtCl_4 with PPh_3

0.050 g of K_2PtCl_4 (1.21×10^{-4} mole) was dissolved in 15 mL methanol with a little base (KOH)in it. 0.100 g PPh_3 (excess) was added. This solution was stirred at room temperature for 24 hours, and then was kept in an oil bath (T=80°C) for 2 hours. The color of the solution changed from colorless to dark red. Slow evaporation in the cold room formed a sticky red solid. Silica gel column was used to separate the red solid and a clear brown solution

obtained in the methanol. Further attempts for crystalization are still under way.

17. Reaction of K_2PtCl_4 with $Ag_2(C_2O_4)$

0.050 g of K_2PtCl_4 ($1.21x10^{-4}$ mole) was dissolved in 5 mL of water. Addition of 4 eq. of $Ag_2(C_2O_4)$ (0.149g) did not change the color of the solution. Brown precipitate formed when the light-yellow solution was put in an oil bath (T=72°C). The solvent was filtered and the precipitate resulted in the purple powder which was insoluble in either water or benzene and solvents in between.

18. Reaction of $K_2Pt(NO_2)_4$ with L-Proline ($C_5H_9NO_2$)

0.050 g of $K_2Pt(NO_2)_4$ ($1.09x10^{-4}$ mole) was dissolved in 2 mL of water. With addition of 4 eq. of proline (0.050 g), the solution was stirred at room temperature for 48 hours. The color of the solution remained the same. The solvent volume was reduced by rotovapor but no crystal formed during slow evaporation at cold temperature.

19. Reaction of $K_2Pt(NO_2)_4$ with tartaric acid

0.050 g of $K_2Pt(NO_2)_4$ ($1.09x10^{-4}$ mole) was dissolved in 2 mL of water. After addition of 4 eq. of proline (0.050 g), 0.16 M HNO_3 was used to adjust the pH to 1. The solvent was removed partially in vacuum and left under room temperature for slow evaporation. The color of the solution turned red. When the solvent was gone, tiny red crystals formed. X-ray characterization proved then to be KNO_3.

20. Reaction of K_2PtCl_4 with L-Proline

0.050 g of K_2PtCl_4 (1.21×10^{-5} mole) was dissolved in 5 mL of methanol and 1 mL of DMSO. Addition of 4 eq. of proline (0.0557 g) and stirring the solution at room temperature for 6 hours changed the color of the solution from yellow to opaque-white with white precipitate. The white precipitates were separated from the solvent through filteration. Small crystals were grown from the solution when the white precipitate was redissolved in methanol. Unfortunately the size of the crystal was not large enough to solve the structure.

21. Reaction of $K_2Pt(NO_2)_4$ with Glycine (H_2NCH_2COOH)

0.050 g of $K_2Pt(NO_2)_4$ (1.09×10^{-4} mole) was dissolved into 3 mL of water. 4 eq. of glycine (0.0327 g) was added into the solution and no color change happened. The solution was stirred at room temperature overnight and the solvent was removed in vacuum. The residue was a white solid. The solid was dissolved in water under cold temperature, but no crystals were found.

22. Reaction of $K_2Pt(NO_2)_4$ with D-Tartaric acid

0.050 g of $K_2Pt(NO_2)_4$ (1.09×10^{-4} mole) was dissolved in a minimum amount of water. 4 eq. of tartaric acid (0.090 g) was added into the solution. It was heated at 85°C for 20 minutes. The solvent was removed in vacuum and a green solid resulted. The green solid was neutralized with a

minimum of water and K_2CO_3 to adjust the pH of the solution to 7. The solution changed to yellow with white and yellow precipitates in it. White ones were considered to be unreacted K_2CO_3 while the yellow ones were found to be $(CHOH)_2(COOK)_2$.

23. Reaction of $Pt_2(HPy)_2(CH_3)_4(Py)_2$ with CCl_3COOH

0.005 g of $Pt_2(CH_3)_4(HPy)_2(Py)_2$ was dissolved in a small amount of chloroform. With the addition of an excess amount of CCl_3COOH, the color of the solution changed from orange to pale yellow. ^1H NMR was used, but the spectrum was too complicated to predict any kind of product. After several months, a tiny needle-like single crystal was grown in the solution and x-ray study was applied to characterize the structure. Unfortunately the crystal was not of sufficient quality to solve the structure, this complex was assumed as CCl_3COO^- ligand coordinated at axial position. The following unit cell parameter was obtained: a=10.891 Å, b=14.416 Å, c=15.542 Å, α=69.289°, ß=84.270°, γ=71.113°. With space group P 1_7 V=2146.1 $Å^3$.

24. Reaction of $Pt_2(CH_3)_4(HPy)_2(Py)_2$ with CF_3COOH

0.005 g of $Pt_2(CH_3)_4(HPy)_2(Py)_2$ was dissolved in a small amount of chloroform. With the addition of an excess (20 eq.) of CF_3COOH, the 1H NMR spectrum immediately changed. The whole spectrum seemed shifted towards lower field and the color of the solution became gradually light

yellow. Integration and single-frequency decoupling were used to try to identify the different resonances, but it was still not clear of the product. Removing the solvent only obtained light yellow powder. Finally the tiny crystals were grown out of an acetone solution. X-ray crystallography study was under way and the unit cell of the crystal was: a=9.1209 Å, b=15.5650 Å, c=17.0275 Å, α=95.236°, ß=92.360°, γ=90.736°. Space group P 1, V=2452.74 $Å^3$.

25. Reaction of Pt(MHPy) with CO

Carbon monoxide was bubbled through a solution of $Pt_2(CH_3)_4(MHPy)_2(Py)$ (5 mg) in about 0.4 mL of chloroform for about 3 minutes. The color of the solution did not change much, but ^1H NMR measurement immediately showed several new resonances formed. These new resonances are presumably the $Pt_2(Py)(CO)$ or $Pt_2(CO)_2$ (HT) complexes. After a day or two, the color of the solution changed to light yellow from orange-yellow and the new resonances kept increasing while the Pt(MHPy) resonances decreased. The sample was left at the cold temperature for the crystalization. Unluckily there were black precipitates in the solution indicating the instability of either the product or the reactant under the influence of the CO attack. Further NMR studies showed the presence of the CH_3 group bonding to the Pt ion due to the presence of Pt-CH_3 satellite. It was concluded that at least one monomer with

a MHPy group still existed. Since the attempt of the reaction was to use the least steric hindered CO to interact with Pt(MHPy), the proper method to keep the product from decomposing was to separate the precipitates from the solution. Attempts to achieve crystalization at very cold temperature failed.

26. Reaction of Pt(MHPy) with KOH

An excess of concentrated KOH solution was added to $Pt_2(CH_3)_4(MHPy)_2(Py)$ (5 mg) in chloroform. The color of the solution changed from orange to black at once and a black solid precipitated. The Pt complex was totally destroyed by the strong base.

27. Reaction of Pt(MHPy) with KCN

A mixture of $Pt_2(CH_3)_4(MHPy)_2(Py)$ (5 mg) with 2 eq. of KCN (1 mg) was dissolved in chloroform and water. The solution was stirred for 2 hours. The solvent was removed in vacuum and the residue was dissolved in the chloroform again (sometimes heating in a water bath was necessary to accelerate the reaction).

The color of the solution, originally orange, became colorless. It was likely to form the $K[Pt_2(CH_3)_4(MHPy)_2(Py)(CN)]$ (HT), but ^1H NMR spectrum showed only a monomer was possible. Besides there was no indication of the Pt-CH_3 bond presence due to the absence of the Pt-CH_3 satellite in the ^1H NMR spectrum. IR spectrum showed there

was a Pt-CN band (2100 cm^{-1}) in the product and MHPy resonance was still observerable. So $Pt(CN)_2(MHPy)$ was a plausible product in the reaction.

28. Reaction of Pt(MHPy) with KSCN

A mixture of $Pt_2(CH_3)_4(MHPy)_2(Py)$ in chloroform and an excess amount of KSCN in water was stirred for several hours and the solvent was removed in vacuum. The white residue was dissolved in the chloroform again. The solution by now was colorless and the ^1H NMR spectrum showed there was no sign for Pt dimer structure, since one did not find the two corresponding satellite resonances for a dimer in the spectrum. It was more likely a decomposed product--a monomer might have formed. Slow evaporation of the solution did not produce crystals suitable for x-ray diffraction studies.

29. Reaction of Pt(HPy) with CH_3COOH

A mixture of $Pt_2(CH_3)_4(MHPy)_2(Py)_2$ (5 mg) with an excess of CH_3COOH in the chloroform was stirred and hoped to transfer Pt(HPy) (HT) to Pt(HPy) (HH). The reaction seemed to go fairly fast and a cloudy precipitate formed. NMR spectrum showed a mess and did not prove the conversion between HT to HH. No further characterization of the precipitate was made.

30. Reaction of Pt(HPy) with pyrazine

An excess of pyrazine (7 mg) was added to $Pt_2(CH_3)_4(HPy)_2(Py)$ (5 mg) in chloroform and also ^1H NMR technique was used to trace and detect the reaction. From the NMR spectrum, it was clear that new resonances appeared fairly soon in the aromatic and methyl regions when the reaction began. The color of the solution gradually changed from orange yellow to light yellow possibly indicating more less-polar compound formation. It was assumed that the pyrazine ligand functioned as an axial bonding with the Pt ion, replacing pyridine, when more pyrazine was added in the solution, the new resonances kept increasing. Nuclear Overhauer (NOE) experiment was tried. Results showed that Pt(HPy) with pyrazine bonded with one axial position and the two Pt(HPy) bonded by pyrazine as a bridging ligand formed.

31. Reaction of Pt(HPy) with 4-methyl pyridine (picoline)

An excess of picoline (C_6H_7N) was added to $Pt_2(CH_3)_4(HPy)_2(Py)$ (5 mg) in chloroform. ^1H NMR was used to find the intermediate or product of this reaction. The color of the solution changed from orange yellow to light yellow. The ^1H NMR spectrum was at first complicated. The reaction turned out to be rapid. The picoline attacked the axial position and formed the Pt-N bond. Approximately the rate of the reaction was classified as Pt(HPy) (HH)-Picoline > Pt(HPy) (HH)-Pyrazine > Pt(HPy) (HH)-Py. The possible

explanation of the series of the rate was due to the trans-effect and the electron donating ability of the incoming ligand. Apparently the methyl group of picoline functioned giving more electrons to the aromatic ring, hence increasing the electron density overall.

32. Reaction of Pt(MHPy) with pyridine

An excess of pyridine was added in the chloroform solution of $Pt_2(CH_3)_4(MHPy)_2(Py)$ and ^1H NMR spectrum showed no indication of $Pt_2(CH_3)_4(MHPy)_2(Py)_2$ formation. From the steric point of view of the Pt(MHPy) structure, it was not difficult to conclude that the bulky methyl group on the MHPy bridge kept the incoming ligand bonding from the metal ion.

33. Reaction of Pt(MHPy) with pyrazine

An excess of pyrazine was added into the solution of $Pt_2(CH_3)_4(MHPy)_2(Py)$ in chloroform. ^1H NMR spectrum also showed no Pt(MHPy) (HT) forming due to the steric effect of the methyl group on the bridge ligand. However dark red crystals formed after the product was recrystalized in acetone. X-ray crystallography characterized this compound as pyrazine substituted pyridine in the axial position.

34. Reaction of Pt(MHPy).($Et^2$2S) with pyrazine

1/2 eq. mole of pyrazine (1 mg) was added into the solution of $Pt_2(CH_3)_4(MHPy)_2(Py)(Et_2S)$ (5 mg) in chloroform. ^1H NMR was used to follow the reaction. This reaction went

very fast but NMR could record the very beginning of the reaction and the increase of the new resonances as well. The color of the solution changed from orange yellow to light yellow over a period of several days. Further addition of pyrazine resulted in the increasing of the new resonances and the disappearance of free diethylsulfide resonance. As diethylsulfide is more volatile than pyrazine, it was clear from the spectrum that diethylsulfide was substituted by the addition of pyrazine. Also there was substantial yellow precipitate in the chloroform solution which was separated from the solution later. This yellow powder has very low solubility in chloroform and benzene, and almost nonsoluble in methanol, acetone, and cyclohexane. From the NMR spectrum, this compound proved to be a mixture of Pt with pyrazine in axial position and Pt-pyrazine-Pt complex with pyrazine functioning as bridge. Efforts to obtain crystals of the complex are still under way.

35. Reaction of $Pt(HPy)$ with C_2H_4

Ethylene gas was bubbling through the chloroform solution of $Pt_2(CH_3)_4(HPy)_2(Py)$ compound and immediate ^1H NMR was measured. The NMR spectrum indicated clearly that there was no new compound formation. Measurements were repeated over several days and no new resonances were formed, thus the possibility that the reaction between the reactants might go very slowly was eliminated.

36. Reaction of Pt(HPy) with HCl (diluted)

$Pt_2(CH_3)_3(HPy)_2(Py)$ was dissolved in chloroform and mixed with the water solution of HCl. There was no obvious color change. The intention of the reaction was to find out how stable the Pt(III) dimer is and if it could stand for the strong acid involvement and the possibility of chloride coordinating the Pt complex in the anion form, hence increase the solubility of the Pt complex in polar solvent. After several days' measurement, there was no indication of the new complex formation.

37. Reaction of Pt(MHPy) with H_2S

H_2S gas was bubbling through the $Pt_2(CH_3)_4(MHPy)_2(Py)$ solution in chloroform. The color of the solution did not change immediately. After a short time (30 minutes), ^1H NMR showed the new product formed and the color of the solution turned foggy. This product's resonance increased very rapidly in NMR and very likely the Pt-S complex formed. After two days reaction, there was a dark-yellow solid sticking on the wall of the NMR tube. Further NMR measurement did give a totally different spectrum without evidences for $Pt-CH_3$ bonding. The structure determination of the dark-yellow solid is still being attempted.

B. Structure Determination

X-ray crystallography data collection:

Crystals of the platinum complexes were carefully examined under a microscope. Those suitable for x-ray diffraction studies were coated with a thin film of epoxy cement and mounted on a glass fiber. X-ray diffraction intensity data were collected on a Nicolet R3mE four circle diffractometer equipped with graphite monochromated Mo Kα radiation (λ = 0.71069 Å). Those data were processed by polarization, Lorentz and absorption corrections. Details of the definition of data for the equipment will follow each platinum complex.

Structure solution for $K_2[Pt_2(NO_2)_4(OH)_2]\cdot 1.5\ H_2O$

A light yellow plate-shaped crystal measuring 0.013 x 0.36 x 0.50 mm was coated with epoxy cement and mounted on the tip of a glass fiber. Unit cell dimensions were obtained by least squares refinement using 15 centered reflections. Three check reflections, monitored every 100 reflections, showed 15% loss of intensity over the course of data collection.

Data reduction, including Lorentz and polarization corrections, gave 4540 independent reflections in the range $4° < 2\Theta < 65°$ of which 1877 with $I > 3\sigma(I)$ were used for structure refinement. The data showed orthorhombic symmetry and systematic absences indicated the space group Ibca. A Patterson function map yielded the platinum positions and

the remaining non-hydrogen atoms were located by difference Fourier maps. These positions were refined with anisotropic thermal parameters by block cascade least squares, minimizing $\Sigma w([Fo]-[Fc])^2$ with 99 parameters refined in each full matrix block.

Absorption corrections were calculated by Gaussian integration using indexed planes to approximate the crystal shape with measured crystal dimensions. Atomic scattering factors, including terms for anomalous scattering, were taken from Cromer and Weber (66). The weighting scheme used was $w=k(\sigma^2(Fo)+0.0001Fo^2)^{-1}$. Final R and Rw were 0.065 and 0.058 respectively. Crystal data and information on data collection appear in Table 13. Atomic positions, thermal parameters, interatomic distances and bond angles appear in Tables 19-22 respectively.

Table 13. Crystallographic Parameters for $K_2[Pt_2(NO_2)_4(OH)_2]\cdot 1\frac{1}{2}\ H_2O$

Formula	$K_2[Pt_2(NO_2)_4(OH)_2]\cdot 1\frac{1}{2}\ H_2O$
Crystal system	Orthorhombic
Space group	Ibca
a Å	11.879 (6)
b Å	13.094 (4)
c Å	32.060 (11)
α deg.	90.0
ß deg.	90.0
γ deg.	90.0
V Å^3	4987(4)
Z	16
Temperature (K)	298
$D_{cal.}$ g/cm^3	3.80
μ (Mok_α) cm^{-1}	233.90
F(000)	5104
Radiation Mok_α (A)	0.71069
Scan mode	Θ-2Θ
Data collection range (2Θ deg.)	4 - 65
Total unique reflections	4540
obs. reflections, I > 3σ(I)	1877
Number of parameters refined	99
data range (hkl)	16, 18, 46
Trans factor, max. min.	58.5%, 5.9%
R^a	0.067
$R_w{}^b$	0.058
Quality of fit indicator^c	1.72
Largest shift/esd, final cycle	0.005
Largest peak, e/Å^3	2.480

a. $R=\Sigma([[F_o]-[F_c]])/\Sigma[F_o]$

b. $R_w=\Sigma([[F_o]-[F_c]])W^{1/2}/\Sigma[F_o]W^{1/2}$

c. Quality of fit indicator$=\Sigma([[F_o]-[F_c]])W^{1/2}/(m-n)^{1/4}$

$W= (\sigma F^2)^{-1}$

Structure solution of $K_5[Pt_4O_3(NO_2)_9]\cdot 3H_2O$

A thin yellow plate-shaped crystal, stable at room temperature and measuring 0.085 x 0.34 x 0.70 mm, was coated with epoxy cement and mounted on a glass fiber. Unit cell

dimensions were obtained from 25 reflections. Structure refinement parameters were about the same as those described for the dimer structure determination procedure. Lorentz, polarization and absorption corrections were applied. The heavy atom positions were determined from a Patterson function map and subsequent difference Fourier maps revealed the remaining non-hydrogen atoms. $w=k(\sigma^2(Fo) + 0.0003F_o^2)^{-1}$ was used as weighting scheme. Least squares refinement resulted in R factors of R=0.0322, R_w=0.0325. Crystal data and information on data collection appear in Table 14. Atomic positions, thermal parameters, interatomic distances, and bond angles appear in Tables 23-26 respectively.

Structure solution of $[Pt_2(CH_3)_4(MHPy)_2(PPh_3)]\cdot 2CH_3COCH_3$

A thin yellow irregular-shaped crystal, measuring 0.15 x 0.36 x 0.16 mm, was coated with epoxy cement and mounted on a glass fiber. Unit cell dimension was obtained by least-squares refinement from 21 centered reflections for which $22° < 2\sigma < 27°$. Three check reflections, monitored every 100 reflections, showed no significant loss of intensity over the course of data collection. Data reduction including corrections for Lorentz and polarization effects gave 8261 independent reflections in the range 3° - 55° of which 2335 with $I > 3\sigma(I)$ were used for structure refinement. Axial photo and diffraction data all showed the systematic absence. Symmetry determined the space group as

Table 14. crystallographic parameters for $K_5[Pt_4(O)_3(NO_2)_9]\cdot 3H_2O$

Formula	$K_5[Pt_4(O)_3(NO_2)_9]\cdot 3\ H_2O$
Crystal system	triclinic
Space group	P 1
a Å	9.940(2)
b Å	10.069(2)
c Å	15.206(3)
α deg.	72.15(1)
ß deg.	74.69(1)
γ deg.	72.24(1)
V $Å^3$	1354.9(4)
Z	2
Temperature (K)	298
D_{cal}.g/cm^3	3.66
$\mu(Mok_\alpha)$ cm^{-1}	217.3
F(000)	1336
Radiation Mok_α (Å)	0.71069
Scan mode	Θ-2Θ
Data collection range (2σ deg.)	4 - 65
Total unique reflections	9836
Obs.reflections, I>3σ(I)	7753
Number of parameters refined	385
Data range (hkl)	±14, ±14, +23
Trans factor, max. min.	16.5%, 0.6%
R^a	0.032
$R_w{}^b$	0.032
Quality of fit indicator[c]	1.480
Largest shift/esd, final cycle	0.011
Largest peak, e/$Å^3$	1.505

a. $R=\Sigma([[F_o]-[F_c]])/\Sigma[F_o]$

b. $R_w=\Sigma([[F_o]-[F_c]])w^{1/2}/\Sigma[F_o]w^{1/2}$

c. Quality of fit indicator = $\Sigma([[F_o]-[F_c]])w^{1/2}/(m-n)^{1/4}$

$w=(\sigma F^2)^{-1}$

monoclinic P $2_1/n$. The platinum positions were determined from a Patterson map. The remaining non-hydrogen atoms' positions were located by difference Fourier maps. The positions of solvent atoms were located by fixing the distances and bond angles among them due to their disordered behavior. The structure was refined by Block-cascade least squares refinement. Absorption corrections were calculated by Gaussian integration using measured crystal dimension between indexed crystal faces. No correction for extinction was needed. The weighting scheme used for final structure refinement was $W=k(\sigma^2(F_o)+0.00001(F_o)^2)^{-1}$. Information on data collection is on Table 15. Crystallographic data appear in Tables 27-30.

Structure solution of $Pt_2(CH_3)_4(C_6H_7NO)_2(C_4H_4N_2)$

A bright red irregular-cubic crystal, measuring 0.18 x 0.16 x 0.42 mm, was mounted on a glass fiber. Unit cell dimensions were obtained from 20 centered reflections. Axial photo and least-squares refinement showed the space group as uncentrosymetrical P $2_12_12_1$. This determination was later confirmed successfully by structure solution. Data reduction gave 3654 unique reflections in the range $4° < 2\sigma < 60°$, of which 2036 with $I > 3\sigma(I)$ were used for structure solution. The platinum positions were calculated from a Patterson synthesis. Other non-hydrogen atoms were obtained from difference maps. Absorption correction was

Table 15. Crystallogaphic parameters for $[Pt_2(CH_3)_4(MHPy)_2(PPh_3)]\cdot 2CH_3COCH_3$

Formula	$Pt_2(CH_3)_4(C_6H_6NO)_2(PPh_3)$
Crystal system	monoclinic B
Space group	P $2_1/n$
a Å	9.593
b Å	17.957
c Å	20.897
α deg.	90.00
ß deg.	92.74
γ deg.	90.00
V Å^3	3595.61
Z	4
Temperature (K)	298
$D_{cal.}$ g/cm^3	1.72
μ ($M_o k_\alpha$) cm^{-1}	79.3
F(000)	1775
Radiation $M_o k_\alpha$ (Å)	0.71069
Scan mode	Ω
Data collection range (2Θ)	3 - 55
Total unique reflections	8261
obs.reflections, I>3σ(I)	2335
Number of parameters refined	207
Data range (hkl)	±13, 21, 28
Trans factor, max., min.	42.3%, 25.2%
R^a	0.0663
$R_w{}^b$	0.0512
Quality of fit indicator^c	1.599
Largest shift/esd, final cycle	0.005
Largest peak, e/Å^3	1.640

a. $R=\Sigma([[F_o]-[F_c]])/\Sigma[F_o]$

b. $R_w=\Sigma([[F_o]-[F_c]])w^{1/2}/\Sigma[F_o]w^{1/2}$

c. Quality of fit indicator= $\Sigma([[F_o]-[F_c]])w^{1/4}/(m-n)^{1/4}$

$w=(\sigma F^2)^{-1}$

Table 16. Crystallogaphic parameters for $Pt_2(CH_3)_4(C_6H_6NO)_2(C_4H_4N_2)$

Formula	$Pt_2(CH_3)_4(C_6H_6N_O)(C_4H_4N_2)$
Crystal system	Orthorombic
Space group	P $2_12_12_1$
a Å	9.4890
b Å	11.8210
c Å	19.7860
α deg.	90.0
ß deg.	90.0
γ deg.	90.0
V Å^3	2219.38
Z	8
Temperature (K)	298
$D_{cal.}$ g/cm^3	2.16
μ (Mok_α) cm^{-1}	127.4
F(000)	1359
Radiation M_ok_α(Å)	0.71069
Scan mode	Θ/2Θ
Data collection range (2Θ)	4 - 60
Total unique reflections	3654
Obs.reflections, I > 3σ(I)	2036
Number of parameters refined	254
Data range (hkl)	11, 13, 22
Trans.factor, max. min.	19.2% 7.0%
R[a]	0.0478
R_w[b]	0.0484
Quality of fit indicator[c]	1.018
Largest shift/esd, final cycle	0.004
largest peak, e/Å^3	1.606

a. $R=\Sigma([[F_o]-[F_c]])/\Sigma[F_o]$

b. $R_w=\Sigma([[F_o]-[F_c]])w^{1/2}$

c. Quality of fit indicator$=\Sigma([[F_o]-[F_c]])w^{1/2}/(m-n)^{1/4}$

$w=(\sigma F^2)^{-1}$

calculated. No extinction corrections were needed. The final structure was refined with anisotropic thermal parameters for all atoms and weighting scheme as $W=k(\sigma^2(F_o)+0.0013(F_o)^2)^{-1}$. Crystallographic data is on Table 16. Atomic coordination parameters are given in Table 31, thermal parameters appear in Table 32. Bond lengths and bond angles are given in Tables 33-34 separately.

Structure solution of cis-$PtCl_2(Et_2S)_2$

A greenish yellow crystal with dimensions 0.06 x 0.31 x 0.25 mm was coated with epoxy cement and mounted on a glass fiber. A Nicolet R3mE diffractometer was used to collect 5367 unique reflections of which 1849 had $I \geq 3\sigma(I)$. Lorentz and polarization corrections were applied. The crystallographic parameters and procedural data are summerized in Table 17. Platinum atom coordinates were obtained from a Patterson map, the other atoms were located in an alternating series of difference electron density maps and least squares refinement. Atomic scattering factors, including anomalous scattering, were also taken from Cromer and Weber (66). The weighting scheme used was $W=k[\sigma^2(F_o)+0.0004(F_o)^2]^{-1}$. The structure was refined to satisfactory low residuals of R=0.0467 and R_w=0.0420 for treating all atoms anisotropically while omitting hydrogen atoms entirely. Other crystallographic data are shown in Tables 35-38.

Table 17. Crystallogaphic parameters for cis-$PtCl_2(Et_2S)_2$

Formula	$PtCl_2[(CH_2CH_3)_2S]_2$
Crystal system	monoclinic
Space group	P $2_1/n$
a Å	10.797
b Å	11.393
c Å	12.209
α deg.	90.00
ß deg.	100.64
γ deg.	90.00
V $Å^3$	1476.60
Z (molecules/cell)	4
Temperature (K)	298
$D_{cal.}$ g/cm^3	2.01
μ ($M_o k_\alpha$) cm^{-1}	102.1
F(000)	848
Radiation $M_o k\alpha$ (Å)	0.71069
Scan mode	Θ-2Θ
Data collection range (2Θ deg.)	4 - 65
Total unique reflections	5367
Obs.reflections, I > 3σ(I)	1849
Number of parameters refined	118
Data range (hkl)	±16, 17, 18
Trans factor, max. min.	52.10%, 16.80%
R^a	0.046
$R_w{}^b$	0.042
Quality of fit indicator[c]	1.16
Largest shift/esd, final cycle	0.080
Largest peak, e/$Å^3$	1.262

a. $R=\Sigma([[F_o]-[F_c]])/\Sigma[F_o]$

b. $R_w=\Sigma([[F_o]-[F_c]])w^{1/2}/\Sigma[F_o]w^{1/2}$

c. Quality of fit indicator$=\Sigma([[F_o]-[F_c]])w^{1/2}/(m-n)^{1/4}$

$w=(\sigma F^2)^{-1}$

Structure solution of trans-$PtCl_2(Et_2S)_2$

An orange yellow crystal with dimensions of 0.22 x 0.78 x 0.68 mm was mounted on a glass fiber with epoxy cement. A Nicolet R3mE diffractometer was used to collect 3769 unique datum in which 1601 had reflections with $I \geq 3\sigma(I)$. Lorentz, polarization and absorption corrections were made. No decay correction was necessary as no loss of intensity was found over the course of the data collection. Relevent crystal parameters and data are given in Table 18. The platinum atom position was obtained from a Patterson function. Alternating least squares cycles and difference Fourier maps revealed the remaining non-hydrogen atoms. Structure was refined to satisfactory low residuals of R=0.045 and R_w=0.047 by treating all atoms anisotropically while omitting hydrogen atoms entirely. Bond angles, bond lengths, positional and thermal parameters are shown in Tables 39-42.

X-ray crystallographic results:

The structural results of the various complexes for which crystals of sufficient quality were obtained are described in the following section; supplying results follow the x-ray crystallographic structures. The observed and calculated structure factors for the listed compounds (**1-6**) are available in Department of Chemistry of Montana State University.

Table 18. Crystallogaphic parameters for trans-$PtCl_2(Et_2S)_2$

Formula	$PtCl_2[(CH_2CH_3)_2S]_2$
Crystal system	monoclinic
Space group	$P2_1/n$
a Å	7.669
b Å	7.772
c Å	12.035
α deg.	90.00
ß deg.	94.05
γ deg.	90.00
V $Å^3$	715.5
Z	2
$D_{cal.}$ g/cm^3	2.07
Temperature (K)	298
$\mu(M_o k\alpha)$ cm^{-1}	105.3
F(000)	424
Radiation $M_o k_\alpha$ (Å)	0.71069
Scan mode	Ω
Data reflections range (2Θ deg.)	3 - 75
Total unique reflections	3769
Obs.reflections, $I>3\sigma(I)$	1601
Number of parameters refined	61
Data range (hkl)	±13, 13, 20
Trans factor, max., min.	14.60%, 1.90%
R^a	0.045
$R_w{}^b$	0.047
Quality of fit indicator[c]	1.09
Largest shift/esd, final cycle	0.003
Largest peak, $e/Å^3$	0.861

a. $R=\Sigma([[F_o]-[F_c]])/\Sigma[F_o]$

b. $R_w=\Sigma([[F_o]-[F_c]])w^{1/2}/\Sigma[F_o]w^{1/2}$

c. quality of fit indicator$=\Sigma([[F_o]-[F_c]])w^{1/2}/(m-n)^{1/4}$
$w=(\sigma F^2)^{-1}$

Structure of $K_2[Pt_2(NO_2)_4(OH)_2]\cdot 1.5H_2O$

An ORTEP view of the molecule is shown in Figure 22. Tables 19 and 20 contain the final atomic coordinate and

anisotropic thermal parameters. Tables 21 and 22 list the bond lengths and bond angles respectively.

This structure displays the features of platinum dimer bridged by hydroxo ligands. The N-Pt-N bond angle is 98.1 degrees and makes each platinum atom nearly square planar. The torsion angle between N-Pt-O is about 170.8 degrees. The ligands are nearly coplanar with platinum atoms. The oxidation state of the platinum is based on the approximately square-planar geometry of the metal ion. X-ray crystallographic data do not permit an absolute determination of whether the bridging ligand is an oxo group or hydroxo group. If the bridging ligands are oxo groups, the platinum valence state would be Pt(III) due to the charge balance of the molecule. A Pt(III) complex should form a platinum-platinum bond. There is no structure evidence of the metal-metal bond formation in the x-ray characterization. Hence the oxidation state of the platinum is most likely assigned as Pt(II).

A striking feature of this structure is the short distance between platinum ions in adjacent dimer molecules. In dimer A, (Figure 28), the nitrite ligand is distorted. This distortion appears to be relative to the interaction between the two dimers. These two paired dimers are related by a crystallographic two-fold axis, and the hydrogen bonding

involves the proton of the bridging groups and nitrito oxygen, and a lattice water molecule located on the two-fold axis. Thus, distortion results. The distance between platinum 1 and platinum 1' is 3.29(5) Å which is short between two molecules, suggesting a substantial interaction between Pt ions. This interaction could not come from platinum ions, because they both have positive charge and the interaction would be repulsive. In a related compound, it has been proposed that there is a charge repulsion between the platinum atoms of the paired dimer units, resulting in a small displacement (0.09 Å) of the platinum atoms from their ligand planes (48). No significant displacement is seen for the analogous platinum atoms in the anion pair we have studied. The close approach between platinum 1 and platinum 1' paired cations is the consequence of hydrogen bonding between the proton on the hydroxo bridge and the two ligand atoms (Pt-N-H .... O-Pt). The average Pt-O bond length is 2.035 Å.

Structure of $K_5[Pt_4O_3(NO_2)_9]\cdot 3H_2O$

An ORTEP drawing of the molecule is shown in Figure 23. Table 23 and Table 24 consist of final atomic coordinated and anisotropic thermal parameters. Table 25 and Table 26 list the bond lengths and bond angles of the molecule.

This structure features one 6 coordinated platinum ion linked symmetrically to each of three 4 coordinated

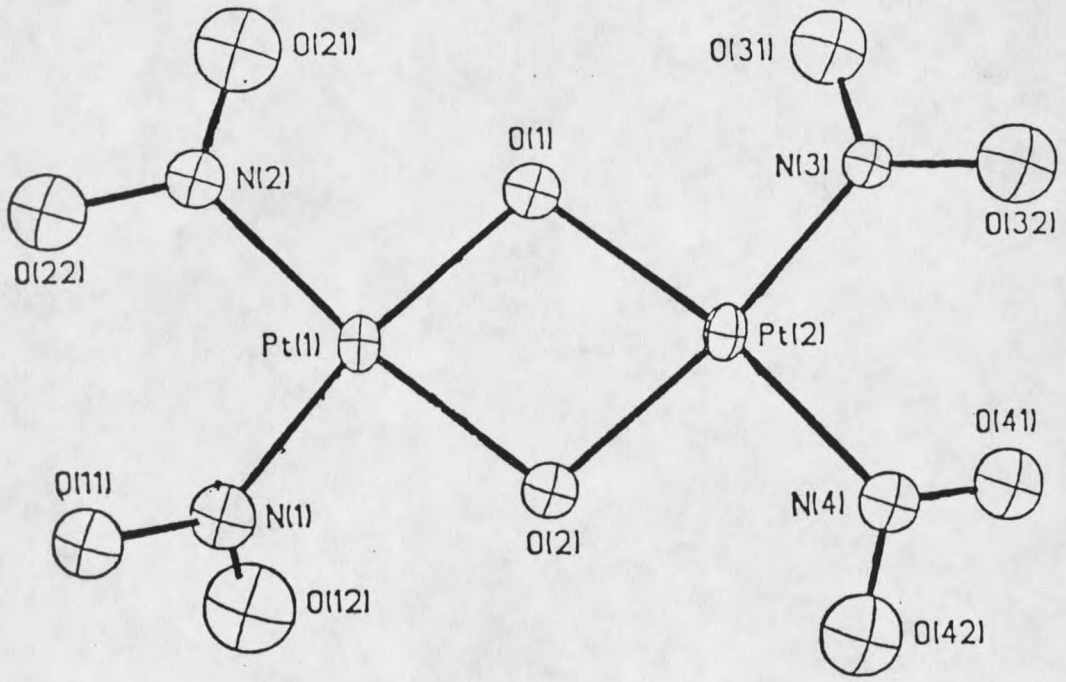

Figure 22. ORTEP view of $K_2[Pt_2(NO_2)_4(OH)_2]\cdot 1.5H_2O$

Table 19. Atom coordinates and isotropic temperature factors (Å²) with standard deviations for $K_2[Pt_2(NO_2)_4(OH)_2]\cdot 1\frac{1}{2}H_2O$

	x/a	y/b	z/c	U
Pt(1)	0.5117(1)	0.1249(1)	0.6098(1)	0.019(1)[a]
Pt(2)	0.2657(1)	0.1370(1)	0.6415(1)	0.020(1)[a]
O(1)	0.426(1)	0.112(1)	0.664(1)	0.025(4)
O(2)	0.351(1)	0.124(1)	0.587(1)	0.024(4)
N(1)	0.569(2)	0.133(2)	0.555(1)	0.032(5)
O(11)	0.648(2)	0.193(1)	0.542(1)	0.033(4)
O(12)	0.534(2)	0.076(2)	0.529(1)	0.068(7)
N(2)	0.658(2)	0.114(1)	0.640(1)	0.027(4)
O(21)	0.656(2)	0.113(1)	0.677(1)	0.056(6)
O(22)	0.750(2)	0.110(1)	0.619(1)	0.047(5)
N(3)	0.208(2)	0.153(1)	0.697(1)	0.019(4)
O(31)	0.252(2)	0.109(1)	0.726(1)	0.045(5)
O(32)	0.120(2)	0.206(1)	0.706(1)	0.046(5)
N(4)	0.120(2)	0.152(1)	0.610(1)	0.028(5)
O(41)	0.032(2)	0.125(1)	0.625(1)	0.040(5)
O(42)	0.119(2)	0.183(1)	0.575(1)	0.050(6)
O(3)[b]	0.5000	0.2500	0.721(1)	0.027(5)
O(4)[b]	0.535(2)	0.0000	0.7500	0.041(7)
O(5)[b]	0.2500	0.446(2)	0.0000	0.070(10)
K(1)[b]	0.3895(4)	0.5866(4)	0.1947(3)	0.067(3)[a]
K(2)[b]	0.1183(5)	0.0981(5)	0.0514(3)	0.080(3)[a]

[a]Equivalent isotropic U defined as one-third of the trace of the orthagonalized U_{ij} tensor. [b]Not shown in Figure 22.

Table 20. Anisotropic thermal parameters (Å² x 10^3) with standard deviation for $K_2[Pt_2(NO_2)_4(OH)_2]\cdot 1\frac{1}{2}H_2O$

	U_{11}	U_{22}	U_{33}	U_{23}	U_{13}	U_{12}
Pt(1)	14(1)	19(1)	25(1)	-2(1)	3(1)	0(1)
Pt(2)	14(1)	18(1)	27(1)	1(1)	2(1)	-2(1)
K(1)	49(3)	64(3)	88(6)	0(3)	-4(4)	2(2)
K(2)	53(4)	110(5)	78(7)	-5(4)	0(4)	-10(3)

The anisotropic temperature factor exponent takes the form: $-2\pi^2(h^2a^{*2}U_{11} + \ldots + 2hka^*b^*U_{12})$

Table 21. Bond lengths (Å) with standard deviations for $K_2\{Pt_2(NO_2)_4(OH)_2]\cdot 1\frac{1}{2}H_2O$

Pt(1)-O(1)	2.02(2)	Pt(1)-O(2)	2.05(2)
Pt(1)-N(1)	1.90(3)	Pt(1)-N(2)	1.99(2)
Pt(2)-O(1)	2.06(2)	Pt(2)-O(2)	2.04(2)
Pt(2)-N(3)	1.90(2)	Pt(2)-N(4)	2.01(2)
N(1)-O(11)	1.28(3)	N(1)-O(12)	1.19(4)
N(2)-O(21)	1.19(4)	N(2)-O(22)	1.28(3)
N(3)-O(31)	1.22(4)	N(3)-O(32)	1.29(3)
N(4)-O(41)	1.20(3)	N(4)-O(42)	1.20(4)

Table 22. Bond angles (°) with standard deviation for $K_2[Pt_2(NO_2)_4(OH)_2]\cdot 1\frac{1}{2}H_2O$

O(1)-Pt(1)-O(2)	81(1)	O(1)-Pt(1)-N(1)	171(1)
O(2)-Pt(1)-N(1)	90(1)	O(1)-Pt(1)-N(2)	91(1)
O(2)-Pt(1)-N(2)	171(1)	N(1)-Pt(1)-N(2)	98(1)
O(1)-Pt(2)-O(2)	80(1)	O(1)-Pt(2)-N(3)	92(1)
O(2)-Pt(2)-N(3)	171(1)	O(1)-Pt(2)-N(4)	170(1)
O(2)-Pt(2)-N(4)	90(1)	N(3)-Pt(2)-N(4)	98(1)
Pt(1)-O(1)-Pt(2)	99(1)	Pt(1)-O(2)-Pt(2)	99(1)
Pt(1)-N(1)-O(11)	127(2)	Pt(1)-N(1)-O(12)	119(2)
O(11)-N(1)-O(12)	114(3)	Pt(1)-N(2)-O(21)	118(2)
Pt(1)-N(2)-O(22)	120(2)	O(21)-N(2)-O(22)	122(3)
Pt(2)-N(3)-O(31)	121(2)	Pt(2)-N(3)-O(32)	125(2)
O(31)-N(3)-O(32)	115(2)	Pt(2)-N(4)-O(41)	122(2)
Pt(2)-N(4)-O(42)	121(2)	O(41)-N(4)-O(42)	117(3)

platinums through oxo bridges. The structure looks like a "crown" in that the four platinum ions form a trigonal pyramidal frame. The oxidation state of the platinum ions are simply based on the configuration of the metal ions and the charge balance of the molecule. The unique Pt ion is Pt(IV) and the other three are Pt(II). The Pt(II)-O bond lengths average 2.04 Å, but the unique Pt(IV)-O bond lengths average 2.029 Å which is even shorter than that in the dimer case. It is only true when the oxidation state of the platinum ion has a higher positive charge, so it makes a stronger bond with its negative charged ligands, thus the shorter bond length. The bond angles between platinum with its ligands (ave. 81.67 degrees) indicate that the geometry of each coordination is distorted due to strong steric repulsion between nitrite groups.

Structure of $Pt_2(CH_3)_4(C_6H_6NO)_2(PPh_3)$

An ORTEP view of the molecule is shown in Figure 24. Table 27 and Table 28 contain the final atomic coordinate and anisotropic thermal parameters. Table 29 and Table 30 list the bond lengths and bond angles respectively.

The molecular structure consists of a binuclear platinum(III) molecule with two MHPy bridging ligands coordinating the two platinum ions in a polar (HH) fashion. The Pt-Pt bond distance is 2.615 Å. The one axial ligand is PPh_3 while another axial position is unoccupied. The PPh_3

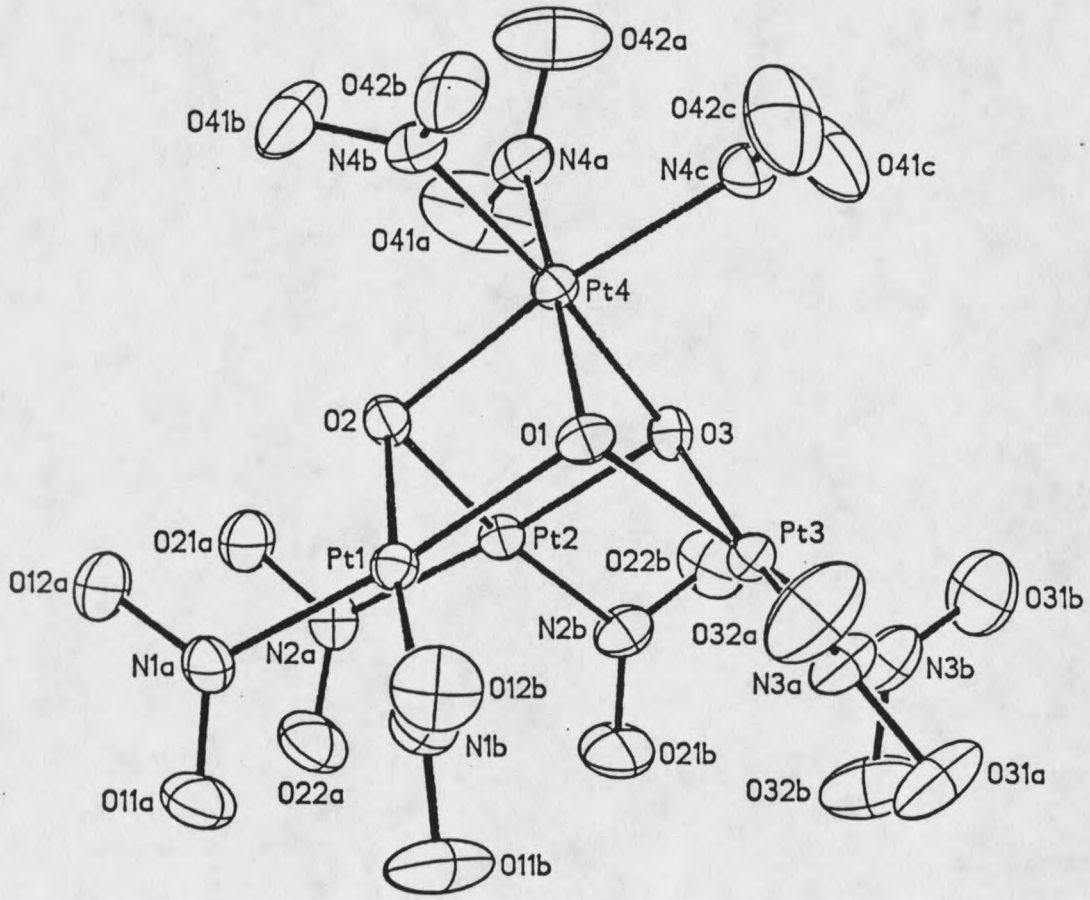

Figure 23. ORTEP view of $K_5[Pt_4(NO_2)_9(O)_3]\cdot 3H_2O$

Table 23. Atom coordinates and equivalent isotropic temperature factors ($Å^2$) with standard deviations for $K_5[Pt_4(NO_2)_9(O)_3]\cdot 3H_2O$

	x/a	y/b	z/c	U_{eq}[a]
Pt(1)	0.0595(1)	0.2004(1)	0.3804(1)	0.019(1)
Pt(2)	0.3470(1)	0.2656(1)	0.2632(1)	0.019(1)
Pt(3)	0.0567(1)	0.3895(1)	0.1702(1)	0.021(1)
Pt(4)	0.2142(1)	0.0715(1)	0.2104(1)	0.019(1)
O(1)	0.0208(5)	0.1977(5)	0.2555(4)	0.022(2)
O(2)	0.2601(5)	0.0920(5)	0.3273(3)	0.022(2)
O(3)	0.2651(5)	0.2652(5)	0.1545(3)	0.022(2)
N(1a)	0.1197(7)	0.1843(7)	0.4976(4)	0.027(2)
O(11a)	0.0990(7)	0.2879(7)	0.5306(4)	0.042(3)
O(12a)	0.1876(8)	0.0669(7)	0.5370(4)	0.050(3)
N(1b)	-0.1353(6)	0.3177(7)	0.4201(5)	0.029(2)
O(11b)	-0.1522(7)	0.4334(8)	0.4379(6)	0.055(3)
O(12b)	-0.2441(6)	0.2814(8)	0.4236(5)	0.044(3)
N(2a)	0.4272(6)	0.2470(7)	0.3753(4)	0.024(2)
O(21a)	0.5086(7)	0.1288(7)	0.4046(4)	0.040(2)
O(22a)	0.3939(7)	0.3417(8)	0.4172(5)	0.045(3)
N(2b)	0.4210(7)	0.4363(7)	0.1885(5)	0.031(2)
O(21b)	0.4032(8)	0.4510(7	0.2193(5)	0.052(3)
O(22b)	0.4782(7)	0.4380(8)	0.1050(4)	0.047(3)
N(3a)	-0.1514(7)	0.4880(7)	0.1818(5)	0.031(2)
O(31a)	-0.1948(7)	0.6213(7)	0.1554(6)	0.050(3)
O(32a)	-0.2400(7)	0.4159(8)	0.2103(6)	0.058(3)
N(3b)	0.1150(7)	0.5662(7)	0.0893(5)	0.035(3)
O(31b)	0.1705(10)	0.5740(8)	0.0065(5)	0.063(4)
O(32b)	0.1040(8)	0.6665(8)	0.1236(6)	0.061(4)
N(4a)	0.4176(7)	-0.0449(7)	0.1688(5)	0.032(2)
O(41a)	0.5182(9)	-0.0252(14)	0.1857(10)	0.089(7)
O(42a)	0.4337(10)	-0.1332(12)	0.1253(9)	0.074(5)
N(4b)	0.1551(7)	-0.1150(7)	0.2809(5)	0.028(2)
O(41b)	0.2281(7)	-0.2031(7)	0.3366(5)	0.048(3)
O(42b)	0.0438(7)	-0.1367(7)	0.2723(5)	0.043(3)
N(4c)	0.1623(7)	0.0800(7)	0.0880(4)	0.029(2)
O(41c)	0.2461(9)	0.1192(10)	0.0155(5)	0.062(4)
O(42c)	0.0519(8)	0.0539(10)	0.0867(6)	0.068(4)
O(4)[b]	0.2670(8)	0.1887(9)	0.6794(5)	0.057(3)
O(5)[b]	0.2707(8)	0.8320(9)	-0.1090(6)	0.060(3)
O(6)[b]	0.4381(8)	0.3946(9)	0.6353(7)	0.068(4)
K(1)[b]	0.5726(2)	0.1415(2)	0.5729(1)	0.036(1)
K(2)[b]	0.7771(2)	0.1172(2)	0.2889(1)	0.038(1)
K(3)[b]	0.1402(3)	0.1202(2)	-0.1333(2)	0.045(1)
K(4)[b]	0.1329(2)	0.5445(2)	0.3703(2)	0.047(1)
K(5)[b]	0.3934(2)	0.3358(2)	-0.0361(2)	0.042(1)

[a]Equivalent isotropic U defined as one-third of the trace of the orthogonalized U_{ij} tensor. [b]The potassium and water oxygen atoms are not shown in Figure 23.

Table 24. Anisotropic thermal parameters ($Å^2x10^3$) with standard deviation for $K_5[Pt_4(NO_2)_9O_3]\cdot 3H_2O$

	U_{11}	U_{22}	U_{33}	U_{23}	U_{13}	U_{12}
Pt(1)	21(1)	18(1)	18(1)	-3(1)	-2(1)	-6(1)
Pt(2)	19(1)	19(1)	21(1)	-5(1)	-3(1)	-7(1)
Pt(3)	25(1)	17(1)	21(1)	-3(1)	-7(1)	-5(1)
Pt(4)	21(1)	17(1)	19(1)	-4(1)	-3(1)	-6(1)
O(1)	20(2)	19(2)	27(2)	-7(2)	-3(2)	-3(2)
O(2)	22(2)	24(2)	19(2)	-6(2)	-5(2)	-4(2)
O(3)	22(2)	24(2)	18(2)	-1(2)	-4(2)	-8(2)
N(1a)	30(3)	28(3)	19(3)	-5(2)	0(2)	-10(2)
O(11a)	49(3)	42(4)	42(3)	-24(3)	-17(3)	-1(3)
O(12a)	76(5)	32(3)	38(4)	-3(3)	-34(4)	6(3)
N(1b)	24(3)	32(3)	31(3)	-12(3)	-3(2)	-5(2)
O(11b)	45(4)	41(4)	89(6)	-41(4)	-17(4)	7(3)
O(12b)	27(3)	52(4)	52(4)	-16(3)	-1(3)	-12(3)
N(2a)	18(2)	31(3)	24(3)	-3(2)	-4(2)	-9(2)
O(21a)	44(3)	36(3)	41(3)	-7(3)	-23(3)	0(3)
O(22a)	49(4)	53(4)	42(4)	-23(3)	-16(3)	-8(3)
N(2b)	31(3)	24(3)	39(4)	-6(3)	-6(3)	-10(2)
O(21b)	81(5)	36(4)	52(4)	-17(3)	-10(4)	-29(4)
O(22b)	56(4)	54(4)	33(3)	-8(3)	10(3)	-32(3)
N(3a)	31(3)	17(3)	43(4)	-3(2)	-12(3)	-2(2)
O(31a)	40(3)	22(3)	83(5)	-3(3)	-23(4)	2(2)
O(32a)	33(3)	40(4)	87(6)	3(4)	-13(4)	-9(3)
N(3b)	31(3)	25(3)	41(4)	3(3)	-4(3)	-8(3)
O(31b)	91(6)	46(4)	44(4)	9(3)	-9(4)	-30(4)
O(32b)	60(4)	33(4)	88(6)	-23(4)	7(4)	-20(3)
N(4a)	33(3)	24(3)	34(4)	-6(3)	3(3)	-6(3)
O(41a)	36(4)	117(10)	143(11)	-85(9)	-33(6)	9(5)
O(42a)	51(5)	65(7)	113(9)	-61(6)	5(5)	-2(5)
N(4b)	34(3)	20(3)	32(3)	-6(2)	-8(3)	-9(2)
O(41b)	56(4)	26(3)	64(5)	8(3)	-32(4)	-12(3)
O(42b)	47(3)	35(3)	50(4)	6(3)	-16(3)	-27(3)
N(4c)	39(3)	26(3)	26(3)	-6(2)	-7(3)	-13(3)
O(41c)	84(5)	91(6)	29(4)	-14(4)	-2(4)	-53(5)
O(42c)	70(5)	95(7)	58(5)	-1(4)	-33(4)	-48(5)
O(4)	57(4)	74(6)	51(4)	-19(4)	-20(4)	-19(4)
O(5)	57(4)	54(5)	61(5)	-8(4)	-8(4)	-14(4)
O(6)	56(4)	51(5)	98(7)	-37(5)	-2(5)	-7(4)
K(1)	38(1)	32(1)	37(1)	-3(1)	-14(1)	-6(1)
K(2)	35(1)	40(1)	41(1)	-8(1)	-7(1)	-15(1)
K(3)	67(1)	33(1)	40(1)	-11(1)	-16(1)	-12(1)
K(4)	49(1)	26(1)	57(1)	-13(1)	7(1)	-10(1)
K(5)	49(1)	41(1)	39(1)	-12(1)	3(1)	-23(1)

The anisotropic temperature factor exponent takes the form: $-2\pi^2(h^2a^{*2}U_{11} + \ldots + 2hka^*b^*U_{12})$

Table 25. Bond lengths (Å) with standard deviations for $K_5[Pt_4(NO_2)_9(O)_3]\cdot 3H_2O$

Pt(1)-O(1)	2.045(6)	Pt(1)-O(2)	2.045(4)
Pt(1)-N(1a)	1.972(7)	Pt(1)-N(1b)	1.983(6)
Pt(2)-O(2)	2.045(5)	Pt(2)-O(3)	2.028(6)
Pt(2)-N(2a)	2.002(7)	Pt(2)-N(2b)	1.979(9)
Pt(3)-O(1)	2.044(5)	Pt(3)-O(3)	2.063(4)
Pt(3)-N(3a)	1.989(6)	Pt(3)-N(3b)	1.982(7)
Pt(4)-O(1)	2.032(4)	Pt(4)-O(2)	2.030(6)
Pt(4)-O(3)	2.035(5)	Pt(4)-N(4a)	2.049(6)
Pt(4)-N(4b)	2.031(7)	Pt(4)-N(4c)	2.030(8)
N(1a)-O(11a)	1.23(1)	N(1a)-O(12a)	1.23(1)
N(1b)-O(11b)	1.23(1)	N(1b)-O(12b)	1.23(1)
N(2a)-O(21a)	1.24(1)	N(2a)-O(22a)	1.22(1)
N(2b)-O(21b)	1.23(1)	N(2b)-O(22b)	1.24(1)
N(3a)-O(31a)	1.25(1)	N(3a)-O(32a)	1.22(1)
N(3b)-O(31b)	1.22(1)	N(3b)-O(32b)	1.24(1)
N(4a)-O(41a)	1.18(2)	N(4a)-O(42a)	1.21(2)
N(4b)-O(41b)	1.23(1)	N(4b)-O(42b)	1.24(1)
N(4c)-O(41c)	1.23(1)	N(4c)-O(42c)	1.21(1)

Table 26. Bond angles (°) with standard deviation for $K_5[Pt_4(NO_2)_9(O)_3]\cdot 3H_2O$

O(1)-Pt(1)-O(2)	81.3(2)	O(1)-Pt(1)-N(1a)	172.7(2)
O(2)-Pt(1)-N(1a)	91.6(2)	O(1)-Pt(1)-N(1b)	94.8(3)
O(2)-Pt(1)-N(1b)	174.7(2)	N(1a)-Pt(1)-N(1b)	92.4(3)
O(2)-Pt(2)-O(3)	81.9(2)	O(2)-Pt(2)-N(2a)	93.2(2)
O(3)-Pt(2)-N(2a)	174.7(2)	O(2)-Pt(2)-N(2b)	173.3(3)
O(3)-Pt(2)-N(2b)	91.5(3)	N(2a)-Pt(2)-N(2b)	93.5(3)
O(1)-Pt(3)-O(3)	81.0(2)	O(1)-Pt(3)-N(3a)	93.9(2)
O(3)-Pt(3)-N(3a)	172.2(3)	O(1)-Pt(3)-N(3b)	173.4(2)
O(3)-Pt(3)-N(3b)	92.7(2)	N(3a)-Pt(3)-N(3b)	92.6(3)
O(1)-Pt(4)-O(2)	82.0(2)	O(1)-Pt(4)-O(3)	82.0(2)
O(2)-Pt(4)-O(3)	82.1(2)	O(1)-Pt(4)-N(4a)	174.8(3)
O(2)-Pt(4)-N(4a)	93.9(3)	O(3)-Pt(4)-N(4a)	94.3(2)
O(1)-Pt(4)-N(4b)	93.9(2)	O(2)-Pt(4)-N(4b)	92.1(3)
O(3)-Pt(4)-N(4b)	173.3(3)	N(4a)-Pt(4)-N(4b)	89.5(3)
O(1)-Pt(4)-N(4c)	93.9(2)	O(2)-Pt(4)-N(4c)	172.3(2)
O(3)-Pt(4)-N(4c)	91.0(3)	N(4a)-Pt(4)-N(4c)	89.8(3)
N(4b)-Pt(4)-N(4c)	94.6(3)	Pt(1)-O(1)-Pt(3)	102.2(3)
Pt(1)-O(1)-Pt(4)	98.0(2)	Pt(3)-O(1)-Pt(4)	97.0(2)
Pt(1)-O(2)-Pt(2)	97.9(2)	Pt(1)-O(2)-Pt(4)	98.1(2)
Pt(2)-O(2)-Pt(4)	96.9(2)	Pt(2)-O(3)-Pt(3)	106.6(2)
Pt(2)-O(3)-Pt(4)	97.3(2)	Pt(3)-O(3)-Pt(4)	96.3(2)
Pt(1)-N(1a)-O(11a)	123.2(5)	Pt(1)-N(1a)-O(12a)	118.4(6)
O(11a)-N(1a)-O(12a)	118.3(8)	Pt(1)-N(1b)-O(11b)	121.3(6)
Pt(1)-N(1b)-O(12b)	121.5(6)	O(11b)-N(1b)-O(12b)	117.1(6)
Pt(2)-N(2a)-O(21a)	116.3(6)	Pt(2)-N(2a)-O(22a)	123.2(5)
O(21a)-N(2a)-O(22a)	120.4(7)	Pt(2)-N(2b)-O(21b)	122.8(5)
Pt(2)-N(2b)-O(22b)	116.5(7)	O(21b)-N(2b)-O(22b)	120.5(7)
Pt(3)-N(3a)-O(31a)	122.3(6)	Pt(3)-N(3a)-O(32a)	119.2(5)
O(31a)-N(3a)-O(32a)	118.3(7)	Pt(3)-N(3b)-O(31b)	120.6(7)
Pt(3)-N(3b)-O(32b)	120.1(6)	O(31b)-N(3b)-O(32b)	119.1(8)
Pt(4)-N(4a)-O(41a)	120.6(8)	Pt(4)-N(4a)-O(42a)	119.1(7)
O(41a)-N(4a)-O(42a)	120.3(9)	Pt(4)-N(4b)-O(41b)	118.5(6)
Pt(4)-N(4b)-O(42b)	121.2(5)	O(41b)-N(4b)-O(42b)	120.2(7)
Pt(4)-N(4c)-O(41c)	116.2(7)	Pt(4)-N(4c)-O(42c)	121.5(5)
O(41c)-N(4c)-O(42c)	122.3(9)		

bonds the platinum ion through the phosphorus atom and the Pt-P bond length is 2.287 Å. The PPh_3 molecule is not colinear with the Pt-Pt vector and the Pt-Pt-P angle is 168.6 degrees, which deviates from the ideal 180 degrees due to the steric repulsion of the hydrogens on methyl groups. Also the PPh_3 molecule is oriented so that the molecule is directed between the methyl groups. The steric repulsion between the methyl groups in the equatorial planes also causes the torsion between metal-metal bond (Figure 26). The torsion angle is 30 degrees in this structure. The average Pt-C bond length is 2.038 Å.

Structure of $Pt_2(CH_3)_4(C_6H_6NO)_2(C_4H_4N_2)$

An ORTEP view is shown in Figure 25. Table 31 and Table 32 contain the final atomic coordinate and anisotropic thermal parameters. Table 33 and Table 34 list the bond distances and bond angles separately.

The structure is very similar to the Pt(MHPy) with one axial pyridine molecule that was discussed before (54). The MHPy bridging ligands bonded the two platinum ions in a polar fashion and the methyl group on the bridging MHPy blocks the axial site, so the molecule has one end with axial pyrazine and the other end is empty. The Pt_2^{6+} unit is bridged tightly. The Pt-Pt bond length is 2.536 Å, which is close to the one just discussed. The axial pyrazine molecule is bent away from the methyl groups and strongly

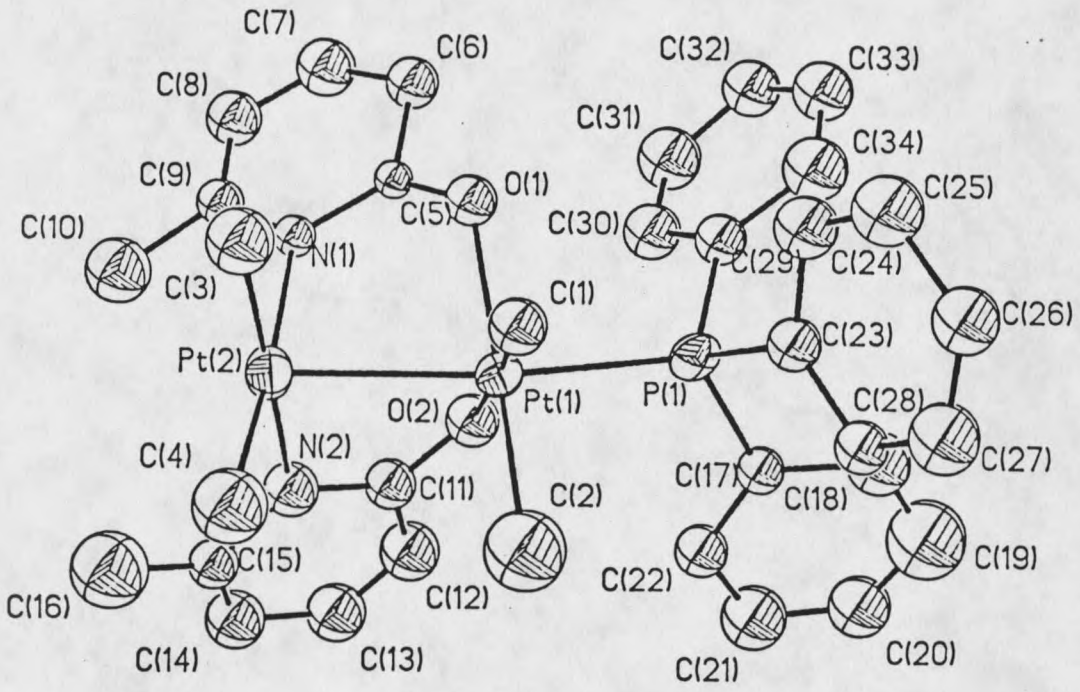

Figure 24. ORTEP view of $Pt_2(CH_3)_4(MHPy)_2(PPh_3)$

Table 27. Atomic coordinates and isotropic temperature factors (Å) with standard deviations for $[Pt_2(CH_3)_4(C_6H_6NO)_2(PPh_3)]\cdot 2CH_3COCH_3$

	x/a	y/b	z/c	U
Pt1	0.0885(1)	0.7302(1)	0.5961(1)	0.031(1)
Pt2	-0.0108(1)	0.7967(1)	0.4923(1)	0.038(1)
C1	0.243(3)	0.803(2)	0.615(1)	0.039(8)
H1a	0.3305	0.7910	0.5901	0.078(2)
H1b	0.2706	0.8001	0.6600	0.078(2)
H1c	0.2104	0.8523	0.6052	0.078(2)
C2	-0.0253(3)	0.787(2)	0.663(2)	0.086(1)
H2a	-0.1150	0.7639	0.6660	0.078(2)
H2b	-0.0374	0.8378	0.6497	0.078(2)
H2c	0.0240	0.7854	0.7040	0.078(2)
C3	0.175(2)	0.8401(6)	0.468(1)	0.056(1)
H3a	0.1837	0.8900	0.4847	0.078(2)
H3b	0.1799	0.8408	0.4227	0.078(2)
H3c	0.2497	0.8101	0.4867	0.078(2)
C4	-0.0604(3)	0.896(2)	0.534(1)	0.070(1)
H4a	-0.1502	0.8913	0.5521	0.078(2)
H4b	-0.0629	0.9342	0.5024	0.078(2)
H4c	0.0086	0.9072	0.5673	0.078(2)
O1	0.213(2)	0.678(1)	0.5272(8)	0.038(5)
C5	0.156(2)	0.657(1)	0.472(1)	0.022(7)
C6	0.223(3)	0.593(2)	0.440(1)	0.042(9)
H6	0.2995	0.5644	0.4577	0.078(2)
C7	0.159(3)	0.580(2)	0.379(2)	0.056(1)
H7	0.1877	0.5359	0.3561	0.078(2)
C8	0.062(3)	0.622(2)	0.350(2)	0.050(9)
H8	0.0293	0.6121	0.3063	0.078(2)
C9	0.010(3)	0.680(2)	0.383(1)	0.034(8)
C10	-0.109(3)	0.726(2)	0.354(1)	0.066(1)
H10a	-0.1367	0.7064	0.3130	0.078(2)
H10b	-0.0769	0.7765	0.3496	0.078(2)
H10c	-0.1849	0.7247	0.3818	0.078(2)
N1	0.055(2)	0.701(1)	0.443(1)	0.026(6)
O2	-0.077(2)	0.659(1)	0.5721(9)	0.044(6)
C11	-0.200(3)	0.683(2)	0.547(1)	0.040(9)
C12	-0.321(3)	0.647(2)	0.564(2)	0.058(1)
H12	-0.3151	0.6049	0.5924	0.078(2)
C13	-0.444(3)	0.670(2)	0.542(1)	0.059(1)
H13	-0.5278	0.6428	0.5516	0.078(2)
C14	-0.453(3)	0.734(2)	0.503(1)	0.057(9)
H14	-0.5424	0.7506	0.4857	0.078(2)
C15	-0.339(3)	0.771(2)	0.491(1)	0.038(8)
C16	-0.338(3)	0.836(2)	0.457(2)	0.086(1)
H16a	-0.4318	0.8505	0.4436	0.078(2)
H16b	-0.2827	0.8318	0.4205	0.078(2)
H16c	-0.2990	0.8762	0.4843	0.078(2)

Table 27. (continued)

	x/a	y/b	z/c	U
N2	-0.205(2)	0.747(1)	0.511(1)	0.046(7)
P1	0.1706(8)	0.6509(2)	0.6748(4)	0.034(3)
C17	0.043(3)	0.611(2)	0.729(1)	0.032(8)
C18	0.097(4)	0.568(2)	0.781(2)	0.060(1)
H18	0.1956	0.5610	0.7879	0.078(2)
C19	0.007(4)	0.536(2)	0.823(2)	0.10(2)
H19	0.0416	0.5120	0.8618	0.078(2)
C20	-0.132(3)	0.538(2)	0.807(2)	0.063(1)
H20	-0.1923	0.5103	0.8335	0.078(2)
C21	-0.190(3)	0.578(2)	0.759(2)	0.068(1)
H21	-0.2896	0.5776	0.7516	0.078(2)
C22	-0.100(3)	0.616(2)	0.720(2)	0.042(9)
H22	-0.1394	0.6464	0.6857	0.078(2)
C23	0.301(3)	0.695(2)	0.729(1)	0.036(8)
C24	0.440(3)	0.701(2)	0.708(2)	0.049(9)
H24	0.4634	0.6817	0.6670	0.078(2)
C25	0.537(3)	0.732(2)	0.747(1)	0.058(1)
H25	0.6311	0.7365	0.7333	0.078(2)
C26	0.502(3)	0.760(2)	0.809(1)	0.050(9)
H26	0.5732	0.7809	0.8379	0.078(2)
C27	0.368(3)	0.758(2)	0.826(2)	0.057(1)
H27	0.3430	0.7794	0.8662	0.078(2)
C28	0.268(3)	0.724(2)	0.788(1)	0.034(8)
H28	0.1736	0.7203	0.8019	0.078(2)
C29	0.243(3)	0.566(2)	0.642(1)	0.039(9)
C30	0.166(3)	0.532(2)	0.594(2)	0.051(1)
H30	0.0821	0.5557	0.5775	0.078(2)
C31	0.206(3)	0.463(2)	0.569(2)	0.07(1)
H31	0.1469	0.4380	0.5369	0.078(2)
C32	0.329(3)	0.431(2)	0.591(2)	0.054(1)
H32	0.3610	0.3860	0.5716	0.078(2)
C33	0.404(3)	0.464(2)	0.638(2)	0.057(1)
H33	0.4882	0.4399	0.6540	0.078(2)
C34	0.366(3)	0.535(2)	0.668(2)	0.061(1)
H34	0.4207	0.5577	0.7018	0.078(2)
C35a	0.52610	0.52884	0.14287	0.1149
C36a	0.48842	0.52680	0.07139	0.1149
C37a	0.56742	0.60105	0.17502	0.1149
O3a	0.51637	0.47200	0.17524	0.1149
C35b	0.57622	0.53953	0.15290	0.1149
C36b	0.45520	0.51409	0.19190	0.1149
C37b	0.60630	0.50017	0.09066	0.1149
O3b	0.65165	0.59091	0.17243	0.1149

* Equivalent isotropic U defined as one third of the trace of the orthogonalised U_{ij} tensor.

Table 28. Anisotropic thermal parameters ($Å^2x10^3$) for $[Pt_2(CH_3)_4(C_6H_6NO)_2(PPh_3)]\cdot 2CH_3COCH_3$

	U_{12}	U_{22}	U_{33}	U_{23}	U_{13}	U_{12}
Pt(1)	33(1)	32(1)	27(1)	-2(1)	3(1)	3(1)
Pt(2)	47(1)	35(1)	31(1)	2(1)	1(1)	7(1)
P(1)	40(5)	37(6)	24(5)	-13(4)	1(4)	0(4)

The anisotropic temperature factor exponent takes the form: $-2\pi^2(h^2a^{*2}U_{11} + \ldots + 2hka^*b^*U_{12})$

Table 29. Bond lengths (Å) with standard deviation for $[Pt_2(CH_3)_4(C_6H_6NO)_2(PPh_3)]\cdot 2CH_3COCH_3$

Pt(1)-Pt(2)	2.615(2)	Pt(1)-C(1)	1.98(2)
Pt(1)-C(2)	2.01(3)	Pt(1)-O(1)	2.14(2)
Pt(1)-O(2)	2.08(2)	Pt(1)-P(1)	2.287(8)
Pt(2)-C(3)	2.03(3)	Pt(2)-C(4)	2.04(3)
Pt(2)-N(1)	2.12(2)	Pt(2)-N(2)	2.12(2)
O(1)-C(5)	1.30(3)	C(5)-C(6)	1.50(4)
C(5)-N(1)	1.37(3)	C(6)-C(7)	1.41(4)
C(7)-C(8)	1.33(4)	C(8)-C(9)	1.35(4)
C(9)-C(10)	1.51(4)	C(9)-N(1)	1.36(3)
O(2)-C(11)	1.34(3)	C(11)-C(12)	1.39(4)
C(11)-N(2)	1.38(4)	C(12)-C(13)	1.31(4)
C(13)-C(14)	1.41(4)	C(14)-C(15)	1.32(4)
C(15)-C(16)	1.39(4)	C(15)-N(2)	1.40(3)
P(1)-C(17)	1.85(3)	P(1)-C(23)	1.83(3)
P(1)-C(29)	1.82(3)	C(17)-C(18)	1.38(5)
C(17)-C(22)	1.38(4)	C(18)-C(19)	1.38(5)
C(19)-C(20)	1.35(5)	C(20)-C(21)	1.32(5)
C(21)-C(22)	1.41(4)	C(23)-C(24)	1.42(4)
C(23)-C(28)	1.40(4)	C(24)-C(25)	1.33(4)
C(25)-C(26)	1.45(4)	C(26)-C(27)	1.36(4)
C(27)-C(28)	1.36(4)	C(29)-C(30)	1.36(4)
C(29)-C(34)	1.40(4)	C(30)-C(31)	1.42(4)
C(31)-C(32)	1.37(3)	C(32)-C(33)	1.34(4)
C(33)-C(34)	1.47(4)	C(35a)-C(36a)	1.520(1)
C(35a)-C(37a)	1.520(1)	C(35a)-O(3a)	1.230(1)
C(35a)-C(35b)	0.550(1)	C(35a)-C(36b)	1.284(1)
C(35a)-C(37b)	1.459(1)	C(35a)-O(3b)	1.733(1)
C(36a)-C(35b)	1.219(1)	C(37a)-C(36b)	1.953(1)
C(37a)-O(3b)	0.831(1)	O(3a)-C(35b)	1.430(1)
O(3a)-C(36b)	1.028(1)	C(35b)-C(36b)	1.520(1)
C(35b)-C(37b)	1.520(1)	C(35b)-O(3b)	1.230(1)

Table 30. Bond angles (°) with standard deviation for $[Pt_2(CH_3)_4(C_6H_6NO)_2(PPh_3)]\cdot 2CH_3COCH_3$

Pt(2)-Pt(1)-C(1)	96.1(7)	Pt(2)-Pt(1)-C(2)	98.7(9)
C(1)-Pt(1)-C(2)	87.0(1)	Pt(2)-Pt(1)-O(1)	80.6(5)
C(1)-Pt(1)-O(1)	89.5(9)	C(2)-Pt(1)-O(1)	176.0(1)
Pt(1)-Pt(2)-O(2)	80.8(5)	C(1)-Pt(1)-O(2)	176.8(9)
C(2)-Pt(1)-O(2)	93.0(1)	O(1)-Pt(1)-O(2)	90.5(7)
Pt(1)-Pt(2)-P(1)	186.6(2)	C(1)-Pt(1)-P(1)	92.0(8)
C(2)-Pt(1)-P(1)	89.8(9)	O(1)-Pt(1)-P(1)	91.4(5)
O(2)-Pt(1)-P(1)	91.2(5)	Pt(1)-Pt(2)-C(3)	95.1(8)
Pt(1)-Pt(2)-C(4)	97.2(9)	C(3)-Pt(2)-C(4)	90.0(1)
Pt(1)-Pt(2)-N(1)	85.8(5)	C(3)-Pt(2)-N(1)	85.0(1)
C(4)-Pt(2)-N(1)	174.0(1)	Pt(1)-Pt(2)-N(2)	86.7(6)
C(3)-Pt(2)-N(2)	92.1(8)	Pt(1)-O(1)-C(5)	120.0(1)
O(1)-C(5)-C(6)	117.0(2)	O(1)-C(5)-N(1)	120.0(2)
C(5)-C(6)-N(1)	122.6(2)	C(5)-C(6)-C(7)	112.0(2)
C(6)-C(7)-C(8)	126.0(3)	C(7)-C(8)-C(9)	118.0(3)
C(8)-C(9)-C(10)	120.0(3)	C(8)-C(9)-N(1)	125.0(3)
C(10)-C(9)-N(1)	114.3(2)	Pt(2)-N(1)-C(5)	118.0(2)
Pt(2)-N(1)-C(9)	126.0(2)	C(5)-N(1)-C(9)	116.3(2)
Pt(1)-O(2)-C(11)	123.0(2)	O(2)-C(11)-C(12)	119.0(3)
O(2)-C(11)-N(2)	119.0(2)	C(12)-C(11)-N(2)	121.0(3)
C(11)-C(12)-C(13)	121.0(3)	C(12)-C(13)-C(14)	119.0(3)
C(13)-C(14)-C(15)	119.0(3)	C(14)-C(15)-C(16)	124.0(3)
C(14)-C(15)-N(2)	123.0(3)	C(16)-C(15)-N(2)	113.0(2)
Pt(2)-N(2)-C(11)	116.0(2)	Pt(2)-N(2)-C(15)	128.0(2)
C(11)-N(2)-C(15)	116.0(2)	Pt(1)-P(1)-C(17)	117.6(9)
Pt(1)-P(1)-C(23)	112.0(1)	C(17)-P(1)-C(23)	104.0(1)
Pt(1)-P(1)-C(29)	112.0(1)	C(17)-P(1)-C(29)	101.0(1)
C(23)-P(1)-C(29)	109.0(1)	P(1)-C(17)-C(18)	117.0(2)
P(1)-C(17)-C(22)	125.0(2)	C(18)-C(17)-C(22)	118.0(3)
C(17)-C(18)-C(19)	120.0(3)	C(18)-C(19)-C(20)	118.0(4)
C(19)-C(20)-C(21)	125.0(3)	C(20)-C(21)-C(22)	117.0(3)
C(17)-C(22)-C(21)	121.0(3)	P(1)-C(23)-C(24)	119.0(2)
P(1)-C(23)-C(28)	122.0(2)	C(24)-C(23)-C(28)	121.0(3)
C(23)-C(24)-C(25)	119.0(3)	C(24)-C(25)-C(26)	121.0(3)
C(25)-C(26)-C(27)	119.0(3)	C(26)-C(27)-C(28)	121.0(3)
C(23)-C(28)-C(27)	120.0(3)	P(1)-C(29)-C(30)	117.0(2)
P(1)-C(29)-C(34)	122.0(2)	C(30)-C(29)-C(34)	121.0(3)
C(29)-C(30)-C(31)	122.0(3)	C(30)-C(31)-C(32)	119.0(3)
C(31)-C(32)-C(33)	120.0(3)	C(32)-C(33)-C(34)	124.0(3)
C(29)-C(34)-C(33)	115.0(3)		

coordinated with the Pt_2^{6+} unit. The Pt-N (axial) distance is 2.036 Å. The pyrazine is oriented the way that it is directed between the two methyl groups in a cis orientation. The torsion caused by the steric repulsion of the methyl groups along the Pt-Pt axis has a angle which differs quite a bit (28 degrees) from the torsion angle in the platinum(III) complex with axial pyridine (31 degrees). The average Pt-C bond length is 2.038 Å.

Structure of cis-$PtCl_2(Et_2S)_2$

An ORTEP view is shown in Figure 26. Table 35 and Table 36 consist of the final atomic coordinate and anisotropic thermal parameters. Table 37 and Table 38 list the bond lengths and bond angles.

The molecular structure contains a mononuclear square-planar platinum(II) with two chloride ions in a cis fashion while the other two diethylsulfide groups trans to each chloride. The Pt-S bond distance is 2.301 Å. Compared to a Pt-S bond distance (2.35 Å) in binuclear Pt(III) complex, the Pt-S bond distance apparently shortens in Pt(II) complex. The reason for the difference of bond length between Pt(II)-S and Pt(III)-S is probably due to the steric repulsion in Pt(III) complex which caused the increase of bond length. The bond angle between the two diethylsulfide groups is 89.4 degrees which is close enough to be considered as a square-planar configuration. The bond

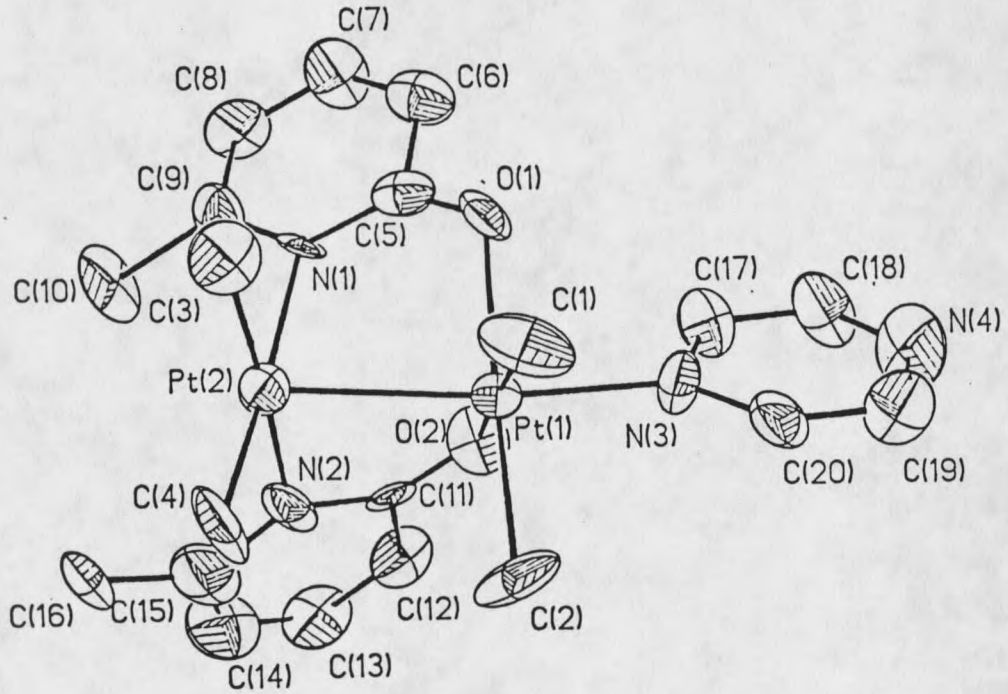

Figure 25. ORTEP view of $Pt_2(CH_3)_4(MHPy)_2(C_4H_4N_2)$

Table 31. Atomic coordinates ($x10^4$) and isotropic thermal parameters ($Å^2x10^3$) with standard deviation for $Pt_2(CH_3)_4$-$(C_6H_6NO)_2(C_4H_4N_2)$

	x/a	y/b	z/c	U
Pt(1)	7079(1)	6341(1)	4217(1)	31(1)*
Pt(2)	6948(1)	4212(1)	4071(1)	39(1)*
C(1)	7046(27)	6427(27)	5251(12)	63(10)*
C(2)	9254(19)	6494(22)	4282(17)	72(11)*
C(3)	5916(26)	3840(23)	4931(13)	55(9)*
C(4)	8747(25)	3844(20)	4564(15)	60(10)*
O(1)	4843(14)	6266(13)	4171(10)	55(6)*
N(1)	4909(15)	4549(14)	3619(10)	34(6)*
C(5)	4313(20)	5535(20)	3774(12)	39(8)*
C(6)	2847(25)	5746(25)	3512(13)	55(8)*
C(7)	2213(28)	4925(24)	3110(16)	67(11)*
C(8)	2896(23)	3915(22)	2947(14)	59(9)*
C(9)	4261(23)	3738(21)	3220(15)	51(8)*
C(10)	5078(30)	2659(21)	3044(17)	71(11)*
O(2)	7095(18)	6340(15)	3127(7)	51(5)*
N(2)	7960(18)	4481(15)	3125(11)	50(7)*
C(11)	7686(16)	5503(16)	2820(12)	32(7)*
C(12)	8214(26)	5676(25)	2133(12)	53(8)*
C(13)	8912(30)	4810(26)	1816(14)	64(10)*
C(14)	9122(33)	3829(29)	2136(17)	76(12)*
C(15)	8668(26)	3670(27)	2750(20)	83(14)*
C(16)	8851(32)	2559(21)	3069(22)	100(17)*
N(3)	6868(19)	8057(14)	4169(11)	50(6)*
C(17)	5890(27)	8473(21)	3743(14)	53(9)*
C(18)	5679(27)	9650(26)	3718(18)	75(12)*
N(4)	6345(28)	10353(20)	4050(15)	79(10)*
C(19)	7329(29)	9970(24)	4541(16)	62(10)*
C(20)	7516(22)	8833(21)	4578(15)	52(9)*

* Equivalent isotropic U defined as one third of the trace of the orthogonalized U_{ij} tensor

Table 32. Anisotropic thermal parameters ($Å^2x10^3$) with standard deviation for $[Pt_2(CH_3)_4(C_6H_6NO)_2(C_4H_4N_2)]$

	U_{11}	U_{22}	U_{33}	U_{23}	U_{13}	U_{12}
Pt(1)	26(1)	32(1)	36(1)	-0(1)	-1(1)	0(1)
Pt(2)	32(1)	32(1)	53(1)	5(1)	-5(1)	1(1)
C(1)	48(13)	99(22)	41(14)	3(15)	11(14)	23(19)
C(2)	30(10)	72(18)	112(26)	70(19)	-23(14)	-23(12)
C(3)	57(14)	59(14)	50(16)	-10(14)	-11(13)	-5(13)
C(4)	61(14)	37(13)	83(21)	-9(14)	-16(15)	34(12)
O(1)	30(6)	41(8)	93(14)	-37(11)	6(9)	9(7)
N(1)	14(6)	35(10)	53(12)	-18(8)	17(8)	4(6)
C(5)	29(10)	53(16)	35(14)	20(11)	1(10)	0(9)
C(6)	47(13)	69(16)	50(15)	11(14)	4(13)	10(15)
C(7)	56(17)	68(18)	78(21)	-26(16)	-29(16)	4(15)
C(8)	38(11)	66(17)	72(18)	-25(13)	-23(14)	-15(13)
C(9)	48(12)	39(12)	67(18)	6(14)	-15(12)	9(12)
C(10)	78(19)	50(15)	85(24)	-57(16)	-20(18)	15(14)
O(2)	69(10)	56(9)	28(8)	5(8)	-9(9)	7(11)
N(2)	23(7)	44(11)	82(15)	-27(10)	-22(11)	13(9)
C(11)	9(8)	37(12)	50(14)	7(9)	-5(8)	-12(7)
C(12)	62(15)	63(15)	33(13)	-15(13)	-2(12)	-16(14)
C(13)	79(18)	80(19)	35(16)	-19(15)	34(15)	-17(18)
C(14)	76(19)	85(24)	66(21)	-36(20)	17(17)	5(19)
C(15)	41(13)	70(19)	139(33)	-38(23)	-34(17)	5(15)
C(16)	56(17)	40(15)	203(46)	23(21)	45(24)	30(14)
N(3)	57(11)	27(8)	65(14)	-11(9)	8(14)	-12(9)
C(17)	67(15)	43(14)	49(16)	0(12)	-2(14)	10(13)
C(18)	54(15)	75(20)	97(27)	-45(20)	-43(17)	24(15)
N(4)	94(17)	47(13)	95(22)	34(15)	-17(17)	14(13)
C(19)	61(16)	59(17)	65(20)	11(15)	-19(14)	-2(13)
C(20)	37(10)	53(15)	66(19)	-34(14)	-2(11)	7(10)

The anisotropic temperature factor exponent takes the form: $-2\pi^2(h^2a^{*2}U_{11} + \ldots + 2hka^*b^*U_{12})$

Table 33. Bond lengths (Å) with standard deviation for $[Pt_2(Ch_3)_4(C_6H_6NO)_2(C_4H_4N_2)]$

Pt(1)-Pt(2)	2.536(1)	Pt(1)-C(1)	2.047(24)
Pt(1)-C(2)	2.079(19)	Pt(1)-O(1)	2.125(13)
Pt(1)-O(2)	2.158(15)	Pt(1)-N(3)	2.041(17)
Pt(2)-C(3)	2.012(26)	Pt(2)-C(4)	2.128(21)
Pt(2)-N(1)	2.168(15)	Pt(2)-N(2)	2.128(21)
O(1)-C(5)	1.271(28)	N(1)-C(5)	1.331(28)
N(1)-C(9)	1.385(31)	C(5)-C(6)	1.506(31)
C(6)-C(7)	1.393(40)	C(7)-C(8)	1.395(38)
C(8)-C(9)	1.419(33)	C(9)-C(10)	1.533(36)
O(2)-C(11)	1.289(26)	N(2)-C(11)	1.375(27)
N(2)-C(15)	1.386(38)	C(11)-C(12)	1.463(33)
C(12)-C(13)	1.470(40)	C(13)-C(14)	1.336(45)
C(14)-C(15)	1.304(50)	C(15)-C(16)	1.467(45)
N(3)-C(17)	1.346(33)	N(3)-C(20)	1.369(32)
C(17)-C(18)	1.406(40)	C(18)-N(4)	1.234(40)
N(4)-C(19)	1.422(40)	C(19)-C(20)	1.358(37)

Table 34. Bond angles (°) with standard deviation for $[Pt_2(CH_3)_4(C_6H_6NO)_2(C_4H_4N_2)]$

Pt(2)-Pt(1)-C(1)	99.3(9)	Pt(2)-Pt(1)-C(2)	98.2(7)
C(1)-Pt(1)-C(20)	87.1(12)	Pt(2)-Pt(1)-O(2)	84.5(4)
C(1)-Pt(1)-O(1)	91.8(9)	C(2)-Pt(1)-O(1)	177.2(8)
Pt(1)-Pt(2)-O(2)	83.4(5)	C(1)-Pt(1)-O(2)	177.1(10)
C(2)-Pt(1)-O(2)	93.1(10)	O(1)-Pt(1)-O(2)	87.9(7)
Pt(2)-Pt(1)-N(3)	167.5(6)	C(1)-Pt(1)-N(3)	89.8(11)
C(2)-Pt(1)-N(3)	90.8(9)	O(1)-Pt(1)-N(3)	86.6(7)
O(2)-Pt(1)-N(3)	87.4(8)	Pt(1)-Pt(2)-C(3)	98.3(8)
Pt(1)-Pt(2)-C(4)	96.7(7)	C(3)-Pt(2)-C(4)	87.5(11)
Pt(1)-Pt(2)-N(1)	84.7(4)	C(3)-Pt(2)-N(1)	87.4(9)
C(4)-Pt(2)-N(1)	174.9(9)	Pt(1)-Pt(2)-N(2)	86.0(5)
C(3)-Pt(2)-N(2)	175.2(9)	C(4)-Pt(2)-N(2)	94.3(9)
N(1)-Pt(2)-N(2)	90.7(7)	Pt(1)-O(1)-C(5)	116.8(13)
Pt(2)-N(1)-C(5)	116.4(14)	Pt(2)-N(1)-C(9)	120.2(13)
C(5)-N(1)-C(9)	123.3(17)	O(1)-C(5)-N(1)	124.7(19)
O(1)-C(5)-C(6)	117.7(20)	N(1)-C(5)-C(6)	117.3(20)
C(5)-C(6)-C(7)	118.7(24)	C(6)-C(7)-C(8)	121.8(24)
C(7)-C(8)-C(9)	117.5(24)	N(1)-C(9)-C(8)	121.3(21)
N(1)-C(9)-C(10)	118.8(20)	C(8)-C(9)-C(10)	119.8(23)
Pt(1)-O(2)-C(11)	118.3(14)	Pt(2)-N(2)-C(11)	115.6(14)
Pt(2)-N(2)-C(15)	125.9(18)	C(11)-N(2)-C(15)	117.7(23)
O(2)-C(11)-N(2)	123.3(21)	O(2)-C(11)-C(12)	118.7(20)
N(2)-C(11)-C(12)	117.8(19)	C(11)-C(12)-C(13)	119.1(24)
C(12)-C(13)-C(14)	124.0(30)	N(2)-C(15)-C(16)	116.6(31)
C(14)-C(15)-C(16)	119.4(32)	Pt(1)-N(3)-C(17)	117.4(16)
Pt(1)-N(3)-C(20)	126.5(16)	C(17)-N(3)-C(20)	115.8(19)
N(3)-C(17)-C(18)	118.8(24)	C(17)-C(18)-N(4)	125.1(28)
C(18)-N(4)-C(19)	119.1(25)	N(4)-C(19)-C(20)	115.9(25)
N(3)-C(20)-C(19)	124.9(24)		

angle between C-S-C is about 99.6 degrees which is a distorted tetrahedral form caused by a lone pair of electrons on the sulfur. The average Pt-Cl bond length is 2.31 Å.

Structure of trans-$PtCl_2(Et_2S)_2$

An ORTEP view is shown in Figure 27. Table 39 and Table 40 contain final atomic coordinate and anisotropic thermal parameters. Table 41 and Table 42 list the bond lengths and bond angles.

The structure is a square-planar Pt(II) with two chloride ions in a trans fashion and two diethylsulfide groups cis to each chloride. The Pt-S bond distance is 2.269 Å, shortened compared with the cis isomer. This is due to the reduced steric interactions between diethylsulfides in the molecule. The polarity of the trans-Pt complex should be much smaller than that of cis-Pt complex. The bond angle between C-S-C group is torsioned (99.9 degrees) by the repulsion of a lone pair of electrons on sulfur and the ethyl groups on both diethylsulfide groups are oriented in such a way that trans-$PtCl_2(Et_2S)_2$ still possesses polarity. The average Pt-Cl bond length is 2.292 Å. The decreasing of Pt-Cl bond length compared with that of cis-Pt complex indicates the stronger trans-effect diethylsulfide groups have been substituted by weaker trans-effect chlorides; the bond between Pt-Cl gets stronger.

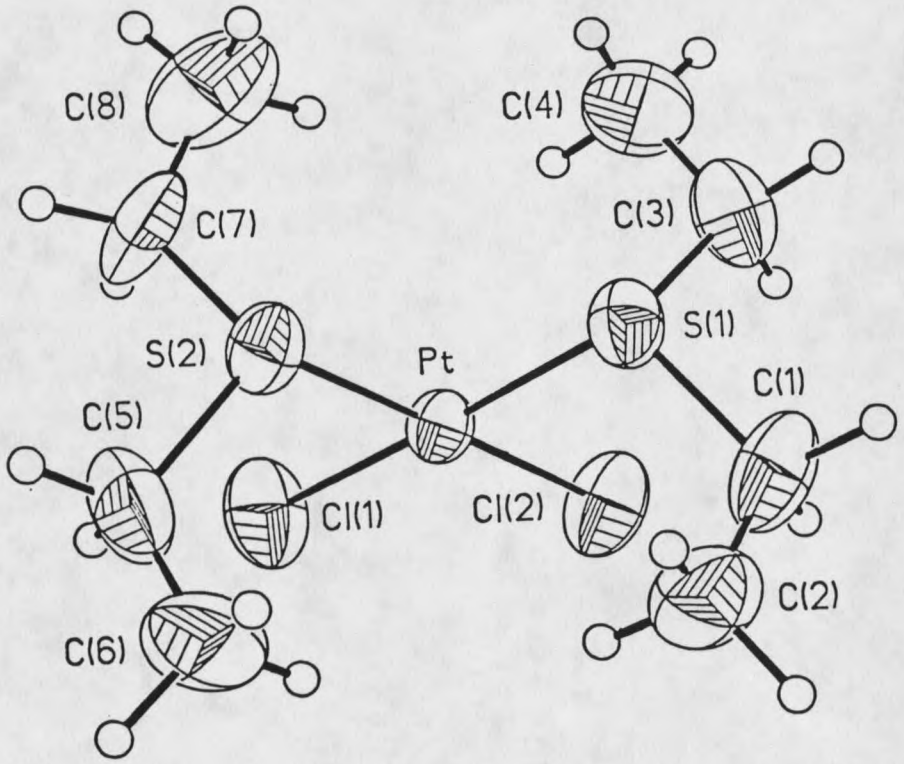

Figure 26. ORTEP view of cis-$PtCl_2(Et_2S)_2$

Table 35. Atomic coordinates and isotropic temperature factors ($Å^2$) with standard deviations for cis-$PtCl_2(Et_2S)_2$

	x/a	y/b	z/c	U_{eq}[a]
Pt	0.4509(1)	0.2872(1)	0.2051(1)	0.044(1)
S(1)	0.4984(4)	0.3093(3)	0.0331(3)	0.056(1)
C(1)	0.670(1)	0.299(1)	0.047(2)	0.080(7)
C(2)	0.728(2)	0.398(2)	0.114(1)	0.092(8)
C(3)	0.453(2)	0.173(1)	-0.046(1)	0.086(8)
C(4)	0.316(2)	0.149(2)	-0.053(2)	0.123(10)
S(2)	0.3519(4)	0.4636(3)	0.1796(3)	0.059(1)
C(5)	0.400(2)	0.550(1)	0.304(1)	0.093(8)
C(6)	0.533(2)	0.579(2)	0.322(2)	0.121(10)
C(7)	0.190(2)	0.440(2)	0.187(2)	0.093(8)
C(8)	0.119(2)	0.380(2)	0.090(2)	0.123(11)
Cl(1)	0.3933(5)	0.2650(4)	0.3763(3)	0.086(2)
Cl(2)	0.5609(4)	0.1118(3)	0.2295(4)	0.079(2)

[a] Equivalent isotropic U defined as one-third of the trace of the orthagonalized U_{ij} tensor

Table 36. Anisotropic thermal parameters ($Å^2 \times 10^3$) with standard deviation for cis-$PtCl_2(Et_2S)_2$

	U_{11}	U_{22}	U_{33}	U_{23}	U_{13}	U_{12}
Pt	42(1)	43(1)	48(1)	3(1)	14(1)	1(1)
S(1)	62(2)	57(2)	53(2)	5(2)	21(2)	8(2)
C(1)	64(11)	81(10)	108(13)	27(10)	48(10)	6(10)
C(2)	63(12)	118(14)	96(13)	2(11)	19(10)	-18(11)
C(3)	110(16)	71(10)	82(12)	-20(8)	32(11)	3(10)
C(4)	92(17)	146(17)	123(17)	-60(14)	-4(13)	-17(14)
S(2)	59(2)	47(2)	72(2)	-1(2)	16(2)	11(2)
C(5)	110(17)	83(11)	91(13)	-37(10)	28(12)	4(11)
C(6)	96(16)	104(14)	149(19)	-62(13)	-16(14)	-12(13)
C(7)	48(10)	87(11)	149(17)	-1(12)	31(11)	26(9)
C(8)	65(13)	115(16)	188(23)	12(15)	18(14)	-21(12)
Cl(1)	114(4)	91(3)	67(2)	14(2)	49(3)	5(3)
Cl(2)	80(3)	56(2)	106(3)	26(2)	33(2)	23(2)

The anisotropic temperature factor exponent takes the form: $-2\pi^2(h^2a^{*2}U_{11} + \ldots + 2hka^*b^*U_{12})$

Table 37. Bond Lengths (Å) with standard deviations for cis-$PtCl_2(Et_2S)_2$

Pt-S(1)	2.266(4)	Pt-S(2)	2.271(3)
Pt-Cl(1)	2.302(5)	Pt-Cl(2)	2.315(4)
S(1)-C(1)	1.83(2)	S(1)-C(3)	1.85(2)
S(2)-C(5)	1.80(2)	S(2)-C(7)	1.79(2)
C(1)-C(2)	1.47(2)	C(3)-C(4)	1.48(3)
C(5)-C(6)	1.45(3)	C(7)-C(8)	1.46(3)

Table 38. Bond angles (°) with standard deviation for cis-$PtCl_2(Et_2S)_2$

S(1)-Pt-S(2)	87.5(1)	S(1)-Pt-Cl(1)	177.4(2)
S(2)-Pt-Cl(1)	91.3(1)	S(1)-Pt-Cl(2)	91.0(1)
S(2)-Pt-Cl(2)	177.1(1)	Cl(1)-Pt-Cl(2)	90.4(2)
Pt-S(1)-C(1)	107.9(6)	Pt-S(1)-C(3)	107.8(6)
Pt-S(2)-C(5)	108.4(6)	Pt-S(2)-C(7)	107.5(6)
C(1)-S(1)-C(3)	99.3(8)	C(5)-S(2)-C(7)	99.9(9)
S(1)-C(1)-C(2)	109(1)	S(1)-C(3)-C(4)	111(1)
S(2)-C(5)-C(6)	112(1)	S(2)-C(7)-C(8)	114(2)

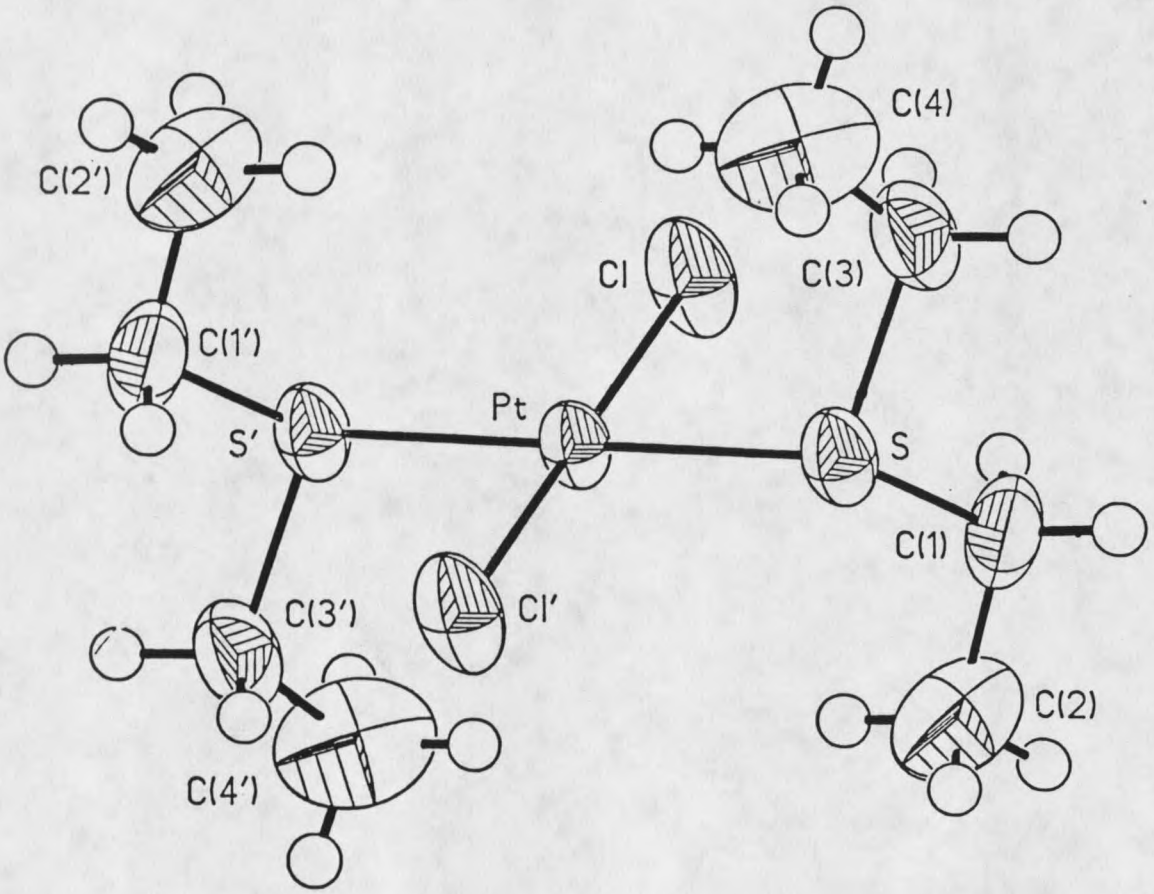

Figure 27. ORTEP view of trans-$PtCl_2(Et_2S)_2$

Table 39. Atomic coordinates and isotropic thermal parameters ($Å^2$) with standard deviation for trans-$Pt((C_2H_5)_2S)_2Cl_2$

	x/a	y/b	z/c	U[a]
Pt	0.5000	0.5000	0.5000	0.038(1)
S	0.6320(3)	0.3572(3)	0.6508(2)	0.048(1)
C(1)	0.446(2)	0.226(2)	0.708(1)	0.068(4)
C(2)	0.331(2)	0.348(3)	0.754(1)	0.097(7)
C(3)	0.770(2)	0.189(2)	0.598(1)	0.066(4)
C(4)	0.927(2)	0.271(2)	0.549(1)	0.113(8)
Cl	0.3922(4)	0.2511(3)	0.4192(2)	0.066(1)

[a]Equivalent isotropic U defined as one-third of the trace of the orthagonalized $\mathbf{U}_{ij}$ tensor.

Table 40. Anisotropic thermal parameters ($Å^2x10^3$) with standard deviation for trans-$Pt((C_2G_5)_2S)_2CL_2$

	U_{11}	U_{22}	U_{33}	U_{23}	U_{13}	U_{12}
Pt	49(1)	29(1)	35(1)	1(1)	-9(1)	-4(1)
S	65(1)	37(1)	40(1)	4(1)	-13(1)	-1(1)
C(1)	88(8)	62(7)	53(5)	21(5)	9(5)	-7(6)
C(2)	81(8)	142(16)	69(8)	5(9)	7(7)	0(11)
C(3)	76(7)	54(6)	66(6)	12(5)	-9(6)	16(6)
C(4)	72(8)	156(18)	109(11)	-23(13)	-2(9)	-7(11)
Cl	95(2)	38(1)	62(1)	-3(1)	-27(1)	-12(1)

The anisotropic temperature factor exponent takes the form: $-2\pi^2(h^2a^{*2}U_{11} + \ldots + 2hka^*b^*U_{12})$

Table 41. Bond lengths (Å) with standard deviation for trans-$PtC((C_2H_5)_2S)_2Cl_2$

Pt-S	2.301(2)	Pt-Cl	2.292(3)
S-C(1)	1.80(1)	S-C(3)	1.83(1)
C(1)-C(2)	1.54(2)	C(3)-C(4)	1.52(2)

Table 42. Bond angles (°) with standard deviation for trans-$PtC((C_2H_5)_2S)_2Cl_2$

S-Pt-Cl	93.0(1)	Pt-S-C(1)	106.7(4)
Pt-S-C(3)	107.6(4)	C(1)-S-C(3)	99.9(5)
S-C(1)-C(2)	108(1)	S-C(3)-C(4)	110(1)

Table 43. Calculated Hydrogen Atom Coordinates ($x10^4$)

cis-$Pt((C_2H_5)_2S)_2Cl_2$				trans-$Pt((C_2H_5)_2S)_2Cl_2$			
H(1a)	695	302	-35	H(1a)	524	146	774
H(1b)	702	217	87	H(1b)	404	146	643
H(2a)	830	393	123	H(2a)	231	273	790
H(2b)	703	394	196	H(2b)	271	425	686
H(2c)	697	480	74	H(2c)	394	431	816
H(3a)	506	101	-4	H(3a)	696	117	534
H(3b)	473	182	-129	H(3b)	814	103	665
H(4a)	292	69	-100	H(4a)	1010	171	518
H(4b)	263	221	-95	H(4b)	1001	343	613
H(4c)	296	140	29	H(4c)	884	355	482
H(5a)	381	501	374				
H(5b)	346	630	295				
H(6a)	556	632	396				
H(6b)	553	627	252				
H(6c)	587	499	332				
H(7a)	147	525	194				
H(7b)	186	388	260				
H(8a)	22	370	100				
H(8b)	160	294	82				
H(8c)	122	431	16				

GENERAL DISCUSSION

Synthetic Procedure

The $K_2Pt(NO_2)_4$ has been proved to be one of the useful starting materials for the synthesis of a class of platinum complexes with various valence states. Early in the 1970's, $K_2Pt(NO_2)_4$ was used to synthesize the binuclear platinum(III) sulfate bridged complex. Because of the liability of the Pt-N bond, many platinum complexes were made out of the reaction with $K_2Pt(NO_2)_4$, thus creating brand new structures that were related to the bond rearrangement. Generally there are two processes involved in the reaction. The first step is to substitute the NO_2 groups; subsequent oxidation adds on the new ligands; and the last step purifies the product.

The classic reaction between $K_2Pt(NO_2)_4$ and H_2SO_4 has proved that it is the only binuclear platinum(III) complex synthesized under the high concentration of acid. Though different kinds of structures were reported under similar conditions, a definite characterization was not made.

The author's work was to investigate this part of chemistry further by changing the Pt/H^+ ratio and setting up a new area for this classic reaction. Therefore people will be able to study consecutively in this area which involves rich structures with distinguished properties. A variety of Pt/H^+ ratios were used, and a strong influence of Pt/H^+ on the formation of the product has been found. In all cases,

the reaction undergoes a series of color changes before it is left for crystallization. The reactants must be heated and mixed well before the solvent is removed. During the solvent removing process, drying agents (concentrated H_2SO_4 and NaOH) are necessary. Also Ar gas flow should be used while acidified water is added in the process to protect the air oxidation. The whole process usually takes about 24 hours. Neutralization of the final solution is critical in forming the product, and generally a larger amount of starting material would yield the desired product comparatively easier. Finally, separation and purification of the product by recrystalization is an effective way to grow crystals for x-ray study. The whole recrystalization may take months to produce crystals large enough for x-ray study. These crystals often stick tightly with the K_2SO_4 which results from neutralization. Filtration is the first step to eliminate the by-product K_2SO_4 or K_2CO_3. One must manually separate the yellow crystals from the filtrate. One then dissolves the yellow crystals with a minimum amount of water and performs a second or third recrystallization to make sure the yellow crystals are pure. Besides, the size of the crystals of the yellow complex may grow larger if they are pure. The crystals are only formed in neutral solution. Attempt to grow crystals in acidic solution failed.

According to Rosenberg's method (45), adjusting the pH

to 6.44 would enable one to collect crystals of their di-μ-hydroxo platinum(II) dimer. This is similar to the condition we have been using, though there is no reaction run under the basic condition.

Efforts to perform the reaction in other Pt/H^+ ratios generally proved futile. What was obtained was non-crystal powders or twined crystals not suitable for x-ray study. Due to the repeated recrystalization process, the yield of the crystal is fairly low (15%).

The means we used to distinguish yellow dimer and yellow tetramer is by the shape of the crystal. If the crystal is a very thin plate, it is probably a platinum(II) dimer. If it is cubic-like, it is likely to be a platinum(II)(IV) tetramer. It is not always effective to distinguish the crystals this way. Despite these drawbacks, the synthetic approach here has exploited another type of chemistry for the tetrameric platinum system.

Cis-$PtCl_2(Et_2S)_2$ is a useful starting material for platinum complex synthesis. Its stability in air, good solubility in different organic solvents and substitution availibility are the main properties used in the reaction. Its isomerization in the solution, however, was previously studied kinetically and thermodynamically. The mechanism for the isomerization explains the liability of the Pt-S bond. It also indicates that polarity-favors trans-$PtCl_2(Et_2S)_2$ is actually the main product of the

isomerization.

The binuclear platinum(III) complexes bridged by oxo-pyridonate ligands were synthesized from the reaction of cis-$PtCl_2(Et_2S)_2$ as starting material. This cis-$PtCl_2(Et_2S)_2$ was methylated by CH_3Li under inert gas protection in dry benzene. A grey-white Et_2S bridged platinum(II) dimer is formed. This Et_2S bridged Pt(II) dimer is further oxidized by a Ag(oxopyridonate) salt in dry benzene at room temperature. A black oily material results after the reaction runs for 36 hours. The black oily material is filtered several times with benzene. After this material is flashed through a short silica gel column by toluene-pyridine mixture (3:1), the solution turns red. Removing the solvent by rotavaping, one ends up with a red-orange powder; ^1H NMR shows that the binuclear platinum(III) complex is formed.

In the author's work, different ligands were used to try to substitute the axial ligand on the binuclear platinum(III) pyridine substituted complexes and find the reactivity of the attacking ligands and the binuclear Pt(III) complexes themselves. PPh_3 was the first one used in the reaction. It was obvious that new resonances formed in the NMR spectra, but no crystal formed in chloroform, indicating that there might be a mixture of products or an excess of PPh_3 left with the product to hinder the crystal growing. It has been found that PPh_3 has a larger

solubility in ethanol. Hence ethanol was used to remove the excess PPh_3 presented in solid state interfering with the single crystal formation. Then different solvents were tried. Single crystals suitable for x-ray crystallography were only found in acetone.

Pyrazine has two available electron donor sites, and it was used in the reaction with the intention of forming a two platinum(III) dimer bridged by this pyrazine ligand. New resonances were also found in NMR spectrum. There were no crystals formed when the solvent evaporated. Because pyrazine has a high vapor pressure, it does not have the problem of excess material left in the reaction mixture interfering with crystal formation. After this red powder was redissolved in acetone under room temperature for the time when the solvent was gone, the author found bright red crystal formed in the evaporation container.

CF_3COOH and CCl_3COOH were both acidic ligands used in the reaction with Pt(III) complex. NMR studies could not supply the detailed information of the product structure. While no crystals formed in chloroform, the crude product was dissolved in acetone. A single crystal suitable for x-ray study was found. The significant point about this product is that this is the first compound made out of an anionic ligand to coordinate to a Pt(III) neutral complex. Pt(III) + CCl_3COOH produced a needle-like complex in chloroform. Crystal was also found, and x-ray structure unit cell was

taken, but the whole data set was just not good enough to solve the structure. The study of Pt(III) + CF_3COOH product is underway.

As with most platinum cluster bridged by the electron donation ligands, this special arrangement in structure leads to the conclusion that ligands with suitable electron donor sites could all be used in the complex synthesis. Efforts were also focused on tartaric acid, proline, glycine and oxalate as potential bridging ligands in the reaction with platinum starting materials. Some of the products were extremely insoluble in most of the solvents selected from non-polar to very polar. No crystals were found in these reactions. New experimental conditions need to be considered.

Structural Comparisons

The yellow platinum(II) dimer displays features that are characteristic of complex with hydroxo bridging ligands. The Pt-N (N-nitrite group) distances and N-Pt-N bond angles are best represented as a square-planar configuration. Compared with the Pt-N bond distance in Pt(III) complex, the Pt-N bond length in yellow dimer seems much shorter. Similar structures were determined by x-ray crystallography in the $[Pt_2(NH_3)_4(OH)_2]^{+2}$ cation while the anionic forms were nitrate and carbonate (44, 45). Pt-N bond lengths in these complexes are on the average longer than in

yellow dimer. This indicates that nitrite ligands interact more strongly with the platinum ions than with ammine ligands, which is reasonable if one recongnizes the negative charges on nitrite ligands. The existence of the hydroxo bridge is also confirmed by IR spectroscopy (Table 44). A band at about 1000 cm^{-1} was observed in the IR spectrum in the previously cationic platinum(II) dimers and assigned as Pt-OH bending vibration mode. A similar band was recorded in the yellow platinum(II) dimer at 946.54 cm^{-1}. Infrared spectroscopy studies on some binuclear hydroxo bridged complexes of Co(II), Cr(III) and Cu(II) as well as transition metal complexes with terminal OH groups always reveal the existence of a band in the region 900-1200 cm^{-1}. Those data are close to the upper limit of transition metal-OH bending mode. Therefore, a Pt-OH bond was assumed.

Another important aspect of the structure is that the distance between the metals in the two platinum(II) dimer molecule is rather short, meaning a strong interaction between the two platinum(II) molecules. This interaction could not be due to an attractive force between the two platinum ions, because in this compound the platinum atoms are both out of a plane drawn through directly bonded atoms (Figure 28). The displacement is in the direction expected if the interaction between metal ions is net repulsive. Moreover, the negative charge on the dimeric units will also

Table 44. Infrared spectral results for $K_2[Pt_2(NO_2)_4(OH)_2]\cdot 1.5H_2O$

Band (cm^{-1})	Intensity	Assignment
3474	s	ν_s and ν_{as} O-H stretching mode
1628	m	H-O-H bending mode
1473	vs	ν_{as} (NO_2)
1417		
1332	vs	ν_s (NO_2)
947	m	Pt-O-H bending mode
834	s	δ (ONO)
585	s	ρ_w (NO_2)
567		
476	w	ν (M-N)

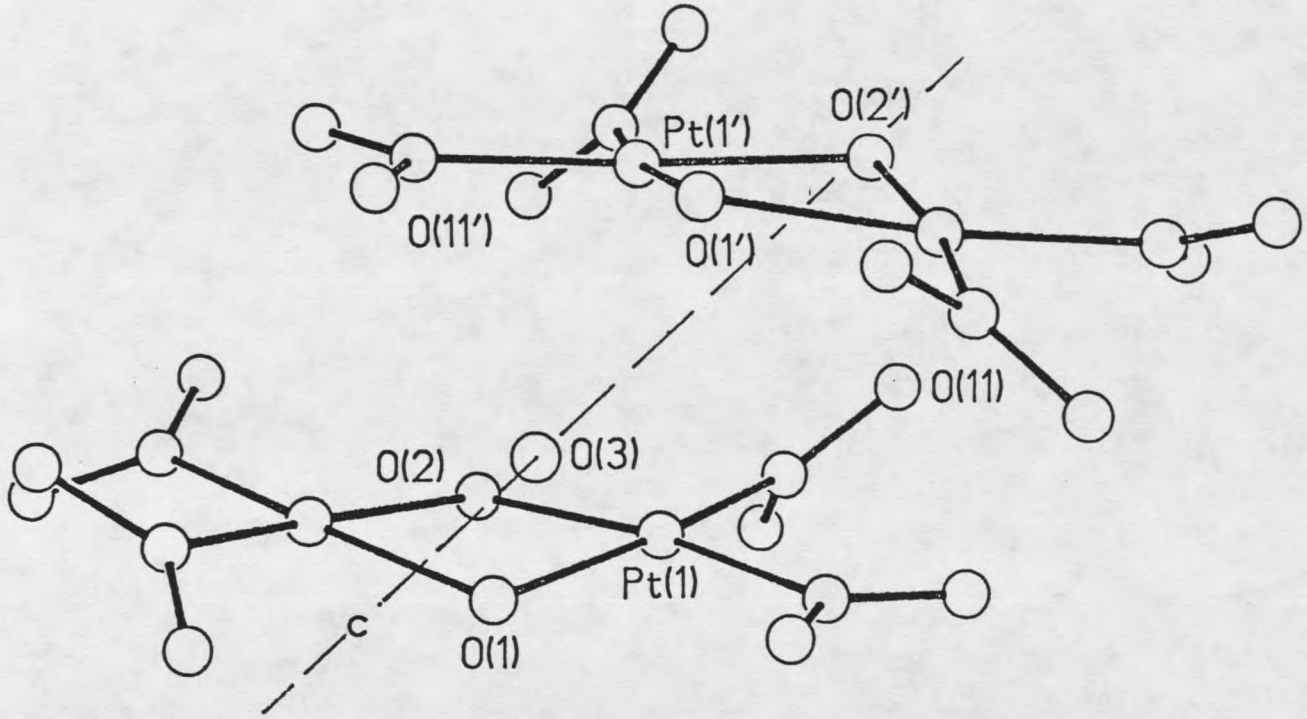

Figure 28. ORTEP view of molecular arrangement in $K_2[Pt_2(NO_2)_4(OH)_2]\cdot 1.5H_2O$

be a cause for repulsion. There must be another interaction holding the two anions in this arrangement.

Similar arrangement occurs in the Pt(II) carbonate cationic complex (45). It has been proposed that the close approach of Pt_a and $Pt_{a'}$ is the consequence of hydrogen bonding between hydrogens on hydroxo bridges and the nitrogens on NH_3 ligands. Such a hydrogen bonding would arise from hydrogens from hydroxo bridge and oxygens on nitrite ligands in this yellow dimer. This hydrogen bonding is responsible for the distortion of the plane around each platinum. In addition, it can be seen from [15] that planes formed by the ligand atoms are twisted relative to the platinum atom plane.

Compared with the synthetic methods of the two different kinds of platinum(II) complex, it is remarkable that yellow anionic platinum(II) complex stacks just the way cationic platinum(II) complex does, despite a substantial difference in forming the hydrogen bonding.

The structure of yellow platinum tetramer reveals the oxo bridging groups and the arrangement of Pt(II) and Pt(IV) mixed valence states in one molecule. The Pt-N bond length in Pt(IV) atom is apparently shorter than that of Pt(II)-N on nitrite groups. N-Pt(IV)-O bond angle is 91 degrees and N-Pt(II)-N bond angle is 92.3 degrees. These data indicate the deformed octahedral and square-planar configuration around each metal ion. No similar structure was ever

observed, though cyclo-hydroxo bridged tetra-platinum (II) complex and a mixed valence tetranuclear platinum(I,II) complex have been reported. The valence states of the platinum ion in this complex are based on the geometric and charge balance of the molecule. The oxo bridge has been confirmed again by not seeing the band at about 1000 cm^{-1} in IR spectrum (Table 45), which would be expected if hydroxo bridges were present. This mixed oxidation states structure is interesting because in a more acidic solution binuclear Pt(III) complex units are formed. The method of synthesizing binuclear Pt(III) complex from the reverse disproportionation of mixed Pt(II) and Pt(IV) complexes is also under way. Such a mechanism of forming binuclear Pt(III) complex would be very instructive. Due to the presence of Pt(II) and Pt(IV) in one molecule, it is quite likely that the mixed valence platinum complex is an intermediate on the route to form Pt(III) binuclear complex. Finally, pH influence greatly affects the formation of the product.

The primary structures of cis-$PtCl_2(Et_2S)_2$ and trans-$PtCl_2(Et_2S)_2$ have basic square-planar configurations except that the square-planar configuration is distorted by the repulsion of two adjacent diethylsulfide groups for the cis-$PtCl_2(Et_2S)_2$. The Pt-S bond length is 2.301 Å in the cis orientation and 2.266 Å in the trans orientation. The repulsive force in cis orientation could make bond strength

Table 45. Infrared spectral assignment for $K_5[Pt_4(NO_2)_9(O)_3]\cdot 3H_2O$

Band (cm^{-1})	Intensity	Assignment
1627.5	m	Lattice H_2O H-O-H bending mode
1470	vs	ν_{as} (NO_2)
1420		
1335	vs	ν_s (NO_2)
835	s	δ (ONO)
605	s	ρ_w (NO_2)
556		
466	w	ν (M-N)

weaker. Also, the stronger trans-effect of Et_2S and larger polarity of the molecule make cis-$PtCl_2(Et_2S)_2$ an more labile material to start with. With good stability in air and good solubility in organic solvents, cis-$PtCl_2(Et_2S)_2$ functions importantly in organometallic synthesis. In view of the Vrieze's synthetic and spectroscopic results, bis-diethylsulfide bridged complex was produced (52). Based on the bis-diethylsulfide bridged complex, a series of binuclear platinum(III) oxo-pyridonate bridged complexes were synthesized and the structures were also characterized (54). These binuclear platinum(III) complexes have similar features compared with carboxylate bridged platinum(III) complexes. The Pt-Pt bond distances are ranged from 2.543 to 2.556 Å. All these platinum complexes have two cis-methyl groups bonded to each platinum center and two oxo-pyridonate bridging ligands coordinated the two platinum

ions. The difference between oxo-pyridonate bridged platinum(III) complex and carboxylate bridged platinum(III) complex is that oxo-pyridonate bridged Pt complex could have polar and non-polar arrangements which indicates both axial positions may be occupied by axial ligand or one axial position is occupied while another end is empty. This has not been observed in the case of carboxylate bridged complexes.

The non-polar and polar arrangements, however, are characterized in α-pyridone bridged platinum (III) complex, $Pt_2(NH_3)_4(HPy)_2LL'$, where L = L'= NO_3^{-1}; L = NO_3^{-1}, L'= H_2O; L = L'= Cl^{-1} etc; (33). The main difference is that this series of platinum complexes have ammine ligands in the cis orientation. The Pt-Pt bond lengths under this category range from 2.539 - 2.771 Å and are close to the non-polar Pt(III) oxo-pyridonate bridged complexes.

It is found from the structures of oxo-pyridonate bridged Pt(III) complexes that there is a substantial torsion about the Pt-Pt bond due to the steric interactions between the two equatorial coordination planes. This is true whether the structures are polar or non-polar. This torsion exists even though in non-polar form this torsion decreases a little due to the addition of axial ligand. The structures that have been characterized by the author are all polar platinum(III) complexes. Instead of pyridine and diethylsulfide, triphenylphosphine and pyrazine were used as

axial ligands. These structures are very similar to the pyridine substituted platinum(III) complex. The internal torsion angle in pyrazine substituted platinum complex is about 3 degrees less than that found in Py substituted Pt complex. So far, there are four different ligands that were used in the reaction. Accordingly, the trans-effect series would be PPh_3 > Et_2S > pyridine = pyrazine. It is observed that torsion angle in Et_2S substituted Pt complex is much smaller than in pyridine or pyrazine substituted Pt complex, while torsion angle in PPh_3 substituted compound (30 degrees) is similar to the pyridine substituted complex. Hence, it seems that the presence of a stronger trans directing ligand in the axial position weakens the bond trans across the metal-metal bond to it, to the extent that no axial ligand could coordinate with platinum ion. However, the trans-effect of axial ligand does not affect the torsion angle. Rather this torsion angle is dependent upon the size of the axial ligand. It is also suggested that a strong trans-effect axial ligand influences the bond formation, because a stronger trans effect ligand would be able to adjust the electron density on the axial position and induce the electron density on the metal ions change. This change would result in the metal-metal bond weakening or strengthening, as the bond lengths change (Figure 29) (Table 46).

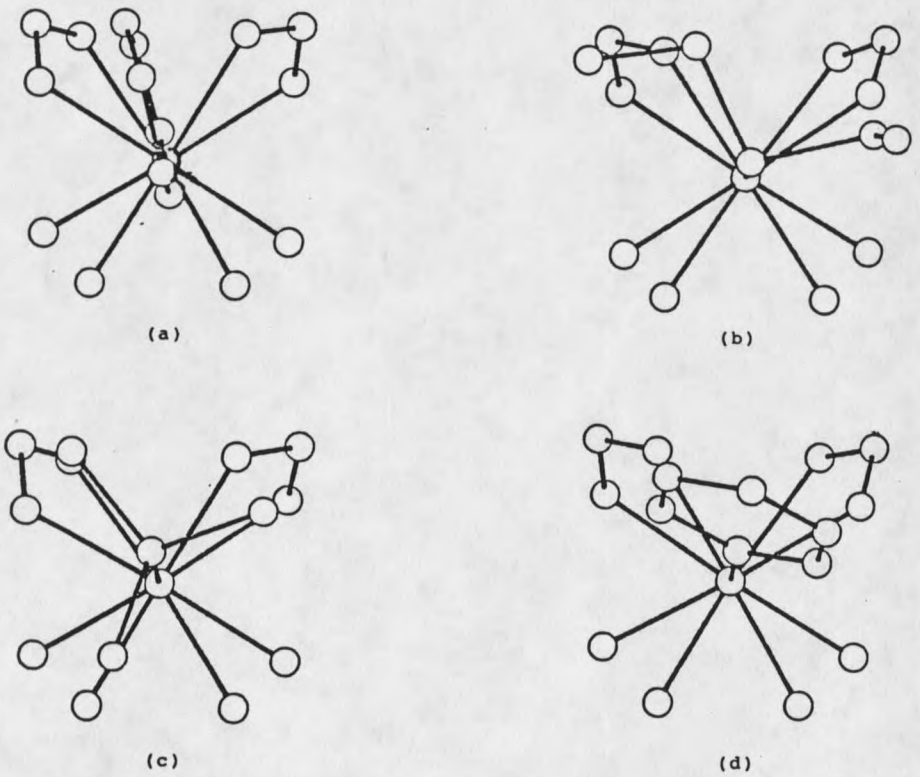

Figure 29. ORTEP view of molecular arrangement of Pt(MHPy) with different axial ligands

Table 46. Relation of the axial ligands vs. torsion angle

Axial ligand		Pt-Pt bond length (Å)	torsion angle (!)
(a)	Pyridine	2.543	31.0
(b)	Et_2S	2.561	24.0
(c)	PPH_3	2.615	29.7
(d)	Pyrazine	2.536	28.2

The comparison between PPh_3 and pyrazine substituted platinum complexes reveals a similar structure configuration. The difference between the two arises because of the different axial ligands. The Pt-Pt bond distance is shorter in pyrazine substituted platinum complex than that of PPh_3 substituted Pt complex. The decrease of bond length might be due to the weaker trans-influence exerted by the pyrazine molecule compared with that of the PPh_3 molecule. The Pt-Pt-P bond angle in PPh_3 substituted complex is closer to 180 degrees than that of pyrazine substituted complex. It shows PPh_3 molecule interacts less sterically with the cis methyl group than pyrazine molecule does.

The structures that have been characterized also indicate the Pt-Pt-C (C-methyl group) bond angle tends to be greater than 90 degrees. This widening of bond angle is explained by the Pt-Pt bond torsion that alleviates the steric repulsion between methyl groups in the equatorial coordination planes. This torsion is not completely reduced, even though it is hindered by the bridging ligands

that would like to choose a planar configuration.

The structures so far characterized only have the head-to-head configuration. From previous studies (54) it is known that, if the substituent on the bridging ligand is small in size, it is likely to convert to the head-to-tail configuration with the addition of an axial ligand. The terms head-to-head and head-to-tail only refer to the polar or non-polar arrangement of the molecule. These two arrangements are, in many ways, similar to each other. From the mechanism study, it seems conclusive that this series of complexes tend to have one strong coordinated axial ligand rather than two weakly coordinated ones. It indicates that polar configuration, despite having a strong torsion force in its bridging ligands and methyl groups, still holds the molecule tightly.

NMR and IR studies

The NMR spectroscopy study mainly involves two parts:

a. Proton NMR assigment for the oxo-pyridonate bridged platinum(III) complexes.

b. Proton NMR study about the mechanism of binuclear platinum(III) complex head-to-head $\rightleftarrows$ head-to-tail interconversion and cis-$PtCl_2(Et_2S)_2$ $\rightleftarrows$ trans-$PtCl_2(Et_2S)_2$ isomerization.

In addition, ^{195}Pt, ^{31}P NMR can be used to aid in the structure determination and to observe coupling constants.

The method of using different nuclei NMR is an advantage because of the sensitivity of the instrument. It shows clearly whether the atoms are present in the molecule or not and tells the atomic ratio in the molecule. The proton NMR study on assignment of binuclear platinum(III) complexes elucidated the nature of the structures. Proton NMR application not only shows the number of hydrogens in each ligand or molecule, but also presents the hydrogen's environment and even the concentration of the species. Proton NMR were also chiefly used in the reaction part in an attempt to determine the actual composition of the product.

Besides those for which structures were determined, a great deal can be learned from the NMR studies discussed in the experimental part. The yellow Pt tetramer is a good example for ^{195}Pt NMR study, but the result is a little disappointing. Pt(II,IV) complex ought to show two resonances with the ratio 3:1 in the spectrum, but only Pt(II) resonance was observed. Failure to show the Pt(IV) resonance might be due to several reasons. One explanation would be that the complex is fluxional in solution. The result of the fluxionality in a molecule such as the yellow tetramer would lead to the loss of the structural information. Another answer lies in the relaxation properties of platinum. As platinum is large, the nuclear spin relaxation time will be shortened so much

that NMR signals are virtually undetectable. We did see platinum FID in a certain range of frequency. However, only Pt(II) resonance was assigned, and there is no definite conclusion for the absence of Pt(IV) resonance.

IR spectra have given considerable insights into the possible structure details of the various synthetic products. The spectra are especially useful finding the specific ligand involved in the reaction and functional groups in the product.

The spectra obtained for the investigation have supplied a critical point in determination of the structure of yellow Pt dimer. The X-ray data set of the complex is very short; therefore the hydroxo bridge was determined, by the charge and geometric balance, to be a more reasonable structure. It is only with information from IR spectra that we can propose that the complex is hydroxo bridged. IR were also used in the reaction product determination. The difficulties involving the complex structure characterization in IR are lacking in reference data and separation of the product, though certain bonds were assigned. On the whole, IR plays a minor part in my research. Only with a combination of NMR and x-ray crystallography and other analytic tools can one obtain a great deal of information about the structure of the molecule.

SUMMARY

The isomerization of cis-$PtCl_2(Et_2S)_2$ ⇄ trans-$PtCl_2(Et_2S)_2$ has been studied. It is noteworthy that the isomerization forms spontaneously. In most organometallic reactions, only cis-$PtCl_2(Et_2S)_2$ is considered a useful material due to the trans-effect influenced labile Pt-Cl bond. The structures of the complexes, though not considered as platinum clusters, are also valuable in understanding in forming platinum cluster.

The second part of this investigation is concerned with the rearrangement between HH and HT configurations in binuclear Pt(III) compounds. The mechanism of Pt(FHPy)(HH) ⇄ Pt(FHPy)(HT) interconversion has been studied. It has been shown that the reaction rate is largely dependent upon the pyridine concentration and temperature. The higher the concentration of pyridine and higher the temperature, the faster the reaction goes. With the bridging ligands coordinating the metal centers and direct metal-metal bond, the rearrangement happens without rupture of the metal-metal bond. Experiment also proves that the bridging ligand is not totally free from the bonding with the metal centers. Further experiment indicates that the reaction rate is closely related to the inductive effect of the substituent of the bridging ligand. Compared with Pt(FHPy) and Pt(HPy), the reaction rate of the Pt(FHPy) is at least 20 times faster than that of the Pt(HPy). Activation entropy and

activation enthalpy of Pt(FHPy) interconversion have been calculated from the temperature dependence of the reaction rate ($\Delta S^{\neq}$= -29 vs. 16 J Mol.$^{-1}$ K^{-1}, $\Delta H^{\neq}$= 84 vs. 105 kJ Mol.$^{-1}$). A mechanism for the interconversion has been postulated as a dissociative concerted process and discussed.

The reactivity of binuclear oxo-pyridonate bridged platinum(III) complexes is such that a variety of reactions can be performed. Different kinds of ligands have been used to study the substitution reaction. Two structures of the derivatives of Pt(III) complexes have been characterized for the first time. Influences of the different axial ligands upon the metal-metal bond length and torsion angle have been observed. With the different axial ligands, the basic configuration remains very much the same, meaning the Pt(III)-Pt(III) bond is strong.

The synthetic method used for preparation of the dinuclear platinum(II) complex and the tetranuclear platinum(II,IV) complex has been proven to be versatile in which a new area of classical reaction has been found. One should notice the unique aspect of the reaction condition that produces both Pt(II) and Pt(II,IV) complexes. The synthesis shows the starting materials undergo a series of color changes, including monomer, dimer, trimer and tetramer. It is easy to assume that these Pt(II) and Pt(II,IV) complexes are intermediates of the reaction, because there is a binuclear Pt(III) complex formation at

low pH value (I). However, Pt(II) and Pt(II,IV) compounds are very stable in air and soluble in water solution. The structures of the yellow Pt(II) dimer and Pt(II,IV) tetramer have been characterized. There are no such structures in the literature so far. From the structure point of view, these platinum compounds have shown diversities in metal-metal bond formation and steric interactions among atoms in these molecules. They have also shown co-existence of the molecules of different oxidation states in the same solution, so as to indicate the plausible way to synthesize Pt(III) compound through the mixture of Pt(II) and Pt(IV) compounds.

Therefore, the research of this category has lead to some important understanding about the platinum cluster complex regarding its bond formation, structure coordination and chemical reactivity. Further efforts of investigation about platinum cluster are needed to gain more knowledge of this "charming" element.

REFERENCES CITED

1. McDonald, D.; Hunt, L.B. "A History of Platinum and Its Allied Metals" Johnson Matthey, London ECI, 1982.

2. Dewar, J.; Scott, A. Chem.News, 1879, 40, 294.

3. Lippard, S.J. "Platinum, Gold and Other Metal Chemotherapeutic Agents" ACS Symposium Series.

4. Thomas, T.W.; Underhill A.E. Chem.Soc.Rev., 1972, 1, 99.

5. Cotton, F.A.; Walton, R.A. "Multiple Bonds Between Metal Atoms" Wiley, New York, 1982.

6. (a) Cotton, F.A.; Deboer, B.G.; Laprabe, M.D.Pipal, J.R.; Ucko, D.A. J.Amer.Chem.Soc., 1970, 92, 2926. (b) Cotton, F.A.; Beboer, B.G.; Laprade, M.D.; Pipal, J.R.; Ucko, D.A. Acta.Cryst., 1971, B27, 1664.

7. Cotton, F.A.; Felthouse, T.R. Inorg.Chem., 1980, 19, 323.

8. Howard, R.A.; Wynne, A.M.; Bear, J.L.; Wendlandt, J. J.Inorg.Chem., 1976, 38, 1015

9. Vezes, M. Ann.Chim.Phys., 1893, 22, 160.

10. Vezes, M. Z.Anorg.Chem., 1897, 14, 278.

11. Blondel, M. Ann.Chim.Phys., 1905, 8, 110.

12. Wohler, L.; Frey, W.Z. Electroch., 1909, 15, 132.

13. Muraeviskaya, G.S.; Kukine, G.A.; Orlova, V.S.; Evestaf'eva, O.N.; Porai-Koshits, M.A. Dokl.Akad.Nauk.SSSR, 1976, 226, 76.

14. Underhill, A.E.; Watkins, D.M. J.Chem.Soc., 1977, 5.

15. Cotton, F.A.; Frenz, B.A.; Shive, L.W. Inorg.Chem., 1974, 14, 649.

16. Cotton, F.A.; Frenz, B.A.; Pederson, E.; Webb,T.R. Inorg.Chem., 1975, 14, 391.

17. Muraveiskaya, G.S.; Abshikin, V.E.; Evestf'eva, O.N.; Golovaneva, I.F. Sov.J.Coord.Chem., 1980, 6, 218.

18. Peterson, E.S. Ph.D Thesis, Montana State University, October, 1987.

19. Bancroft,D.P.; Cotton, F.A.; Falvello, L.R.; Han, S.; Schwotzer, W. Inorg.Chim.Acta., 1984, 87, 147.

20. Muraveiskaya, G.S.; Abashikn, V.E.; Evstaf'eva, O.N.; Golovaneva, I.F.; Shchelokov,R.N. Koord.Khim., 1980, 6, 463.

21. Cotton, F.A.; Falvello, L.R.; Han, S. Inorg.Chem., 1982, 21, 1709.

22. Conder, H.L.; Cotton, F.A.; Falvello, L.R.; Han, S.; Walton, R. Inorg.Chem., 1983, 22, 1887.

23. Che, C.M.; Schaefer, W.P.; Gray, H.B; Dickson, M.K.; Stein, P.B.; Roundhill, D.M. J.Am.Chem.Soc., 1982, 104, 4253.

24. Che, C.M.; Mak, T.C.W.; Gray, H.B.; Inorg.Chem. 1984, 23, 4386.

25. Clark, R.J.H.; Kurmoo, M.; Dames,H.M.; Hursthouse, M.B. Inorg.Chem., 1986, 25, 409.

26. Che, C.M.; Herbstein, F.H.; Schaefer, W.P.; Marsh, R.E.; Gray, H.B. J.Am.Chem.Soc., 1983, 105, 4604.

27. Hoffmann, K.A.; Bugge, G. Chem.Ber., 1908, 41, 312.

28. Davidson, P.J.; Faber, P.J.; Fischer Jr, R.G.; Mansy, S.; Peresie, H.J.; Rosenberg, B.; Van Camp, L. Cancer Chemother.Rep., 1975, 59, 287.

29. Rosenberg, B. Cancer Chemother.Rep., 1975, 59, 589.

30. Speer, R.J.; Ridgeway, H.; Hall, L.M.; Steward, D.P.; Howe, K.E.; Liebman, D.Z.; Newmann, A.O.; Hill, J.M. Cancer Chemother.Rep., 1975, 59, 629.

31. Barton, J.K.; Szalda, D.J.; Rabinowitz, H.W.; Waszczak, J.V.; Lippard, S.J. J.Am.Chem.Soc., 1979, 101, 1434.

32. Hollis, L.S.; Lippard, S.J. J.Am.Chem.Soc., 1981, 103, 6761.

33. Hollis, L.S.; Lippard, S.J. Inorg.Chem., 1983, 22, 2605.

34. Schollhorn, H.; Thewalt, U.; Lippert, B. J.Chem.Soc.Chem.Commu., 1986, 258

35. Kuyper, J.; Vrieze, K. Transition Met.Chem., 1976, 1, 208.

36. Steele, B.R.; Vrieze, K. Transition Met.Chem., 1977, 2, 169.

37. Steele, B.R.; Vrieze, K. Transition Met.Chem., 1977, 140

38. Overbeck, A.R.; Schagen, J.D.; Schenk, H. Inorg.Chem., 1978, 17, 1938.

39. Bellitto, C.; Flamini, A.; Gastaldi, L. Inorg.Chem., 1983, 22, 444.

40. Carrondo, M.A.A.F.de C.T., Skapski, A.C. J.Chem.Soc.Chem.Commun., 1976, 410.

41. Orlova, V.S.; Muraveiskaya, G.S.; Golovanoca, I.F.; Shchelokov, R.N. Zh.Neorg.Khim., 1980, 25, 209.

42. Calabrese, J.C.; Dahl, L.F.; Chin, P.; Longoni, G.; Martinengo, S. J.Am.Chem.Soc., 1974, 96, 2616.

43. Briant, C.E.; Evans, D.G.; Mingos, D.M.P. J.Chem.Soc.Dalton.Trans., 1986, 1535.

44. Moody, D.C.; Ryan, R.R. Inorg.Chem., 1977, 16, 1052.

45. Lippert, B.; Lock, C.J.L.; Rosenberg, B.; Zvagulis, M. Inorg.Chem., 1978, 17, 2971.

46. Faggiani, R.; Lippert, B.; Lock, C.J.L.; Rosenberg, B. Inorg.Chem., 1977, 16, 1192.

47. Rochon, F.D.; Morneau, A.; Melanson, R. Inorg.Chem., 1988, 27, 10.

48. Betz, P.; Bino,A. J.Am.Chem.Soc., 1988, 110, 602.

49. Hollis, L.S.; Lippard, S.J. Inorg.Chem., 1982, 21, 2116.

50. Hollis, L.S.; Lippard, S.J.; Roberts, M.M. Inorg.Chem., 1983, 22, 2637.

51. Lippert, B.; Schollhorn, W.; Thewalt, U. Naturforsch, Teil B, 1983, 38, 1441.

52. Bancroft, D.P., Doctoral Thesis, Texas A&M University, December, 1986

53. Kauffman, G.B.; Cowan, D.O. Inorg.Synthesis, 1960, 6, 211.

54. Turley, P.C.; Haake, P. J.Am.Chem.Soc., 1967, 89, 4617.

55. Roulet, R.; Barbey, C. Helvetica Chimica.Acta., 1973, 56, 2179.

56. Blondtrad, R.J. J.Pr.Chem., 1888, 38, 352.

57. Klason, P. Chem.Ber., 1895, 28, 1493.

58. Werner, A. Z.Anorg.Chem., 1893, 3, 310.

59. Angell, F.G.; Drew, H.D.K.; Wardlaw, W. J.Am.Chem.Soc., 1930, 349

60. Chatt, J.; Wilkins, R.G. J.Am.Chem.Soc., 1952, 273, 4300.

61. Haake, P.; Pfeiffer, R.M. J.Am.Chem.Soc., 1970, 92, 4996.

62. Cooper, D.G.; Powell, J. J.Am.Chem.Soc., 1973, 95, 1102.

63. Tobita, H.; Habazaki, H.; Ogino, H. Bull.Chem.Soc.Jpn., 1987, 60, 797.

64. Sergi, S.; Marsala, V.; Pietropaolo, R.; Faraone, F. J.Organomet.Chem., 1970, 23, 281.

65. Cromer, D.T.; Weber, J.T., "International Table for X-ray Crystallography" Vol.IV; Kynock Press:Birmingham, England, 1974, P72-98, P149-150.

66. O'Halloran, T.V.; Lippard, S.J. Inorg.Chem., 1989, 28, 1289